T.C.

YEDITEPE UNIVERSITY
INSTITUTE OF HEALTH SCIENCES
DEPARTMENT OF PHARMACEUTICAL TECHNOLOGY

DEVELOPMENT OF ANTIPERSPIRANT FORMULATION BASED ON DOUBLE EMULSION

MASTER OF SCIENCE THESIS

DİDEM AYŞE ALABAZ

İstanbul-2018

T.C.
YEDITEPE UNIVERSITY
INSTITUTE OF HEALTH SCIENCES
DEPARTMENT OF PHARMACEUTICAL TECHNOLOGY

DEVELOPMENT OF ANTIPERSPIRANT FORMULATION BASED ON DOUBLE EMULSION

MASTER OF SCIENCE THESIS

DİDEM AYŞE ALABAZ

SUPERVISORS
PROF DR SEYDA MALTA
ASSIST PROF DR GÜLENGÜL DUMAN

İstanbul-2018

THESIS APPROVAL FORM

Institute	: Yeditepe University Institute of Health Sciences
Programme	: Master of Science in Cosmetology
Title of the Thesis	: ''Development of Antiperspirant Formulatıon Based on Double Emulsion''
Owner of the Thesis	: Didem Ayşe Alabaz
Examination Date	: 09/01/2018

This study have approved as a Master/Doctorate Thesis in regard to content and quality by the
Jury.

Chair of the Jury:	PROF. DR. SEYDA MALTA	
Supervisor:	ASSIST. PROF. DR GÜLENGÜL DUMAN	
Member/Examiner:	PROF. DR. ERDAL CEVHER	
Member/Examiner:	ASSOC. PROF. DR ALİ DEMİR SEZER	
Member/Examiner:	ASSIST. PROF. DR CEM LEVENT ALTAN	

APPROVAL

This thesis has been deemed by the jury in accordance with the relevant articles of Yeditepe University Graduate Education and Examinations Regulation and has been approved by Administrative Board of Institute with decision dated 11.01.2018. and numbered 2018/01-03

Prof. Dr. Bayram YILMAZ
Director of Institute of Health Sciences

DECLARATION

I hereby declare that this thesis is my own work and that, to the best of my knowledge and belief, it contains no material previously published or written by another person nor material which has been accepted for the award of any other degree except where due acknowledgment has been made in the text.

22/01/2018

Didem Ayse Alabaz

I would like to dedicate this work to my dearest friend Mey..

ACKNOWLEDGEMENTS

First of all I would like to acknowledge God, for giving me the great opportunity to step in the wonderful world of science, for providing me every day the enthusiasm and wisdom to proceed successfully and above all for offer me the chance to meet amazing people who were the clue for the development of this thesis.

I would like to express my gratitude to a woman that personally I admire and appreciate with all my heart, my coadvisor Prof. Dr. Seyda Malta, for her assistance in all the laboratory issues. I would also like to thank to my advisor Assist. Prof. Dr. Gülengül Duman, for her encouragement and guidance in all the organization and discussion issues.

Moreover, I would like to thank my dear M.Sc. supervisor, Assist. Prof. Dr. Yasemin Yağan Uzuner for her guidance during my M.Sc. I would like to give special thanks to my colleagues in YUKOZ and a lovely women, Fahriye Hamzaoğlu for offering me their friendship and support.

It is a pleasure to thank to three incredible person whom I had the honor to collaborate: Assist. Prof. Dr. Samet Özdemir, Essam Türkmani and Sera Erkeçoğlu. They helped me a lot in different steps of my investigation, providing me their knowledge and direction. Specially, I want to offer my greatest thanks to my best friends Hasine Gündoğan, Hande Arat and Ayşe Vaizoğlu for their invaluable friendship.

I wish to express my most sincere appreciation to my beloved family, for believing in me doing their best in helping me to achieve this goal. Particularly, I would like to thank my parents, Assoc. Prof. Derya Alabaz and Prof. Ömer Alabaz, because for them it was not easy to be away of me and even like this, they offered me all their support and understanding. At last but not least, I would like to thank a fabulous man, for his unconditional support, motivation and love.

TABLE OF CONTENTS

LIST OF TABLES

LIST OF FIGURES

LIST OF SYMBOLS AND ABBREVIATIONS

O/W	: oil-in-water emulsion
W/O	: water-in-oil emulsion
W1/O/W2	: water-in-oil-in-water emulsion
O1/W/O2	: oil-in-water-in-oil emulsion
CMC	: Critical Micellar Concentration
HLB	: Hydrophilic-lipophilic balance
AOT	: Dioctyl sulfosuccinate sodium salt
$Al_2OH_5Cl_2.3\ H_2O$	: Aluminum Chlorohydrate
DLS	: Dynamic Light Scattering
F1	: Double Emulsion (W1/O/W2)
F2	: Double Emulsion Incorporated with Aluminum Chlorohydrate
F3	: Double Emulsion Incorporated with Lavender Oil
F4	: Double Emulsion Incorporated with Aluminum Chlorohydrate and Lavender Oil

ABSTRACT

In this study, lavender oil is used to give pleasent odor and aluminum chlorohydrate is used due to its effect on decreasing the perspiration. Two actives were formulated with suitable emulsifiers to obtain a stable multiple emulsion. Suitable emulsifiers were chosen due to their HLB value according to manuscript and literature. Aluminum salts are the main topical agents for hyperhidrosis which have antiperspirant activity that decreases perspiration. When these salts are used in cosmetics formulations, duration of effect is often limited to 48 hours. By microencapsulating antiperspirant salts the insulation from the surroundings, and controlled released could be achieved, so securing a long shelf life. In order to overcome these problems both were used in small amounts, in a formulation of a double emulsion. So that, both were chosen to be used in small amount by the technique of double emulsion.

The cosmetic products generally contain 10% of aluminum chlorohydrate on the market. The objective of this study was to investigate and to obtain the optimum antiperspirant ratio for formulation of stable double emulsion. In this project the ratio of aluminum chlorohydrate was determined as 1% in double emulsion formulation. For this purposes, optimum conditions were determined according to experimental results of particle size, stability and migration studies. Finally, the most stable double emulsion (F4) resulted poly dispersity index of 0.238 at the end of the 13th day and with an average globule size of 3.9 μm and 1%, which is 10 times lower dosage, containing aluminum chlorohydrate was formulated to be used as antiperspirant cream/roll on.

The second aim is that the aluminum chlorohydrate formulated in the inner phase of the double emulsion stays there or is slowly released for the final product to show desired antiperspirant properties. For this purposes, migration over time was detected. As a result, it was clearly observed that incorparation of viscosity enhancer was delayed the migration. Due to the increased amount of viscosity enhancer, the migration rate was slowed down, improving the stability.

Keywords: Aluminum salts, lavender oil, multiple emulsion, double emulsion, microencapsulation

ÖZET

Bu çalışmada, lavanta uçucu yağı hoş koku vermek için ve alüminyum klorohidrat ise terleme önleyici ajan olarak kullanılmıştır. Stabil bir çoklu emülsiyon, bu iki aktif beraberinde uygun emülgatörler kullanılarak formüle edilmiştir. Literatür ve çoklu emülsiyon sistemine uygun HLB değerindeki emülgatörler seçilmiştir. Alüminyum tuzları, aşırı terlemeyi azaltan en önemli topikal aktif maddelerdir. Bu tuzlar kozmetik formülasyonlarda kullanıldıklarında, etki süresi çoğunlukla 48 saat ile sınırlıdır. Mikroenkapsülleme yöntemi ile alüminyum tuzlarının dış etkilerden izolasyonu ve kontrollü salınımı sağlanarak, böylece ürünün raf ömrü uzatılmış olur. Bu sorunları aşabilmek adına çoklu emülsiyonda çift kat emülsiyon tekniğinden faydalanarak az miktarda aktif madde kullanılması sağlanmaktadır.

Pazarda yer alan kozmetik ürünlerin çoğu %10 alüminyum klorohidrat içermektedir. Bu çalışmada, stabil bir çoklu emülsiyon formüle edebilmek için gerekli olan optimum antiperspiran aktif oranını araştırmak ve belirlemek amaçlanmıştır. Alüminyum klorohidratın oranı %1 olarak belirlenmiştir. Bu oran ile, damlacık boyutu, stabilite ve salınım çalışmalarının deneysel sonuçları optimum koşullar sağlanarak belirlenmiştir. Böylelikle, 13. günün sonunda polidispersite indeksi 0.238 ve damlacık boyutu ortalama 3.9 μm olan, stabil çoklu emülsiyon (F4) formülasyonu, 10 kat daha az alüminyum klorohidrat aktif madde miktarı ile krem/roll-on amaçlı kullnılmak üzere tasarlanmıştır.

Bu projede amaçlanan ikincil hedef ise, beklenen terleme önleyici özelliklerini göstermesi için çoklu emülsiyonun iç fazında yer alan alüminyum klorohidratın dış faza salınımını durdurmak ya da kontrollü bir şekilde sağlamaktır. Bu nedenle, zamana bağlı fazlar arası geçiş gözlemlenmiştir. Sonuç olarak, viskozite ajanının formülasyona eklenmesi stabiliteyi iyileştirerek aynı zamanda fazlar arası aktif madde geçişini ertelediği açıkça gözlenmiştir.

Anahtar kelimeler: Alminyum tuzları, lavanta yağı, çoklu emülsiyon, çift kat emülsiyon, mikroenkapsülleme

1. INTRODUCTION

1.1. Emulsion

An emulsion consist of two phases which known as the two phase system. The phases also consist of two immiscible liquids. One of which is known as discontinuous or internal and the other is continuous or external phase. Discontinuous phase is dispersed as small droplets in continuous phase. Also an emulsifier helps discontinuous phase to disperse throughout the other [1].

There are two types of emulsion systems; oil-in-water (O/W) and water-in-oil (W/O) emulsion. In order to call an emulsion as an oil in water (O/W), aqueous phase needs to be constitute of more than 45% of the total weight where oils are the dispersed phase. W/O emulsions are named where aqueous phase constitutes of less than 45% of the total weight. Also a hydrophillic emulsifier for O/W and lipophillic emulsifier for W/O system helps discontinuous phase to disperse throughout the continuous phase [2].

1.1.1. Emulsion Stability

Positively charged hydrogen atoms and negatively charged oxygen atoms come together and produce water molecules which have polar structure. This tends to hydrogen bonding of water molecules with other materials (Figure 1) [3].

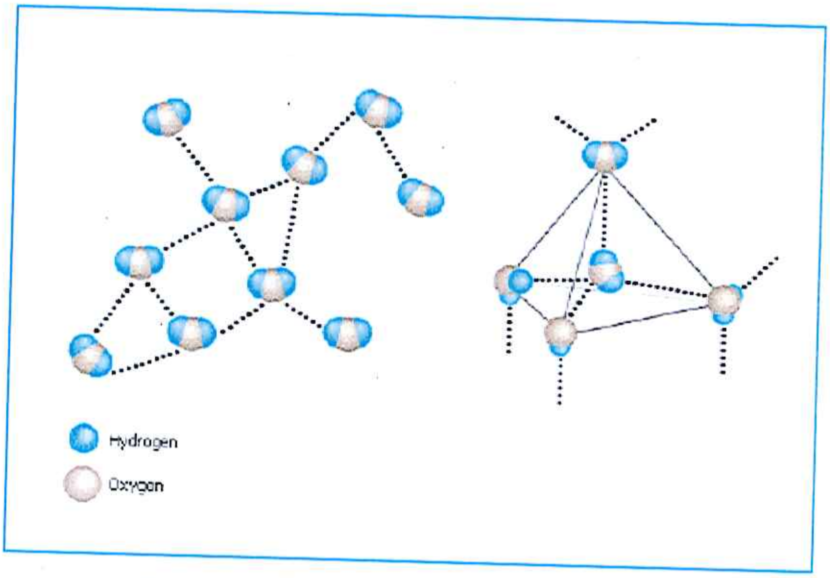

Figure 1: Hydrogen bonding in water [4]

When hydration takes place, hydrogen bonds can come together with an ion or a polar compound. When there is intensive hydration substances can be defined as hydrophilic [3].

On the other hand, when the hydrogen bonds come together with non-polar molecules such as a hydrocarbon chain, the water molecules organized to be in a cage-like structure being more ordered than in the bulk liquid which ends up in a low solubility of the solute (Figure 2). Such non-polar substances are defined as hydrophobic [5].

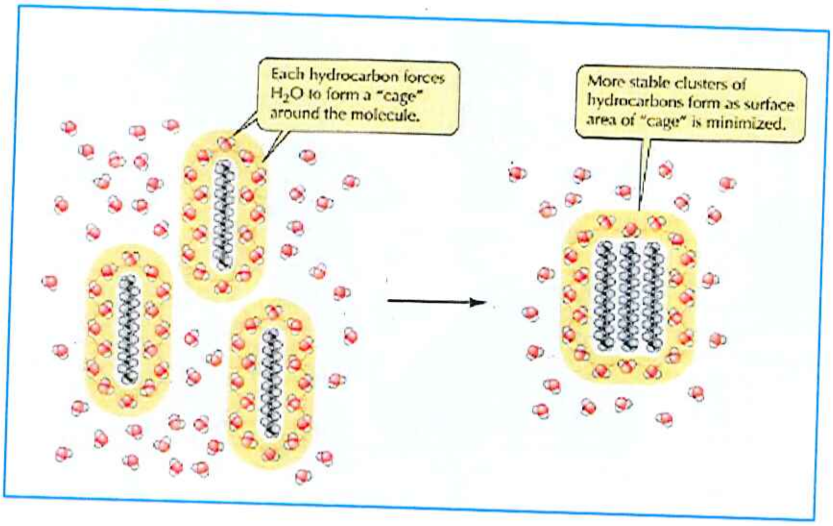

Figure 2: Interactions of Water with Non-Polar Substances [5]

Emulsions are thermodynamically unstable due to hydrophilic-hydrophobic interactions. They are capable of moving into two separate layers over time.

Due to aggregation of emulsion globules the flocculation takes place without distrupting the stabilizing layer at the interface (Figure 3). Flocculation is weak when it is reversible and it is strong when it is irreversible [6]. Coalescence takes place where the globules unite (Figure 4). Coalescence is an irreversible separation.

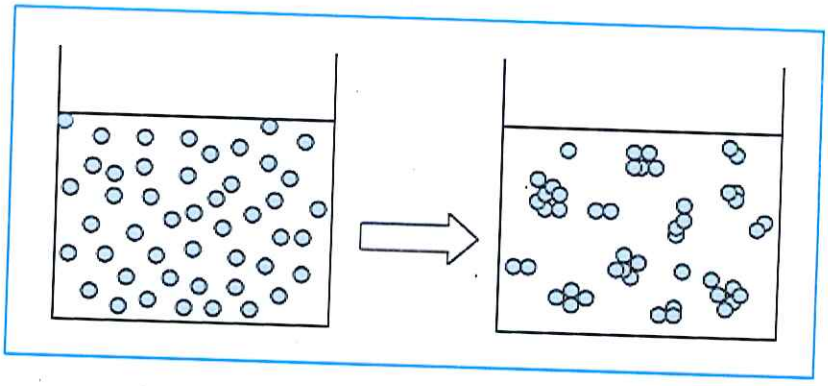

Figure 3: Flocculation / Aggregation [6]

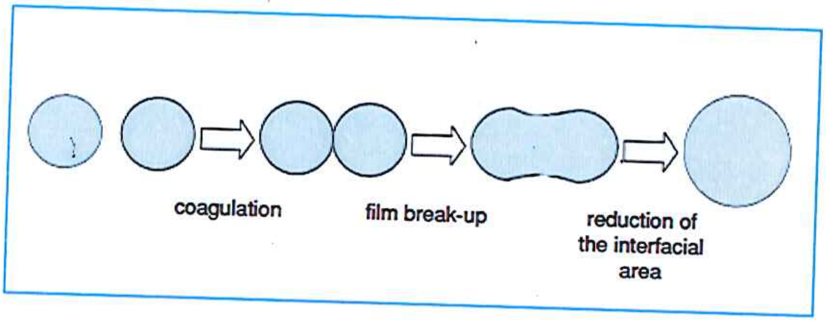

Figure 4: Coalescence of two globules [7]

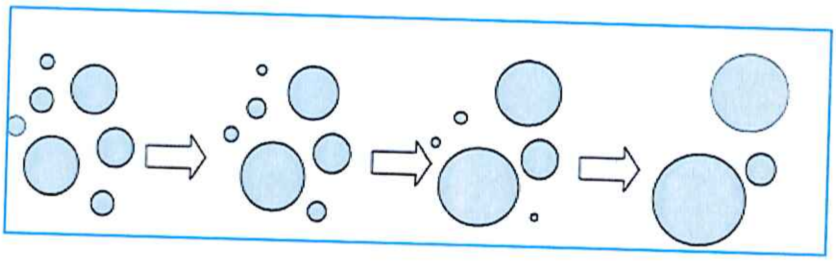

Figure 5: Ostwald ripening [7]

Smaller globules in emulsion dissolve and deposit on larger globules in order to reach a more stable state. This phenomena is called as Ostwald ripening (Figure 5) [7].

Creaming (Figure 6) or sedimentation (Figure 7) takes place when dispersed oil globules unite and arise to top of the O/W emulsion or sink to the bottom in W/O emulsions [8].

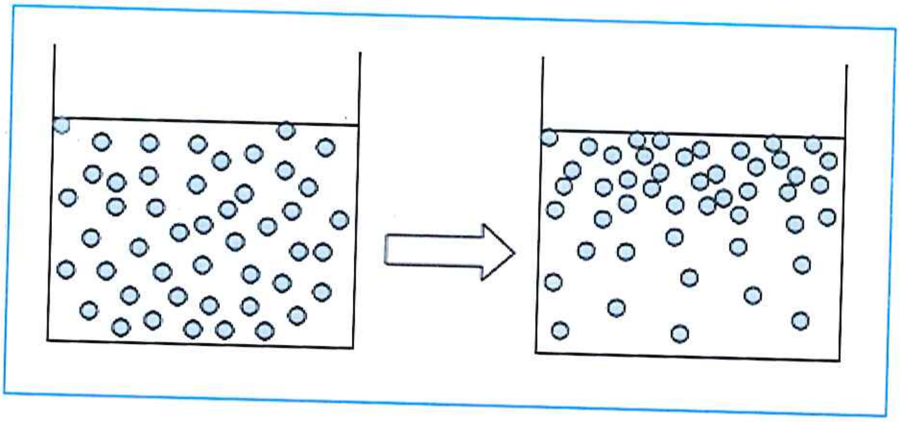

Figure 6: Creaming [8]

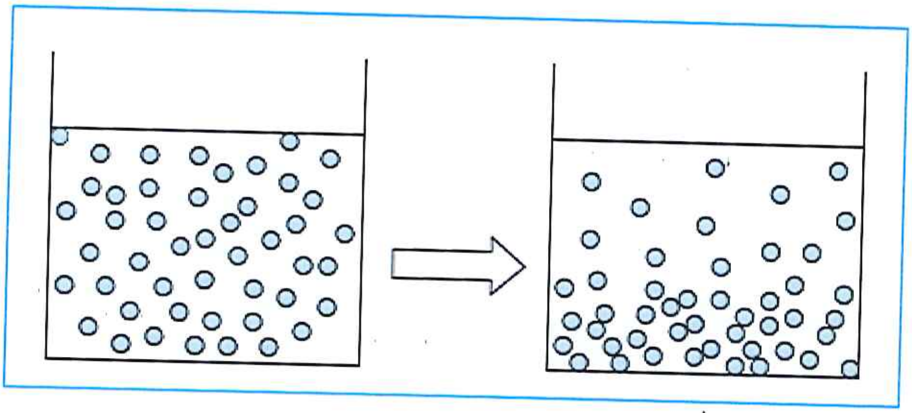

Figure 7: Sedimentation [8]

Commonly, flocculation, coalescence and Ostwald Ripening could lead to enhanced creaming (Figure 8) [6]. Emulsions are thermodynamically unstable due to hydrophilic hydrophobic interactions. In order to stop aggregation making multiple emulsions (W / O / W or O / W / O) could be a worth trying method.

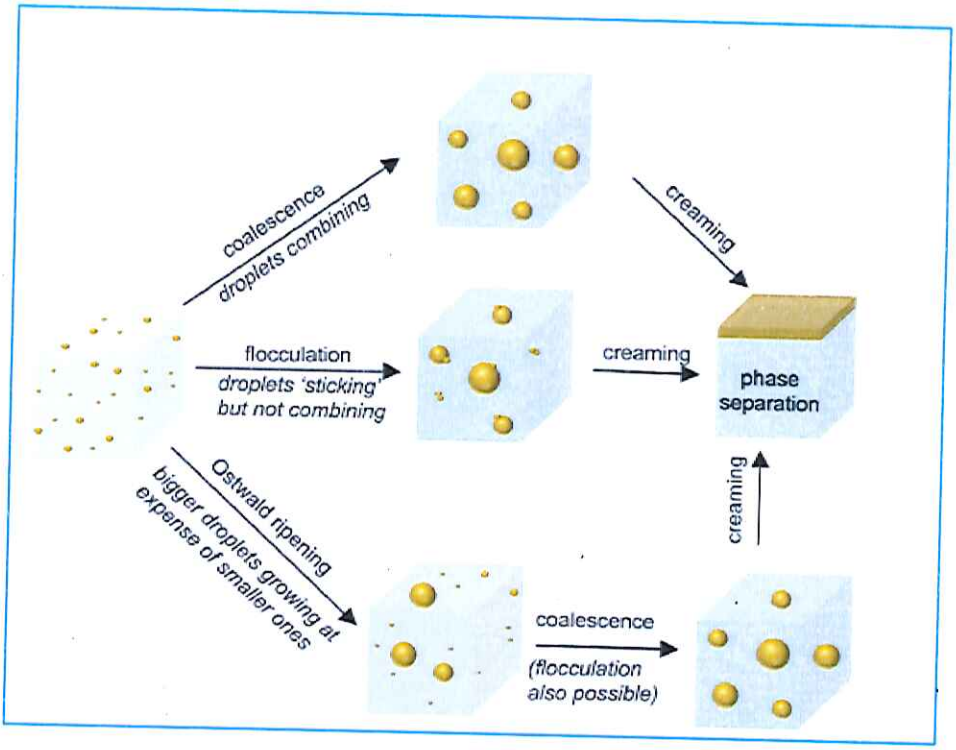

Figure 8: Stability mechanism cycle [8]

1.1.2. Emulsifiers or Surface-active agents or surfactants

Surfactants contain both hydrophilic and hydrophobic parts which is an amphiphillic molecule (Figure 9). They work by lowering the surface tension between two phases as a result formation of the emulsion.

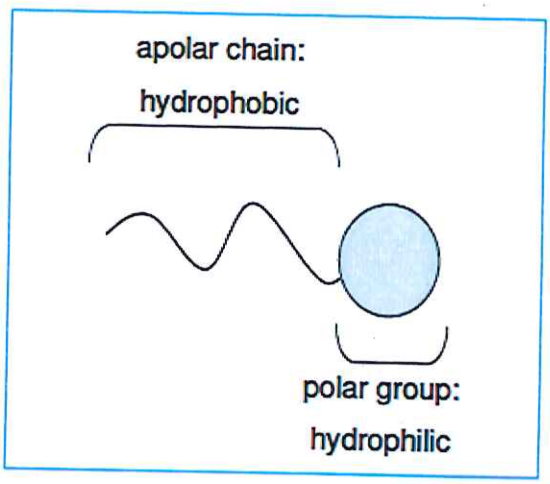

Figure 9: Parts of a surfactant monomer [9]

As the surfactant concentration increases, surface tension decreases. Micelles consist of several clustered surfactant molecules (Figure 10). Micelles are formed at this specific concentration is known as the Critical Micellar Concentration (CMC). At concentrations above the CMC, the surface tension of the solution is constant because the interfacial surfactant concentration does not change any more [9]. Below the CMC the surface tension decreases with increasing surfactant concentration as the number of surfactants at the interface increases.

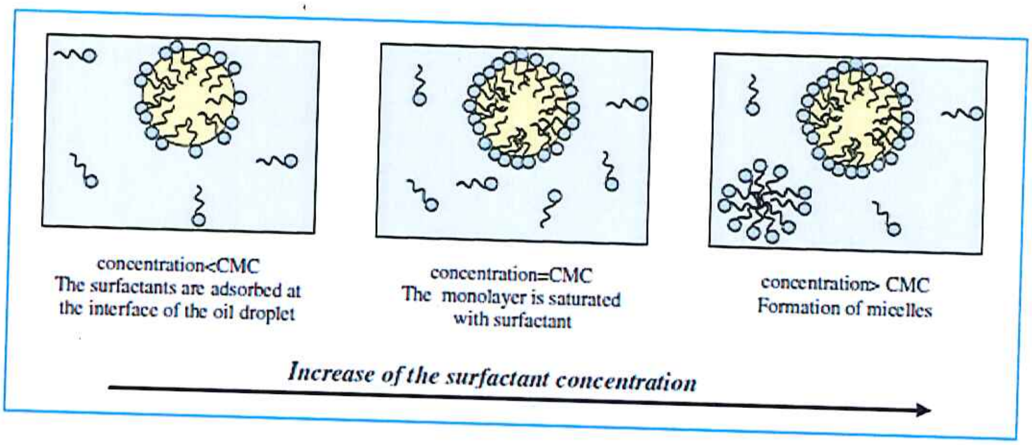

Figure 10: Surfactant adsorption in an O / W emulsion and micelle formation [9]

1.1.3. Hydrophilic Lipophilic Balance (HLB)

Hydrophilic-lipophilic balance (HLB) is an empirical form which shows the relationship between hyrophillic and hydrophobic parts of a surfactant. The HLB values introduced by Griffin evaluated experimentally as a means of predicting emulsion type with a number of emulsion stability tests. The more hydrophilic the surfactant, the higher the HLB value. HLB values range from 0 to 20. In order to make and stabilize a W/O emulsion, the HLB value should be up to 10, and should be between 10-20 for an O/W emulsion [5].

1.2. Classification of Emulsion

S.F. Wong et al. classified emulsions as O/W, W/O and multiple emulsions [10]. It can also be classified in accordance to particle size. Commonly, emulsion droplet size (Figure 11) lies in the micrometer range [11]. Particle size of microemulsions lies in the range 1-100 nm, particle size of nanoemulsions lies in the range 20-500 nm and particle size of macroemulsions lies in the range 20 nm – 10 μm.

1.2.1. Microemulsion

The microemulsion type was first introduced in the 1940s by Hoar and Schulman who produced a transparent solution by the titration of milky emulsion into the hexanol [12]. Microemulsion has an optical transparency and thermodynamically stable liquid solution. It has spherical and lamellar shapes. Low energy methods could be used to prepare [13]. Particle size ranges between 10 to 100 nm.

1.2.2. Nanoemulsion (Miniemulsion)

Nano-emulsions are also known as miniemulsions. Particle size ranges between 20 to 500 nm with narrow droplet size distribution [14-16]. They have some advantages for many practical applications in food, cosmetics, agricultural, chemicals, and pharmaceutical industries over other emulsion types as high kinetic stability, and optical transparency. It can be used as a method as drug delivery systems [17-19], as personal care formulations, as polymerization reaction media etc. [20]. The appearance of nanoemulsions is just like microemulsions, they both are transparent. The main difference between the two systems, is the thermodynamic stability of microemulsions versus the kinetic stability of nanoemulsions [21].

1.2.3. Comparison of Macroemulsions, Nanoemulsions and Microemulsions

The great differences between macroemulsions, microemulsions and nanoemulsions is in droplet size range and stability characteristics, as shown in Table 11. Macroemulsions and nanoemulsions are both thermodynamically unstable, but nanoemulsions are kinetically stable over long time scales due to their small particle size. Microemulsions are thermodynamically stable systems, although they are sensitive to changes in temperature and composition [22].

Table 1: Comparison of different types of emulsions [23]

	macroemulsions	nanoemulsions	microemulsions
	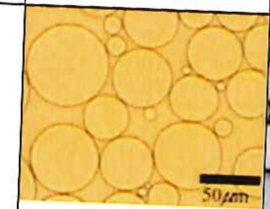	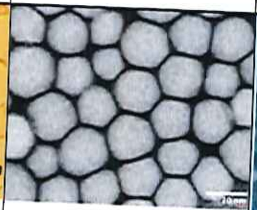	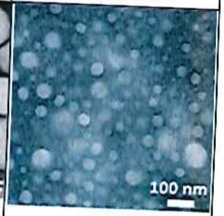
size	1-100μ	20-500 nm	10-100 nm
shape	spherical	spherical	Spherical, lamellar
stability	Thermodynamically unstable, weakly kinetically stable	Thermodynamically unstable, kinetically stable	Thermodynamic ally stable
Method of preparation	High&low energy methods	High&low energy methods	low energy methods
polydispersity	Often high (>40%)	Typically low (<10-20%)	Typically low (<10)

Another major advantage of nanoemulsions over microemulsions, is the lower surfactant concentration desired for the preparation. In fact, 4-8 wt % surfactant is enough while microemulsions need 10-30 wt % surfactant for the preparation.

Advantages of nanoemulsions include small globule size and kinetic stability [6] which is attractive for practical applications in drug delivery systems agricultural, personal care formulations, polymerization reaction etc. Due to small globule size, they have higher stability and because the diffusion rate can be faster than the sedimentation rate; so Brownian motion can avoid sedimentation/creaming, flocculation and coalescence [25].

1.4. Double Emulsion

Both oil in water and water in oil emulsion systems exist at the same structure by producing a complex system named as the multiple emulsion. This complex system was first used by Seifriz in the early 1920s [26]. The most common type of multiple emulsions is called double emulsion. In double emulsions, the dispersed or discontinuous or internal phase itself is another emulsion [27]. The two main types are, water oil water (W/O/W) and oil water oil (O/W/O) double emulsions. O/W/O double emulsion globule was schematically shown in Figure 11 [27].

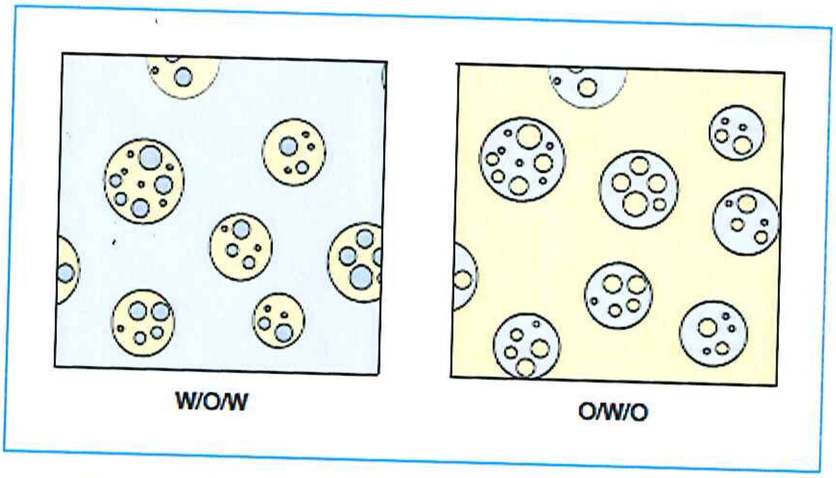

Figure 11: Types of double emulsions [27]

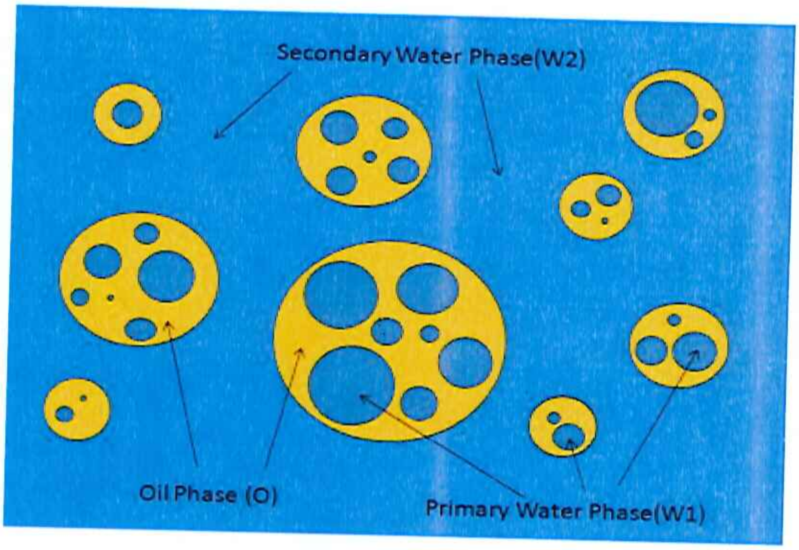

Figure 12: W/O/W double emulsion [27]

The most used first type water-in-oil-in-water (Figure 12) have intensive application area, made up of three phases, where small water droplets are entrapped within larger oil droplets and they are dispersed in continuous water phase. Two types of emulsifiers are used for emulsification of the multiple emulsion system. Lipophilic emulsifier is used for W/O emulsion, hydrophilic emulsifier is used for O/W emulsion. The second type double emulsion named as oil in water in oil, also made up of three phases, where small oil droplets are entrapped within larger water droplets and they are dispersed in continuous oil phase. Hydrophilic emulsifier is used for O/W emulsion, emulsifier is considered W/O emulsion [27].

1.3.2. Double Emulsion Preperation Methods

Three are three main method for the preparation of double emulsions. Phase inversion, two step emulsification, mechanical agitation of a mixture of an aqueous solution of a combination of hydrophilic and lipophilic emulsifier [28].

The two-step emulsification process is the most prevailling way for the production of double emulsion by the existence of hydrophobic and hydrophilic emulsifiers. Firstly W/O or O/W emulsion is prepared with involvement of proper emulsifier. To produce stable double emulsions particle size distribution need to be as narrow as possible. In second emulsification step, primarily produced emulsion is dispersed in convenient continuous phase with the proper emulsifier by the help of a homogenizer at mild level of speed [29]. This process is controllable, convenient and reproducable so that it is the most prevailling type [30].

Double emulsion system is ready to use tecnology for formulation of novel products [30]. They provide several sophisticated applications for industries like fuel energy [31], agrieulture, chemical engineering and separation processes [32][33]. Double emulsions technology is also very popular in food industries to improve emulsions mainly in milk, mayonnaise, etc. [34].

1.3.2. Double Emulsion and Industrial Applications

Davis, [35] said that W/O/W double emulsions have great industrial applications in various fields such as; as to improve the efficiency of the intestinal absorption of immobilized insulin in Engel et al's paper [36], used the double emulsion for production of flavoured mayonnaise in Matsumoto and Kohda's paper [37], they formulated low caloric mayonnaise [38]. Takahashi et al. [39] formulated dressing based on w/o/w double emulsion. Bams [40] prepared edible double emulsion with a dressing-like characterisics and a mayonnaise-like taste based on the same concept. Tadros [41] and Dickinson [42] entrapped the flavor compound inside the double emulsion in order to delay the release of volatile flavor during the production of food. Based on this concept, many patents had been given for foodstuffs and cosmetic products like antiperspirants.

1.4.Antiperspirants

Sweating is a normal process of the human physiology. Hyperhidrosis named as excessive sweating is a disorder that cause physical and psychological disability on the quality of life of human beings. People who have hyperhidrosis have emotional and social deception which leads to a downsizing in self-confidince. Hyperhidrosis originated from the abnormality of chromosomes in human biology, in fact it appear in childhood years. Nowadays there are pharmacological treatments for hyperhidrosis such as topical, oral and iontophoretic. Genarally people try to use cosmetics as an auxiliary solution to pharmacological treatments [43].

Aluminum salts are the main topical agents for hyperhidrosis which have antiperspirant activity that decreases perspiration. Salts of metals such as zirconium, aluminum, zinc, etc. have astringent function based to direct interaction on the excretory eccrine gland epithelium. Although aluminum salts are only effective in moderate cases of hyperhidrosis, there have always been a risk of skin irritation in sensitive individuals presumably related with high concentration of salt.

When these salts are used in cosmetics formulations, duration of effect is often limited to 48 hours. When an individual sweats, antiperspirant salts wash away directly proportional with the level of sweat. Therefore providing more effective, longer lasting antiperspirants is great interest [43]. By microencapsulating antiperspirant salts the insulation from the surroundings, and controlled released could be achieved. In the marketplace, there are available a wide range of cosmetic formulations with unnatural raw materials which are aimed to inhibit perspiration [44].

In the present study, two effective antiperspirant actives were choosen. Lavender oil as natural and aluminum chlorohydrate as unnatural but very effective on decreasing the perspiration. Antiperspirant salts are difficult to encapsulate due to their acidic natüre. Up until now it has been found that most antiperspirant salts rapidly degrade or react with the substances used to form the outer shell of the microcapsule, and essential oils deteriorate by heat, humidity, light and oxygen easily. In order to overcome these problems both were used in small amounts, in a formulation of a double emulsion.

2. MATERIALS AND METHODS

2.1 Materials

In this study following actives and other ingredients (excipients) were used to prepare double emulsion formulations as seen in Table 2.

Table 2: Functions, Purity and Suppliers of Raw Materials

	Function	Raw Material	Purity %	Supplier
actives	Antiperspirant agent	Aluminum Chlorohydrate ($Al_2OH_5Cl_2 . 3\ H_2O$) (Locron® P)	99,5	Clariant
	Antimicrobial agent, odor	Lavender oil (Lavandula Angustifolia)	100	Talya Bitkisel
Other Ingredients	Water phase	Aqua	100	YUKOZ Facility
	Emollient, Oil phase	Isohexadecane (Arlamol™ HD)	100	Croda
	Lipophillic emulsifier	Dioctyl sulfosuccinate sodium salt (AOT)	96	Alfa Aesar
	Hydrophillic emulsifier	Laureth-4 (Ercawax™ LM 4 V/FD)	100	ERCA
	Preservative	Ethylhexylglycerin, Phenoxyethanol (Euxyl™ PE 9010)	90, 10	Schülke & Mayr GmbH
	Viscosity enhancer	Bis-Lauryl Cocaminopropylamine/HDI/PEG-100 Copolymer, Butylene Glycol (Rheoluxe® 812)	30, 55	Elementis Specialties
	pH adjuster	Sodium hydroxide	100	Merck
	pH adjuster	Hydrochloric Acid	100	Merck
	Indicator	Phenolphtalein	100	Merck

Isohexadecane (Arlamol™ HD), main ingredient of oil phase as used as an emollient in the formulation of double emulsion, was obtained from Croda and used as received. Dioctyl sulfosuccinate sodium salt (AOT), an efficient lipophilic emulsifier used in oil phase in the first emulsification process, is supplied by Merck. Laureth-4 (Ercawax™ LM 4 V/FD), a hydrophilic emulsifier used in continuous water phase of double emulsion was supplied from ERCA. Euxyl™ PE 9010 to be used in double emulsion as a preservative to prevent microbial contamination during preparation and storage was supplied from Schülke & Mayr GmbH. Aluminum Chlorohydrate. $3H_2O$ (Locron® P), active used with antiperspirant properties was supplied from Clariant. Lavender oil, antimicrobial essential oil was also supplied from Talya Bitkisel. Rheoluxe® 812 was supplied from Elementis Specialties to be used in double emulsion as a viscosity enhancer to prolong release time. Water was deionized and UV filtered.

2.2. Methods

The experiments were carried out in the Chemical Engineering, Genetics Engineering and Faculty of Pharmacy student laboratories. Set-up is described in detail in experimental procedure part.

2.2.1. UV Spectrophotometry

UV Spectrophotometer measures the absorbance of a beam of light after it passes through a sample. Components of UV Spectrophotometer are, source that generates electromagnetic radiation, monochromator which includes a dispersion device that selects a particular waveband, sample area, detector to measure the intensity of radiation, recorder and lenses.

Figure 13 shows a schematic of a conventional single-beam spectrophotometer. At the beginning light comes to entrance slit of a monochromator, which transfers the light. Then it passes through the sample area to the detector. At that moment the absorbance of a sample is detected by the measurement of the intensity of light. Measurement of the intensity of light that reaches to the detector first done for the blank and then compared with the sample. Evolution 201 UV-Visible Spectrophotometer, Thermo Scientific was used in spectrophotometer analysis [45].

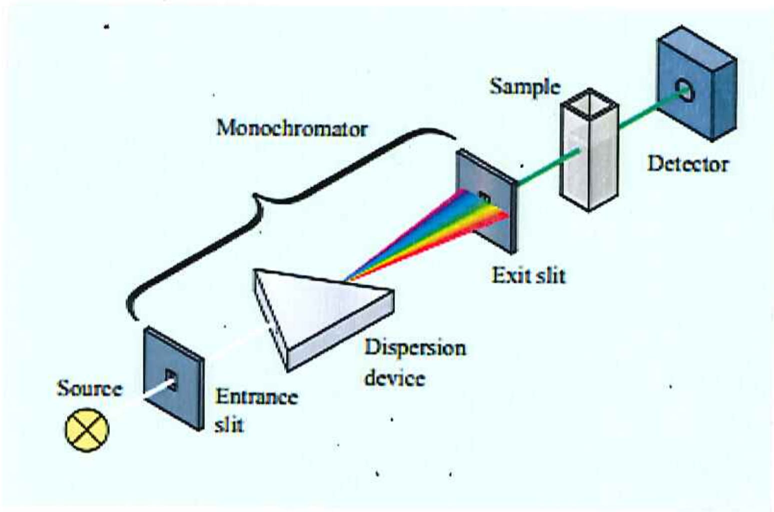

Figure 13: Schematic of a conventional spectrophotometer [45]

2.2.2. Optical Microscopy

Optical microscopy is a first inventrory tool that is used to identify substances from a close viewpoint. The image of a sample is viewed with the magnification of a lens with sending a beam of light as seen in Figure 14. Condenser lens employed to focus the light to sample and then objective lens is employed to magnify the beam. The microscope employed has four magnification levels of 5×, 10×, 20×, and 50× . The projector lens is also employed to make the image observable. NMM-800TRF System Metallurgical Microscope as a light microscope, Industrial Digital Camera as a microscopic camera and software named Argenit Kameram was used in optical analysis [46].

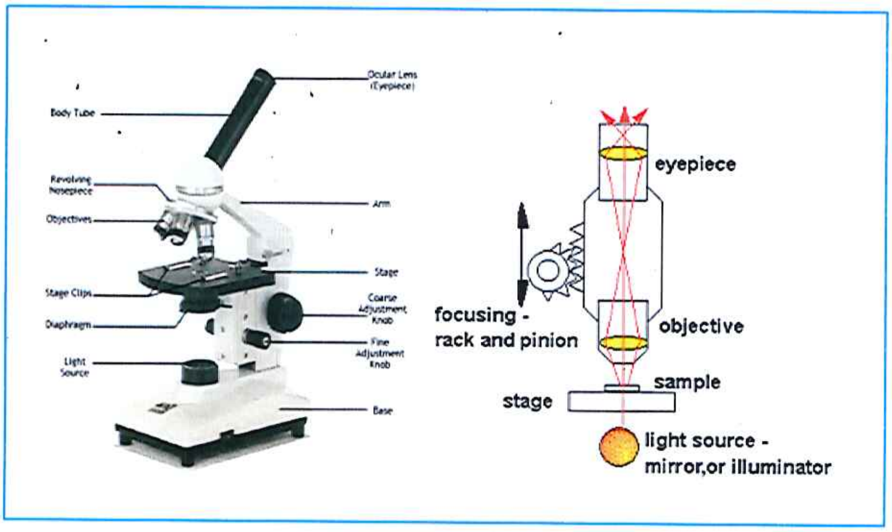

Figure 14: Light Microscopy [47]

2.2.3. Dynamic Light Scattering

Dynamic Light Scattering (DLS) also named as Photon Correlation Spectroscopy (Figure 15) is one of the most common technique that is used to examine the particle size of a solution. Particle size of a solution is examined by the help of laser light reflected onto the moving particle. This moving particle has a Brownian motion and this causes a Doppler Shift which is changing the wavelength of the laser light. The reason why the wavelength of the laser light is changing that is because of the size of the particle is changing also. Dynamic Light Scattering measures the size distribution, diffusion coefficient, polydispersity index to give a result by the autocorrelation function. The mean droplet size and size distribution of the double emulsions were determined by dynamic light scattering (DLS), by using a Malvern Zeta Sizer 3600 (Malvern Instruments, Malvern, U.K.) [48].

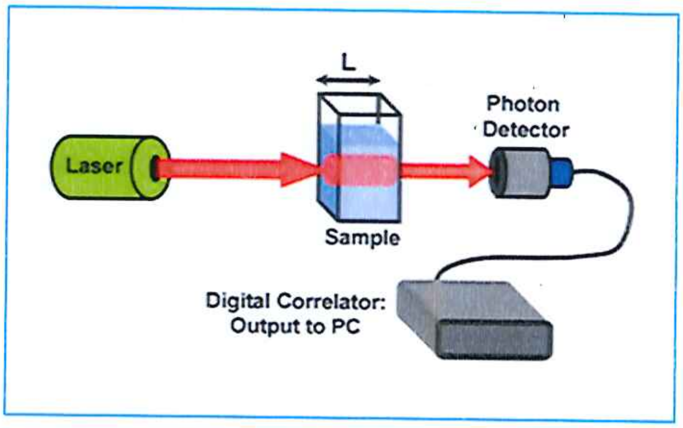

Figure 15: Dynamic Light Scattering [49]

2.2.4. Viscosimetry

To describe the meaning of viscosity is a good way to start this section. It is a quantitative measurement of a fluid's resistance to flow. In order to distinguish the viscosity of a fluid a tool named Viscosimetry is used. The most common type of viscosimetry is the rotational type as shown in Figure 16. Its principal is based on the idea that the value of torque essential to manage the resistance by the rotation of spindle is related with the viscosity of the fluid of viscometers use the idea that the force required to turn an object in a fluid, can indicate the viscosity of that fluid. Rotational viscometers are classified into three types as, coaxial-cylinder, cone-and-plate, and plain spindle [50].

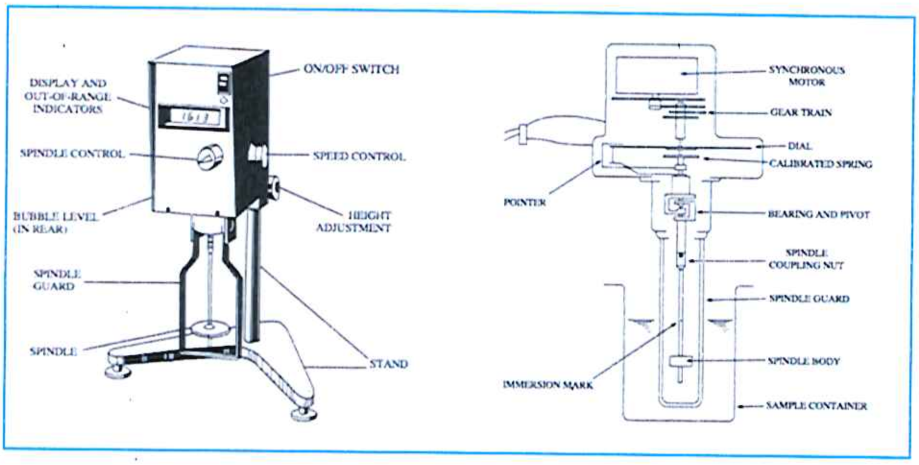

Figure 16: Rotational Viscometer [50]

2.2.5. Homogenizer

Homogenization is a process that reduces the size of droplets in liquid-liquid dispersions as seen in Figure 17 [51]. The machine have rotor blades that provides high-speed rotation. It helps liquid and solid materials to be mixed with a high suction by the movement from bottom to top of the container (Figure 18 (a)).

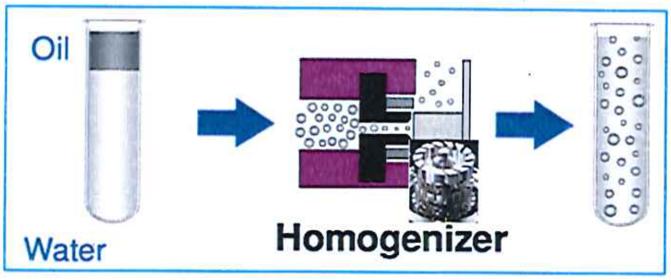

Figure 17: Emulsion processing [51]

Materials move straight through the outer edge where they are exposed to a circulating effect between the rotor and stator by centrifugal force (Figure 18 (b)). This circulatory effect of the horizontal (radial) repulsion and suction into the head is continued by intense hydraulic shear where high velocity takes place (Figure 18 (c)) (Figure 18 (d)) [52].

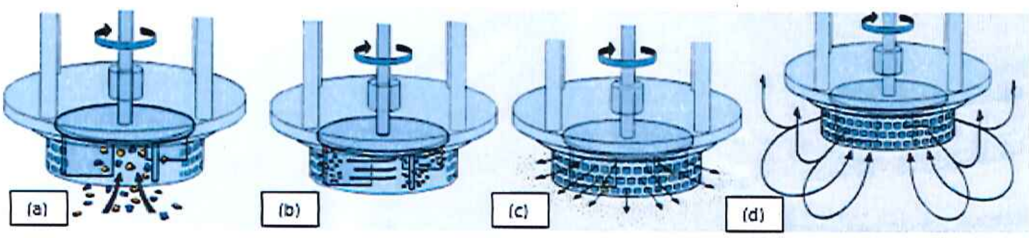

Figure 18: Homogenization processing (a) Stage 1 (b) Stage 2 (c) Stage 3 (d) Stage 4 [52]

2.3. Experimental Procedure

In this study water-in-oil-in-water (W1/O/W2) type of double emulsion was prepared with two emulsifiers via the two-step emulsification technique. For this technique first primary and secondary emulsions were prepared. Then four different types of formulations were coded, respectively, double emulsion (F1) Double Emulsion Incorporated with Aluminum Chlorohydrate (F2), Double Emulsion Incorporated with Lavender Oil (F3), Double Emulsion Incorporated with Aluminum Chlorohydrate and Lavender Oil (F4) as seen in Table 3.

Table 3: Four different type of Double Emulsions, F1, F2, F3, F4

Type of Emulsion	Code
Double Emulsion (W1/O/W2)	F1
Double Emulsion Incorporated with Aluminum Chlorohydrate	F2
Double Emulsion Incorporated with Lavender Oil	F3
Double Emulsion Incorporated with Aluminum Chlorohydrate and Lavender Oil	F4

2.3.1. Preparation of Water in Oil (W1/O) (Inner Phase) Primary Emulsion

In order to prepare W1/O emulsion, firstly 0.5 M AOT in isohexadecane stock solution was prepared by weighing, 11,11 g AOT as emulsifier and 20 ml isohexadecane in a beaker and solution was sonicated until totally dissolved. Secondly, 2 ml of water as an aqueous phase, 10 ml of 0.5 M stock solution and isohexadecane as oil phase was added slowly while stirring up to 50 ml in the volumetric flask, solution became clear at the end of the procedure.

2.3.2. Preparation of Oil in Water (O/W2) (Outer Phase) Secondary Emulsion

In order to prepare O/W2 emulsion, 10 g of isohexadecane as oil phase, 37.5 g water as an aqueous phase and 2.5 g Laureth 4 as an emulsifier were taken in 50 ml beaker separately. Both were put into hot bath, kept at phase inversion temperature of 41°C to put together in beaker then homogenized for 2 minutes at a speed of 10,000 rpm. Then primary emulsion and secondary emulsion was united together in order to obtain a double emulsion as shown in Figure 19.

2.3.3. Preparation of Double Emulsion (W1/O/W2) (F1)

In order to prepare water in oil in water double emulsion (W1/O/W2) as shown in Figure 20, first of all primary (inner phase) emulsion was prepared. Then, to prepare secondary (outer phase) emulsion, 10 g of primary (inner phase) emulsion as oil phase, 37.5 g water as an aqueous phase and 2.5 g of Laureth 4 as emulsifier were taken in 50 ml beaker. Both two beakers were kept at phase inversion temperature of 41°C, then mixed into another beaker and homogenized for 2 minutes at a speed of 10,000 rpm. Finally W1/O/W2 type of double emulsion was obtained and placed into ice bath.

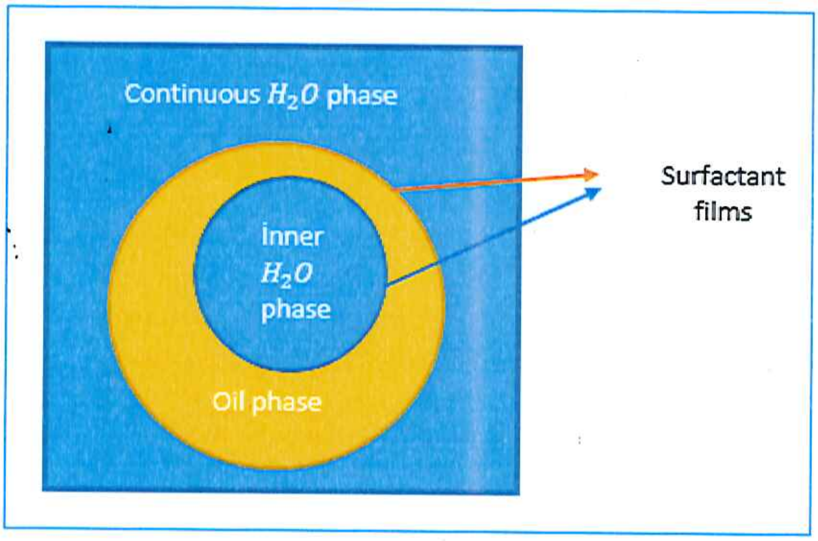

Figure 19: W1/O/W2 Double Emulsion

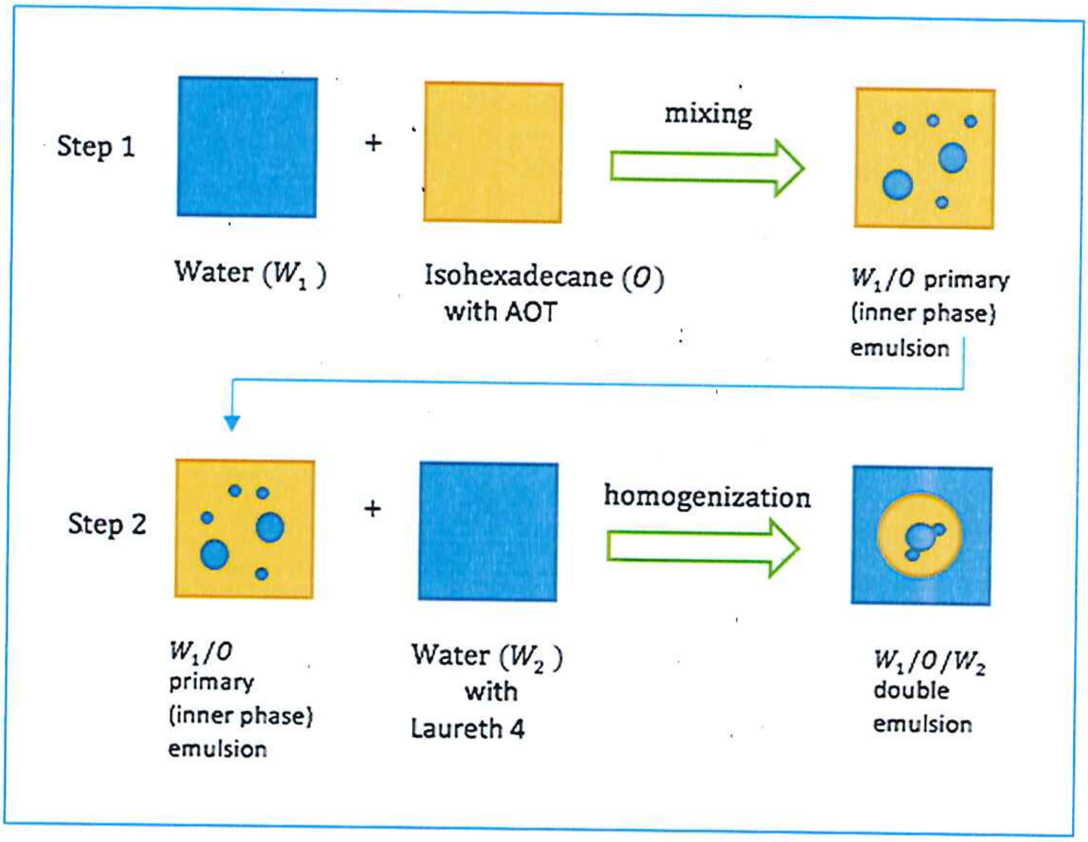

Figure 20: Double Emulsion (F1) Preparation Method

2.3.4. Preparation of Double Emulsion (W1/O/W2) Incorporated with Aluminum Chlorohydrate (F2)

In order to prepare water in oil in water double emulsion (W1/O/W2) with aluminum chlorohydrate as shown in Figure 21, firstly the amount of aluminum chlorohydrate determined by physical appearance, transparency of primary emulsion. Then primary (inner phase) emulsion was prepared by weighing 0.02 g Aluminum Chlorohydrate into aqueous phase and secondary (outer phase) emulsion was prepared by weighing 10 g of primary (inner phase) emulsion as oil phase, 37.5 g water as an aqueous phase and 2.5 g of Laureth 4 as emulsifier in 50 ml beaker. Both two beakers were kept at 41°C then mixed into another beaker and homogenized for 2 minutes at a speed of 10,000 rpm. Finally W1/O/W2 type of double emulsion was obtained and placed into ice bath.

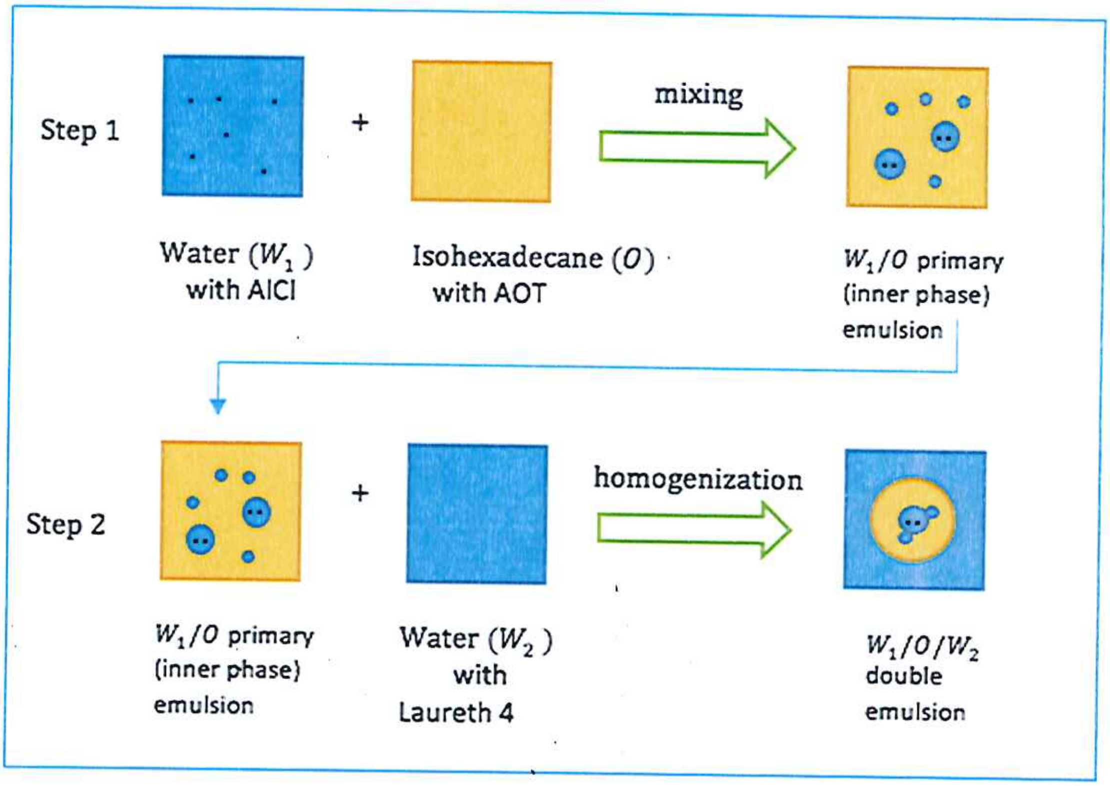

Figure 21: Double Emulsion (F2) Preparation Method

2.3.5. Preparation of Double Emulsion (W1/O/W2) Incorporated with Lavender Oil (F3)

In order to prepare water in oil in water double emulsion (W1/O/W2) with lavender oil as shown in Figure 22, firstly primary (inner phase) emulsion was prepared. Then, to prepare secondary (outer phase) emulsion, 9.5 g of primary (inner phase) emulsion together with 0.5 g of lavender oil as oil phase, 37.5 g water as an aqueous phase and 2.5 g of Laureth 4 as emulsifier were weighed in 50 ml beaker. Both two beakers were kept at 41°C then mixed into another beaker and homogenized for 2 minutes at a speed of 10,000 rpm. Finally W1/O/W2 type of double emulsion was obtained and placed into ice bath.

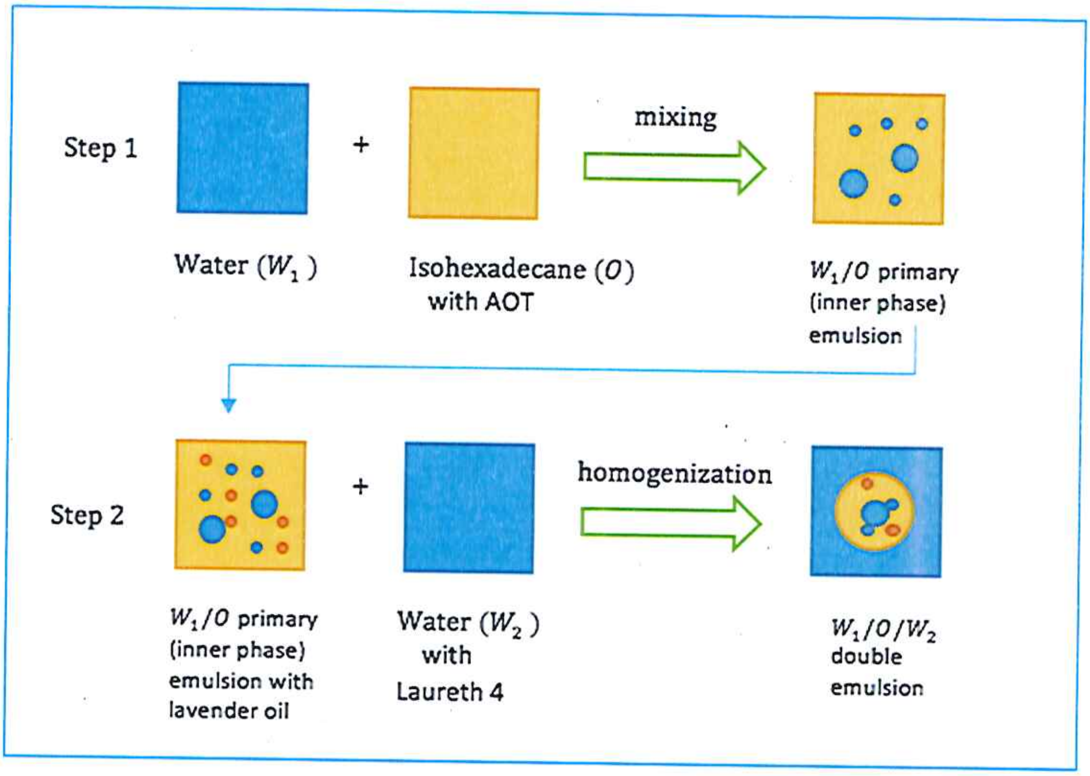

Figure 22: Double Emulsion (F3) Preparation Method

2.3.6.Preparation of Double Emulsion (W1/O/W2) Incorporated Both with Aluminum Chlorohydrate and Lavender Oil (F4)

In order to prepare water-in-oil-in-water double emulsion (W1/O/W2) with aluminum chlorohydrate and lavender oil as shown in Figure 23, firstly primary (inner phase) emulsion was prepared by weighing 0.02 g aluminum chlorohydrate into aqueous phase. Then, to prepare secondary (outer phase) emulsion, 9.5 g of primary (inner phase) emulsion together with 0.5 g of lavender oil as oil phase, 37.5 g water as an aqueous phase and 2.5 g of Laureth 4 as emulsifier were weighed in 50 ml beaker. Both two beakers were kept at 41°C then mixed into another beaker and homogenized for 2 minutes at a speed of 10,000 rpm. Finally W1/O/W2 type of double emulsion was obtained and placed into ice bath.

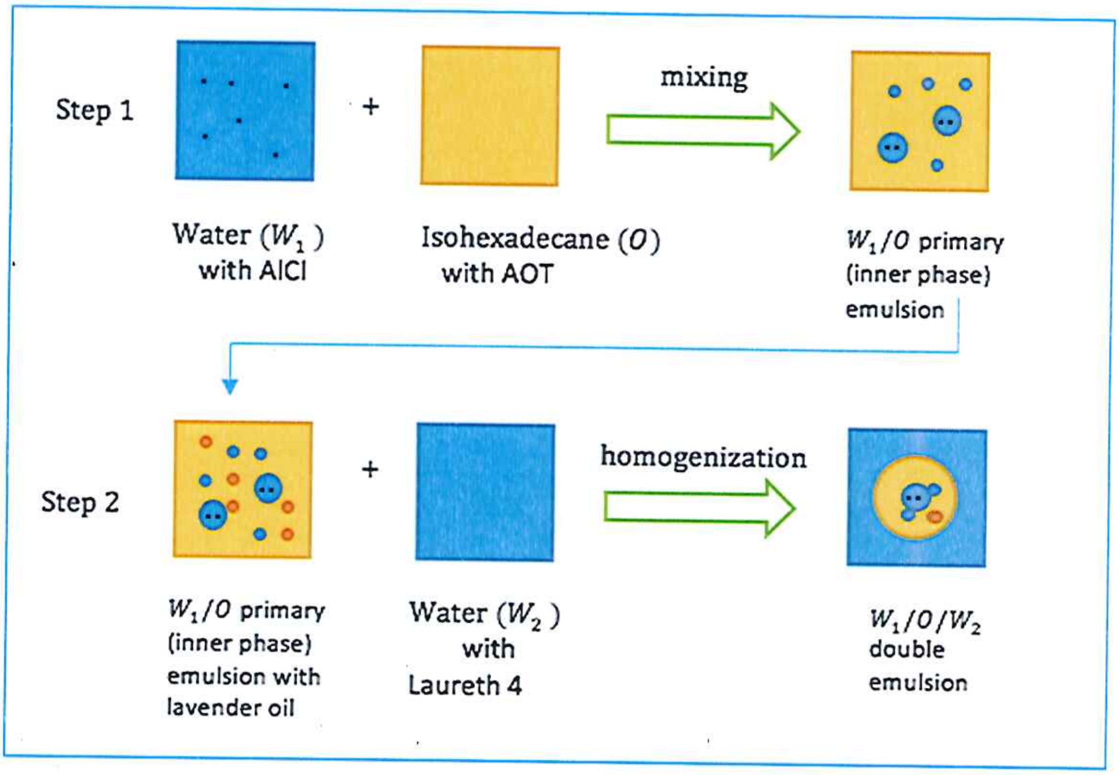

Figure 23: Double Emulsion (F4) Preparation Method

2.4. Migration Of Water Soluble Material

In order to understand how fast the inner water phase migrates to the continuous water phase, the primary (inner phase) emulsion was prepared with 0.3 g of 1 M hydrochloric acid solution. The contiuous water phase contained phenolphtalein as an indicator at pH 11.00 which has a distinct pink color. Therefore if the hydrochloric acid in the inner phase migrates to the continuous water phase, this can be observed as a change in color from pink to white and pH value was obtained as 7 as shown in Figure 24. It can be followed by naked eye and pH measurement over a period of time. To prolong release period between two water phases, respectively 3g, 5g, 7g of viscosity enhancer was added into the W1/O/W2 double emulsion.

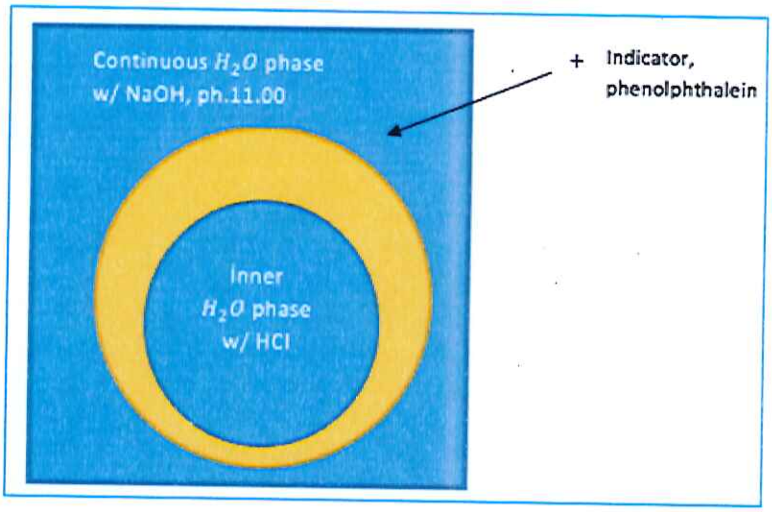

Figure 24: Migration of Water Soluble Material

2.5. Analysis of Double Emulsion

Absorbance of emulsion droplets in formulations of double emulsion were determined using UV Spectrophotometry method at 400 nm. Droplet size and PDI values were examined with Dynamic Light Scattering method. The images of double emulsions with different magnification levels were obtained using optical microscope.

2.5.1. Particle Size Analysis

Particle sizes and distributions of the primary, secondary and double emulsion samples were determined by Dynamic Light Scattering. The measurement parameters were determined according to emulsion structure. Since water phase (W2) of double emulsion was continuous phase, optical properties of dispersant were chosen accordingly with refractive index of 1.33. Considering dispersed phase was oil phase in double emulsion, the optical properties of dispersed (W1/O) phase were chosen accordingly with refractive index of 1.464 and globule absorbance of 0.01.

2.5.2. Optical Imaging

In order to observe the morphological properties of double emulsions, double emulsions were examined under light microscope. Double emulsions were diluted with corresponding W2 phase in order to observe globules clearly. The diluted solutions were mounted evenly onto glass microscope slide as a very thin layer and slide was placed into light microscope. Images were extracted by microscopic camera and analyzed by software named Kameram. The images of double emulsions were taken with four magnification levels (5×, 10×, 20×, and 50×).

3. RESULTS AND DISCUSSION

3.1. Results of Formulation Studies

W/O/W double emulsion was successfully prepared via the two-step emulsification procedure. In the first step, the primary w/o emulsion was formed by incorporating progressively the oily phase containing the lipophilic (AOT) (HLB: 10.5) primary emulsifier into the slowly stirred aqueous phase. The reason why AOT used as lipophillic emulsifier is that it is the most used emulsifier in W/O systems [3]. Water-in-oil (W/O) nanoemulsions had nano-sized water droplets surrounded with surfactant molecules dispersed in oil phase. Due to nanoemulsions with small droplet sizes and narrow globule distributions, the primary W1/O emulsion appeared as transparent, homogeneous [3]. Small droplet size made them stable against sedimentation and creaming processes for a long period of time, hence increasing overall stability of the emulsion.

Generally, droplet size of globules are directly proportional with rotation rate of homogenizer and indirectly proportional with emulsifier ratio. Nanoemulsions can be prepared using lower surfactant concentrations typically between 3 and 10 wt% [5]. In this study maximum amount (10 %) of AOT was used as an emulsifier to prepare nanoemulsion due to low rotation rate of the homogenizer. Nanoemulsions are preferred due to their lower amount of emulsifier usage in contrast to microemulsions with about 20 wt % or higher amount of emulsifier usage. However, nanoemulsions are generally thermodynamically unstable and the size of the droplets tends to increase with time [4].

In the second step, the primary emulsion was added into the secondary emulsion (outer phase) containing the hydrophillic emulsifier (Laureth 4) (HLB: 9.7) at 40 ° C ± 1, at high speed of 10,000 rpm for 2 minutes using homogenizer. The reason why Laureth 4 used as hydrophillic emulsifier is that it is the most used emulsifier in O/W systems [3]. The production of double emulsion usually requires input of high energy with the aids of homogenizers. However in this study, the preparation of double emulsion had not required high input of energy due to lab scale preparation.

Later on, to observe compatibility of two active substances; aluminum chlorohydrate and lavender oil, were incorporated seperately and all together with the obtained W1/O/W2 double emulsion. Firstly optimum W/O/W double emulsion (F2) was prepared with aluminum chlorohydrate as an antiperspirant agent alone as seen in section 2.

In order to obtain the maximum amount of aluminum chlorohydrate physical appearance like transparency and turbidity of primary emulsion was observed and these are reported in Table 4. According to the results, transparent appearance was observed with a maximum loading of 0.02 g aluminum chlorohydrate in 1 ml water.

Table 4: Appearance of primary emulsion with different amounts aluminum chlorohydrate

Aluminum Chlorohydrate (g)	Aluminum Chlorohydrate (%)	Appearance
0.1	5	turbid
0.05	2.5	turbid
0.02	1	transparent

The reason why aluminum chlorohydrate has chosen to be used in this study is that antiperspirant salts are effective, however, can cause skin irritation in sensitive individuals. There are many obvious advantages in microencapsulating antiperspirant salts. Also the conventional antiperspirant formulation on the market contains high amount up to %10. For that reason, in this study aluminum chlorohydrate was encapsulated so, it was used 1:10 times lower amount of active in conventional antiperspirant formulation on the market.

However, antiperspirant salts like aluminum chlorohydrate are difficult to encapsulate due to their acidic nature. Up until now it has been found that most antiperspirant salts rapidly degrade or react with the substances used to form the outer shell of the microcapsule. Microcapsules can also be washed away by sweating just as antiperspirants salts, so a means of keeping the microcapsule securely anchored to skin is also desirable [44]. In this study, aluminum chlorohydrate is water soluble but in order to encapsulate it we would like aluminum chlorohydrate to be in the aqueous phase inside of inner phase instead of being dispersed in the continuous water phase. So, as mentioned above acidic properties of aluminum chlorohydrate has overcome by preparing a double emulsion with lower amount of aluminum chlorohydrate. Final pH of our double emulsion (F2) containing aluminum chlorohydrate (1%) was found to be pH. 5.5 which is suitable for skin applications.

Secondly, optimum W/O/W double emulsion was prepared with lavender oil (F3) itself as seen in section 2, Figure 22. The reason why lavender oil has chosen to be used in this study is that essential oils also have antimicrobial activity and gives pleasent odor. Essential oils are also so effective, however, can cause skin irritation too. As like antiperspirant salts, they are subjected to environmental deterioration by heat, humidity, light, and oxygen. Micro or nanoencapsulation, is a technique which allows isolation of flavours from their environment and controles their release, so securing a long shelf life. Finally, optimum W1/O/W2 double emulsion (F4) was successfully prepared with combination of both aluminum chlorohydrate and lavender oil as seen in Figure 2.11.

A unique property of W1/O/W2 double emulsions compared to simple W1/O emulsion is the diffusion of water through the oil phase because of unbalanced osmotic pressures between the internal and external aqueous phase. The oil layer acts as a membrane separating these two aqueous phases. Polar molecules dissolved in either the internal aqueous phase or the external continuous aqueous phase can pass through the oil layer by diffusion because of the concentration gradient. The aim is that the aluminum chlorohydrate formulated in the inner phase of the double emulsion stays there or is slowly released for the final product to show desired antiperspirant properties. To test this, a new experiment is designed and named as the migration of water soluble material from inner aqueous phase to the continuous phase as mentioned in section 2.

Migration over time represented by Figure 25. from left to right, glass bottles contain following; double emulsion with sodium hydroxide and phenolphtalein in first bottle; double emulsion with sodium hydroxide, phenolphtalein and hydrogen chloride in second bottle; double emulsion with sodium hydroxide, phenolphtalein, hydrogen chloride and 3g of viscosity enhancer in third bottle; double emulsion with sodium hydroxide, phenolphtalein, hydrogen chloride and 5g of viscosity enhancer in fourth bottle and double emulsion with sodium hydroxide, phenolphtalein, hydrogen chloride and 7g of viscosity enhancer in fifth bottle respectively.

It was seen that the two phases were migrated in 12 hours. This was too short for our desired target. To prolong the release period between two water phases, viscosity enhancer, Rheoluxe® 812, was added into the W1/O/W2 double emulsion. When 3g of Rheoluxe® 812 was added double emulsion turned from distinct pink color to white in 24 hours. But addition of 5g and 7g of Rheoluxe® 812 has prolonged the duration of migration in 36 hours and 48 hours respectively as seen in Table 5. As a result, it was clearly observed that incorparation of viscosity enhancer was delayed the migration. Due to the increased amount of viscosity enhancer, the migration rate was slowed down, improving the stability.

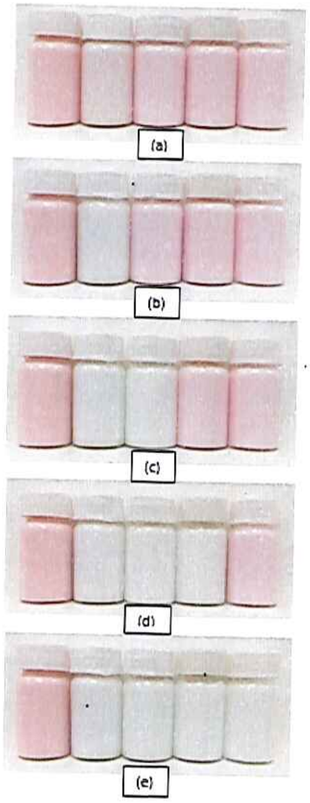

Figure 25. Representation of Migration over time (a) when phases were just combined together (b) after 12 hours (c) after 24 hours (d) after 36 hours (e) after 48h

Table 5: Viscosity and Duration of Migration of Double emulsions

Viscosity enhancer (%)	Viscosity (cp)	Duration of Migration (h)
3	6.000	24
5	15.200	36
7	28.000	48

3.2. Results of Characterization of Formulations of Double Emulsion

Absorbance of formulations of double emulsion, droplet size and PDI values were evaluated with UV Spectrophotometry and Dynamic Light Scattering method as mentioned in Section 2.

3.2.1. Results of Particle Size Analysis

Absorbance values of formulations of double emulsions were tabulated in Table 6. For the duration of 13 days (Time period, 1st, 2nd, 5th, 7th, 13th day) according to absorbance results, almost same values were obtained suggesting that the nanoemulsions remained stable in this time period as shown in Figure 26. Absorbance values of F3 are slighty difference from the other formulations, from 0.694 to 1.562, as can be seen in Table 6.

Table 6: Absorbance values of formulations of double emulsion

Day	F1(nm)	F2(nm)	F3(nm)	F4(nm)
1	0.446	0.493	0.694	0.722
3	0.447	0.551	1.104	0.755
7	0.453	0.490	1.387	0.710
13	0.444	0.541	1.562	0.619

1:1000 dilution, 400 λ (nm)

Since water phase (W2) of double emulsion was the continuous phase, optical properties of dispersant were chosen accordingly with refractive index of 1.33. Considering that dispersed phase to be the was oil phase in double emulsion, the optical properties of dispersed (W1/O) phase were chosen accordingly with refractive index of 1.464 and globule absorbance of 0.01.

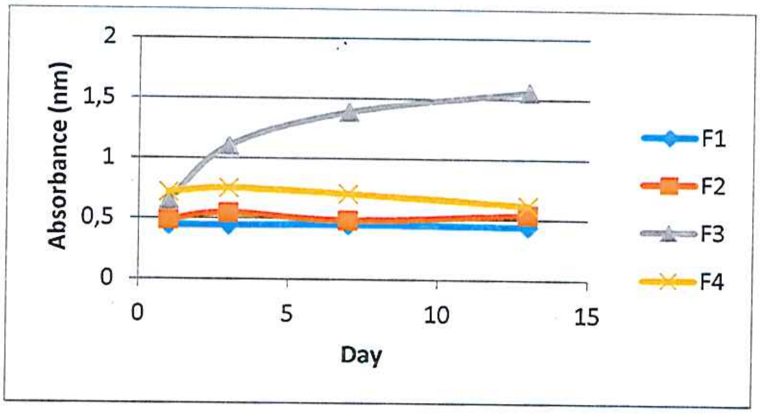

Figure 26. Absorbance vs. day graph

Table 7: Particle Size and size distribution of Double Emulsions over a 13-d period

Time (d)	F1		F2		F3		F4	
	Size (nm)	PDI*	Size (nm)	PDI*	Size (nm)	PDI*	Size (nm)	PDI*
1	-		-		-		-	
3	78.16 ± 39.39	0.249	55.3 ± 44.24	0.333	98.15 ± 45.50	0.368	50.38 ± 25.58	0.346
7	91.28 ± 48.53	0.186	97.81 ± 44.44	0.236	93.22 ± 41.21	0.238	78.31 ± 40.13	0.362
13	104.8 ± 52.97	0.193	118.1 ± 46.94	0.187	155.0 ± 50.71	0.203	117.2 ± 58.89	0.238

*: Poly Dispersity Index

Particle size of double emulsions is the most important parameter since it affects appearance, stability, texture and odour of emulsion. In this study, particle size and distribution have been monitored during thirteen day time period.

The size of formulation of double emulsion F1 obtained, ranged from 78.16 ± 39.39 to 104.8 ± 52.97. In this study, there was no clear particle size difference for double emulsion F1, even identical particle size of double emulsion were observed as can be seen in Figure 27. PDI generally revealed size distribution of dispersion as shown in Figure 28. PDI values were obtained less than 0.4. This was shown a homogenous particle size distribution for all double emulsion formulations.

Time-course stability has shown that particle size of F4 slightly increased from 50.38 ± 25.58 to 117.2 ± 58.89. Instead, increment in particle size was noticed for double emulsion F1 which was comparable to that without the addition of aluminum chlorohydrate and lavender oil. PdI values of F3 were shown good result meaning there was no attaractive and repulsive forces in dispersed system so the slight difference in absorbance values were not a big deal. Coalescence risk could be minimized by using less amount of essential oil in F3. Eventually, absorbance and PdI values of F4 were found stable.

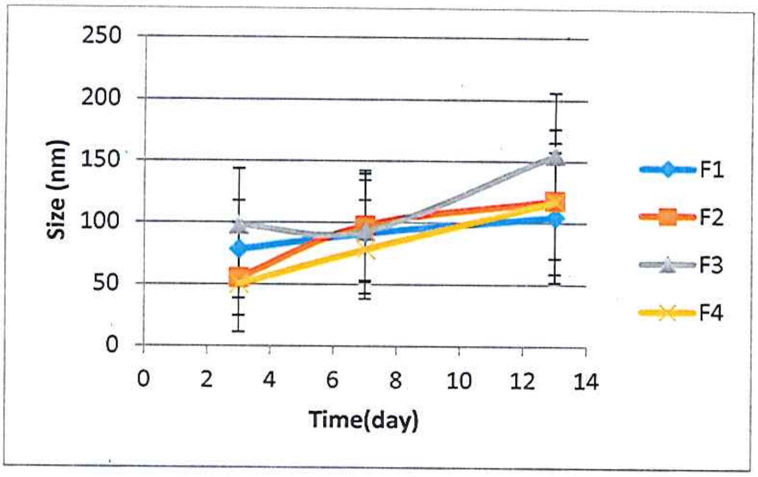

Figure 27. Particle size versus time graph

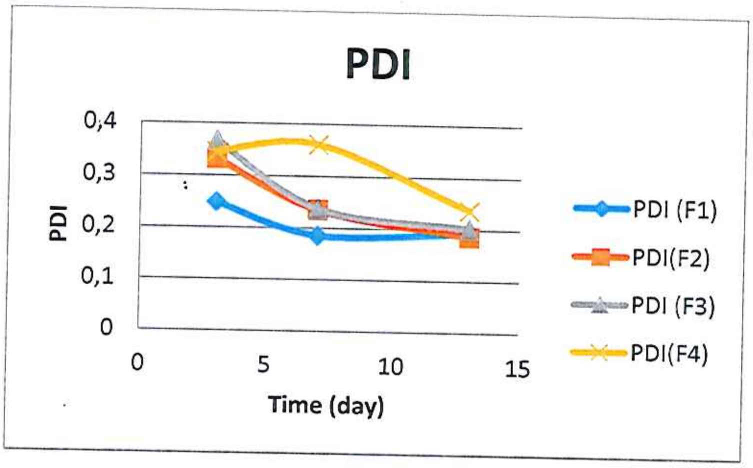

Figure 28. PDI versus time graph

3.2.2. Results of Optical Imaging of the Outer Core

Particle size of the droplets were similar to each other and size distribution was concentrated around 3,8 – 4,8 μm. At the end of the 13th day homogeneous and stable particle size disribution was shown in Figure 29. There were no clear difference between images between 3rd and 13th day for both F1 and F4. At the end of six months microscopy image (Figure 30) was prooved that F4 is stable and homogeneous emulsion.

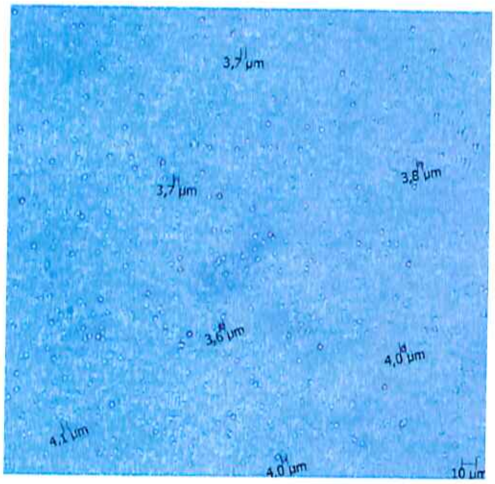

(F1 3rd day)

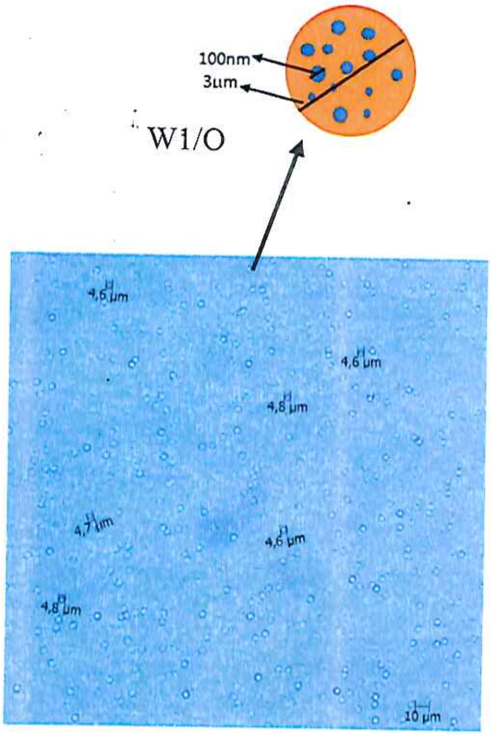

(F1 13th day)

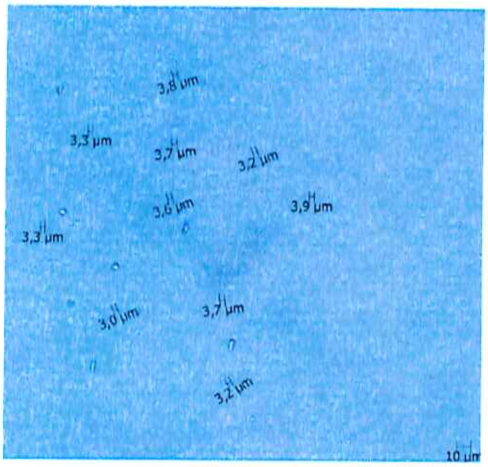

(F4 3rd day)

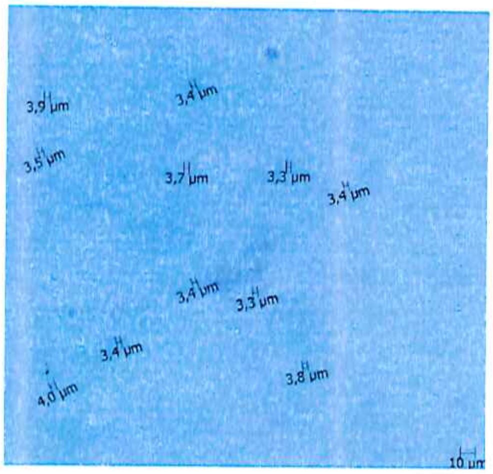

(F4 13th day)

Figure 29: Light Microscopy imaging of F1, F4 double emulsions at 1:100 dilution over a 13 day period

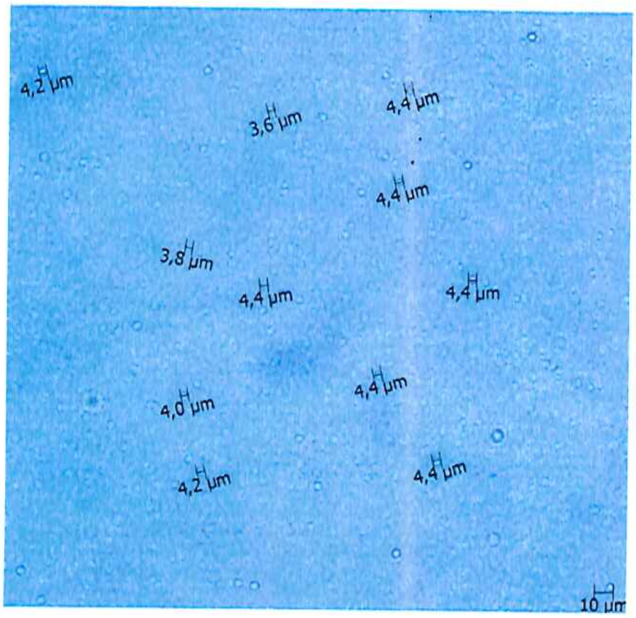

Figure 30. Light Microscopy imaging of F4 double emulsions at 1:100 dilution after six months

The aim is that the aluminum chlorohydrate formulated in the inner phase of the double emulsion stays there or is slowly released for the final product to show desired antiperspirant properties. To test this, migration over time was detected. It was seen that the two phases were migrated in 12 hours. This was too short for our desired target. To prolong the release period between two water phases, 3, 5, 7 grams of viscosity enhancer. As a result, it was clearly observed that incorparation of viscosity enhancer was delayed the migration. Due to increased amount of viscosity enhancer, the migration rate was slowed down, improving the stability. Absorbance of formulations of double emulsion, droplet size and PDI values were evaluated with UV Spectrophotometry and Dynamic Light Scattering method as mentioned in Section 2.

The most used first type water-in-oil-in-water have intensive application area, made up of three phases, where small water droplets are entrapped within larger oil droplets and they are dispersed in continuous water phase. Two types of emulsifiers are used for emulsification of the multiple emulsion system. Lipophilic emulsifier is used for W/O emulsion, hydrophilic emulsifier is used for O/W emulsion. The second type double emulsion named as oil-in-water-in-oil, also made up of three phases, where small oil droplets are entrapped within larger water droplets and they are dispersed in continuous oil phase. Hydrophilic emulsifier is used for O/W emulsion, emulsifier is considered W/O emulsion [27].

One of the main aims of the present work was to establish the relationship between W/O nano-emulsion in W/O/W double emulsion formation and stability with the nature of the phases formed during the emulsification process. Double emulsion have been prepared using the two step emulsification process and the stability has been assessed by determining the changes in droplet size by DLS as a function of time.

In this study, microencapsulation and nanoencapsulation of antiperspirant salts and essential oil also provides controlled release of the internal constituents, hence lengthening the effective period of the antiperspirant. Desirable property of double emulsion is the controlled and triggered release of encapsulated actives (lavender oil as an odor and aluminum chlorohydrate as an antiperspirant compound in cosmetic product). The potential, particularly for cosmetic application of structure that deliver intense burst of flavour under arm or hide the unpleasent odor.

In this study, the aim was that the aluminum chlorohydrate formulated in the inner phase of the double emulsion stays there or is slowly released for the final product to show desired antiperspirant properties. To test this, migration over time was detected. It was seen that the two phases were migrated in 48 hours. To prolong the release period between two water phases, weight of viscosity enhancer can also be increased.

Many studies has shown that the nanoemulsions made with emulsifier mixtures accomplish better by decreasing the rate of Ostwald ripening in emulsions. So, as future work more than one emulsifier in nano emulsion can be used. Also, in usage emulsifiers can be placed with proper ones and the ratio of the emulsifiers can be changed also. The work done in this thesis was a lab scale work. In order to bring this project on to market, research and development level kinetic stability work should be done for future.

In order to see whether there is irritation when product applied to skin or not, patch test could be done. Microbiological testing and challenge tests are also must have ones for the microbiological quality of the product. Lavender oil amount over time in the formulation could be determined by the method GC-MS. In order to prolong migration between phases secondary surfactant, Laureth-4 can be replaced by a different surfactant with an HLB value between 0-10 by improving the shelf life.

5. REFERENCES

1. Hamley, I.W., Introduction to Soft Matter: Polymers, Colloids, Amphiphiles and Liquid Crystals. 2000, Chichester: John Wiley & Sons, Ltd.
2. Duman, G., Pharmaceutical Technology 1: Dosage Forms and Contemporary Practice,2014
3. Barnes, G.T. and I.R. Gentle, Interfacial Science: An Introduction. 2005: Oxford University Press.
4. Atkins, P. and J. de Paula, Atkins' Physical Chemistry, 9th Edition, P. Atkins, Editor. 2010, Oxford University Press
5. Interaction of water and non-polar substances. Available from the New Jersey's Science and Technology University, Federated Departments of Biological Sciences: http: / / newarkbioweb.rutgers.edu / bio301s / lecture%20slides / lec2-1.jpg.
6. Binks, B.P., Chapter 1: Emulsions - Recent Advances in Understanding, in Modern Aspects of Emulsion Science, B.P. Binks, Editor. 1998, The Royal Society of Chemistry: Cambridge.
7. Yuyama, H., et al.., Preparation and analysis of uniform emulsion droplets using SPG membrane emulsification technique. Colloids and Surfaces A: Physicochemical and Engineering Aspects, 2000. 168: p. 159-174.
8. Robins, M.M. and D.J. Hibberd, Emulsion Flocculation and Creaming, in Modern Aspects of Emulsion Science, B.P. Binks, Editor. 1998, The Royal Society of Chemistry: Cambridge.
9. Kabalnov, A.S., Chapter 7: Coalescence in Emulsions, in Modern Aspects of Emulsion Science, B.P. Binks, Editor. 1998, The Royal Society of Chemistry: Cambridge.
10. S.F. Wong et al. / Journal of Petroleum Science and Engineering 135 (2015) 498–504
11. Forgiarini, A., et al.., Formation of Nano-Emulsions by Low-Energy Emulsification Methods at Constant Temperature. Langmuir, 2001. 17: p. 2076-2083.
12. Shinoda, K. and Friberg, S. (1975) Adv. Colloid Interface Sci., 4, 281.
13. Adamson, A.W. (1969) J. Colloid Interface Sci., 29, 261.3.
14. Kunieda, H. and Shinoda, K. (1980) J. Colloid Interface Sci., 75, 601.
15. T.P. Hoar, J.H. Schulman, Transparent water-in-oil disper- sions: the oleopathic hydro-micelle, Nature 152 (1943) 102– 103.
16. J.H. Schulman, W. Stoeckenius, L.M. Prince, Mechanism of formation and structure

of micro emulsions by electron microscopy, J. Phys. Chem. 63 (1959) 1677–1680.

17. I. Danielsson, B. Lindman, The definition of a microemul- sion, Colloids and Surfaces 3 (1981) 391–392.
18. K. Shinoda, B. Lindman, Organised surfactant systems: microemulsions, Langmuir 3 (1987) 135–149.
19. L.M. Prince, A theory of aqueous emulsion. I. Negative interfacial tension at the oil / water interface, J. Colloid Interface Sci. 23 (1967) 165–173.
20. D. Fennell Evans, H. Wennerstrom, Micro- and macro- emulsions, in: The Colloidal Domain — Where Physics, Chemistry, Biology and Technology Meet. 1st Edition, Vol. 1, VCH Publishers, 1994, pp. 451–469.
21. Nakajima, H.; Tomomasa, S.; Okabe, M. Preparation of Nanoemulsions. In Proceedings of First Emulsion Conference, Paris, 1993; EDS: Paris, 1993; Vol. 1, p 1-11/162.
22. D. J. McClements, Soft Matter, 2012, 8, 1719–1729.
23. N. Anton and T. F. Vandamme, Pharm. Res., 2011, 28, 978–985.
24. Izquierdo, P., et al.., Formation and Stability of Nano-Emulsions Prepared Using the Phase Inversion Temperature Method. Langmuir, 2002. 18: p. 26- 30.
25. Morales, D., et al.., A Study of the Relation between Bicontinuous Microemulsions and Oil / Water Nano-emulsion Formation. Langmuir, 2003. 19: p. 7196-7200.
26. Matsumoto, S., and W. Kang, J. Dispersion Science and Technology 10 (4&5) (1989) 455.
27. Matsumoto, S., J. Texture Stud. 17 (1986) 141.
28. Gaonkar, A., US patent number 5,322,595. Assigned to Kraft General Foods Inc. USA (1994b).
29. A.T.FlorenceandD.Whitehill,J.ColloidInterfaceSci., 79 (1981) 243.
30. Kanouni, M., & Rosano, H. L. (2005). 22 - Preparation of Stable Multiple Emulsions as Delivery Vehicles for Consumer Care Products: Study of the Factors Affecting the Stability of the System (w1/o/w2). In M. R. Rosen (Ed.), Delivery System Handbook for Personal Care and Cosmetic Products (pp. 473- 497). Norwich, NY: William Andrew Publishing.
31. Lin, C.-Y., & Wang, K.-H. (2003). The fuel properties of three-phase emulsions as an alternative fuel for diesel engines. Fuel, 82(11), 1367-1375.

32. Aserin, A. (2008). Multiple Emulsion: Technology and Applications: Wiley,pp 85-120.
33. Garti, N., & Aserin, A. (1996). Double emulsions stabilized by macromolecular surfactants. Advances in Colloid and Interface Science, 65(0), 37-69.
34. Sjoblom, J. (2001). Encyclopedic Handbook of Emulsion Technology: Taylor & Francis, pp 601-605.
35. Davis S., Chemistry and Industry 3 (1981) 683.
36. Engel, R., S. Riggi and J. Fahrenbach, Nature 219 (1968) 856.
37. Matsumoto, S., and M. Kohda, in: Food Texture and Rheology. Ed. by P. Sherman, pp. 437. Academic Press, London 1979.
38. Matsumoto, S., in: Macro and Micro Emulsions: Theory and Applications. Ed. by D. O. Shah, pp. 272, 415. ACS Symposium Series, ACS, Washington D.C. 1985.
39. Takahashi, Y., S. Aizawa, S. Tamai, T. Yoshida and T. Takahashi, U.S. patent number 4,632,840. Assigned to Meiji Milk Products Company Limited, Tokyo, Japan (1986).
40. Bams, G., U.S. patent number 4,650,690. Assigned to Thomas J Lipton Inc, Englewood Cliffs, N.J. (1987).
41. Tadros, T. F. (2013). Emulsion Formation, Stability, and Rheology Emulsion Formation and Stability (pp. 1-75): Wiley-VCH Verlag GmbH & Co. KGaA.
42. Dickinson, E. (2010). Double Emulsions Stabilized by Food Biopolymers. Food Biophysics, 6(1), 1-11.
43. Hyperhidrosis: Anatomy, Pathophysiology and Treatment with Emphasis on the Role of Botulinum Toxins
44. https://www.google.com/patents/US20030206973
45. Principles and applications of UV-visible spectroscopy
46. Virginia Tech, ''The Optical Microscope'', http://www.sv.vt.edu/classes/MSE2094_NoteBook/96ClassProj/experimental/optical.html [retrieved 9 August 2014].
47. Figure. (http://infohost.nmt.edu/~klathrop/Microscopes.htm)
48. http://216.92.172.113/courses/phys39/light%20scattering/DLS%20LabView%20UCSD.pdf
49. http://www.ipc.uni-stuttgart.de/AKStubenrauch/research/equipment/lightscattering/
50. (ftp://ftp.unicauca.edu.co/Facultades/FIET/DEIC/Materias/Instrumentacion%20Industrial/Instrument_Engineers__Handbook_-_Process_Measurement_and_Analysis/Instrument%20Engineers%27%20Handbook

%20-%20Process%20Measurement%20and%20Analysis/1083ch8_63.pdf)
51. Food Structure and Functionality Laboratories
52. Department of Food Science & Biotechnology University of Hohenheim Garbenstrasse 21, 70599 Stuttgart, Germany

APPENDIX A

			Diam. (nm)	% Intensity	Width (nm)
Z-Average (d.nm):	148.1	Peak 1:	164.3	95.3	83.92
PdI:	0.324	Peak 2:	4990	4.7	614.8
Intercept:	0.954	Peak 3:	0.000	0.0	0.000
Result quality :	Good				

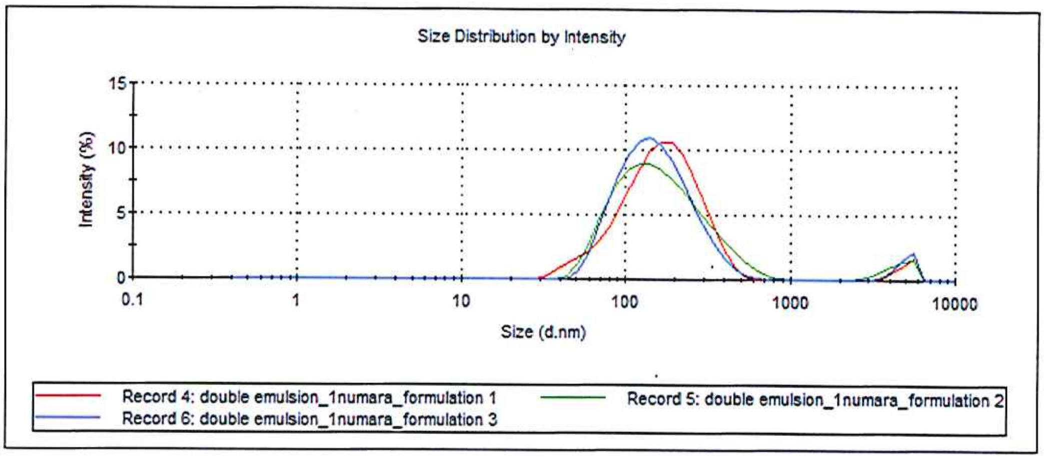

Figure A1: Size Distribution by Intensity of double emulsion at 1:1000 dilution (4.7.2017)

			Diam. (nm)	% Intensity	Width (nm)
Z-Average (d.nm):	167.5	Peak 1:	212.1	98.5	117.9
PdI:	0.243	Peak 2:	4925	1.5	655.3
Intercept:	0.945	Peak 3:	0.000	0.0	0.000
Result quality :	Good				

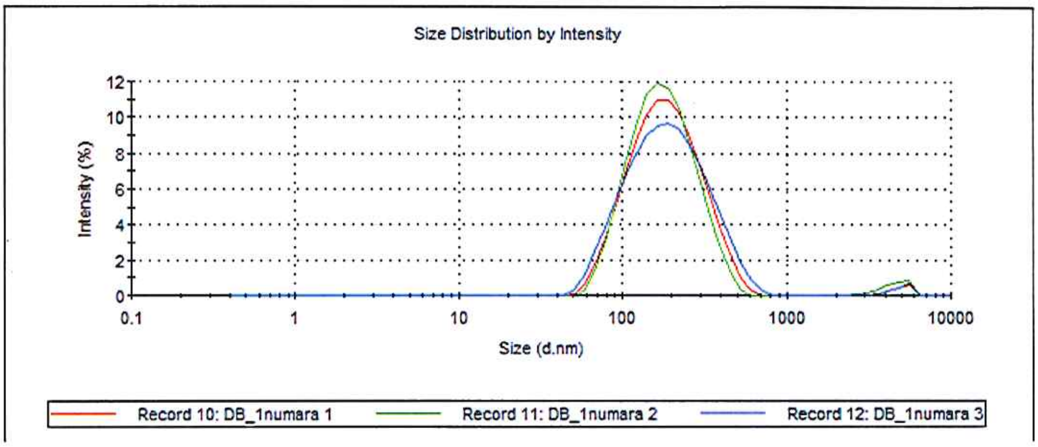

Figure A2: Size Distribution by Intensity of double emulsion at 1:1000 dilution (4.11.2017)

			Diam. (nm)	% Intensity	Width (nm)
Z-Average (d.nm):	155.1	Peak 1:	183.3	97.5	94.11
PdI:	0.249	Peak 2:	4972	2.5	622.0
Intercept:	0.938	Peak 3:	0.000	0.0	0.000
Result quality :	Good				

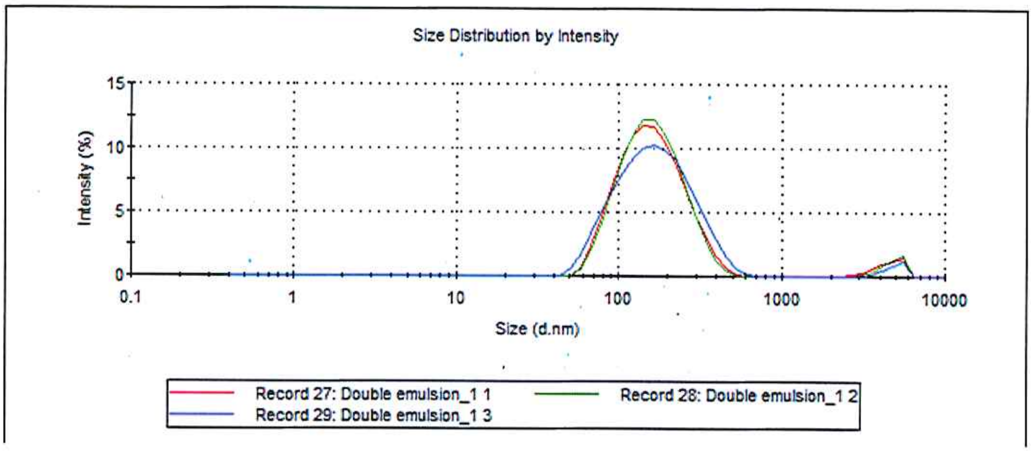

Figure A3: Size Distribution by Intensity of double emulsion at 1:1000 dilution (4.17.2017)

			Diam. (nm)	% Intensity	Width (nm)
Z-Average (d.nm):	151.8	Peak 1:	175.2	98.3	74.15
PdI:	0.198	Peak 2:	4811	1.7	718.9
Intercept:	0.948	Peak 3:	0.000	0.0	0.000
Result quality :	Good				

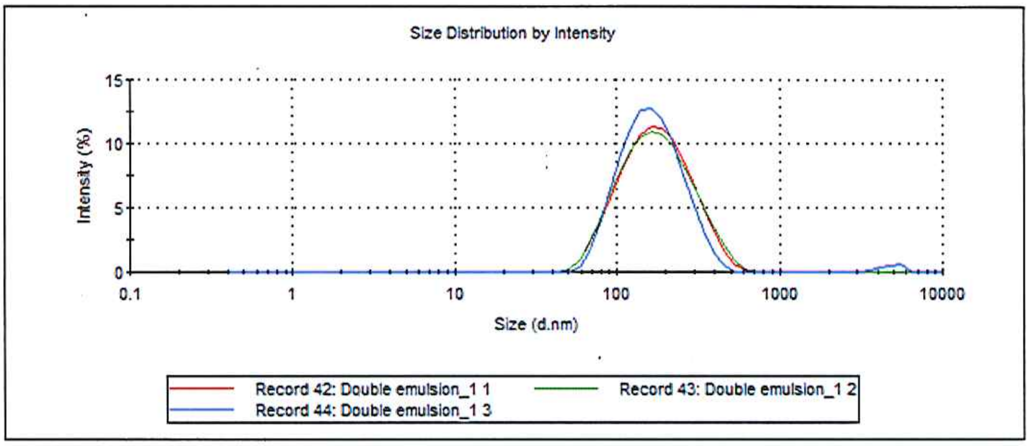

Figure A4: Size Distribution by Intensity of double emulsion at 1:1000 dilution (4.19.2017)

			Diam. (nm)	% Intensity	Width (nm)
Z-Average (d.nm): 153.4		Peak 1:	192.7	100.0	94.36
PdI: 0.186		Peak 2:	0.000	0.0	0.000
Intercept: 0.943		Peak 3:	0.000	0.0	0.000
Result quality : Good					

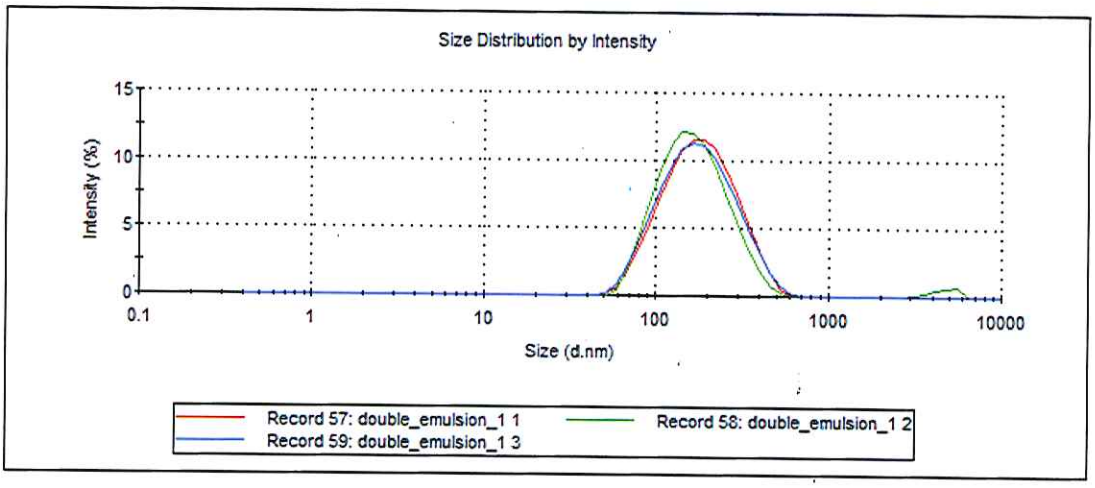

Figure A5: Size Distribution by Intensity of double emulsion at 1:1000 dilution (4.21.2017)

			Diam. (nm)	% Intensity	Width (nm)
Z-Average (d.nm): 162.8		Peak 1:	194.9	100.0	90.06
PdI: 0.193		Peak 2:	0.000	0.0	0.000
Intercept: 0.951		Peak 3:	0.000	0.0	0.000
Result quality : Good					

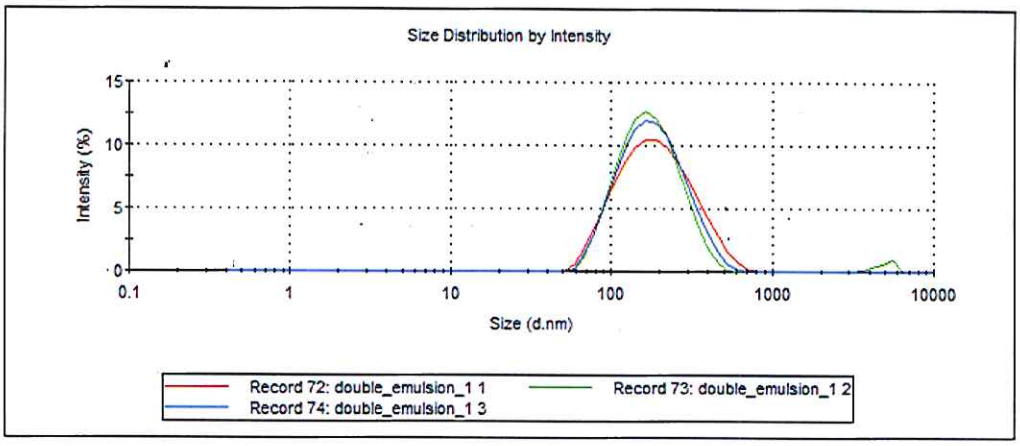

Figure A6: Size Distribution by Intensity of double emulsion at 1:1000 dilution (4.27.2017)

			Diam. (nm)	% Intensity	Width (nm)
Z-Average (d.nm):	179.8	Peak 1:	201.3	100.0	65.13
PdI:	0.109	Peak 2:	0.000	0.0	0.000
Intercept:	0.953	Peak 3:	0.000	0.0	0.000
Result quality :	Good				

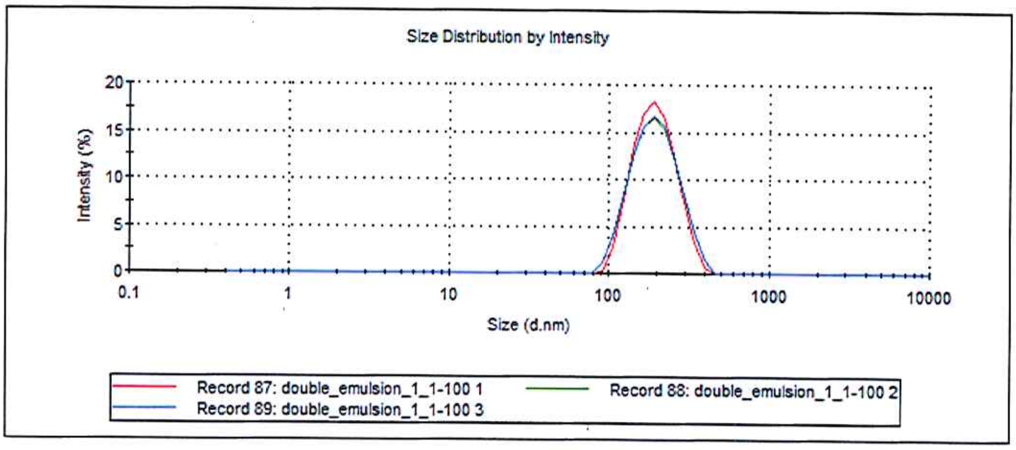

Figure A7: Size Distribution by Intensity of double emulsion at 1:100 dilution (5.10.2017)

APPENDIX B

			Diam. (nm)	% Number	Width (nm)
Z-Average (d.nm):	148.1	Peak 1:	77.09	100.0	35.49
PdI:	0.324	Peak 2:	0.000	0.0	0.000
Intercept:	0.954	Peak 3:	0.000	0.0	0.000
Result quality :	Good				

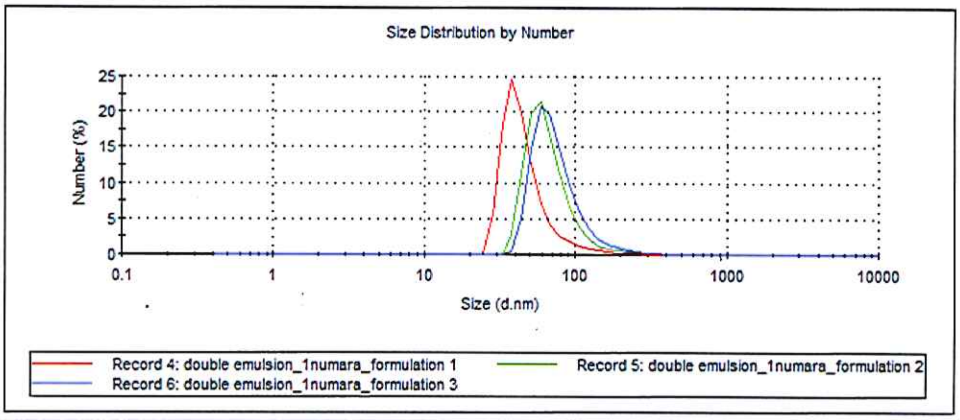

Figure B1: Size Distribution by Number of double emulsion at 1:1000 dilution (4.7.2017)

			Diam. (nm)	% Number	Width (nm)
Z-Average (d.nm):	155.1	Peak 1:	78.16	100.0	39.39
PdI:	0.249	Peak 2:	0.000	0.0	0.000
Intercept:	0.938	Peak 3:	0.000	0.0	0.000
Result quality :	Good				

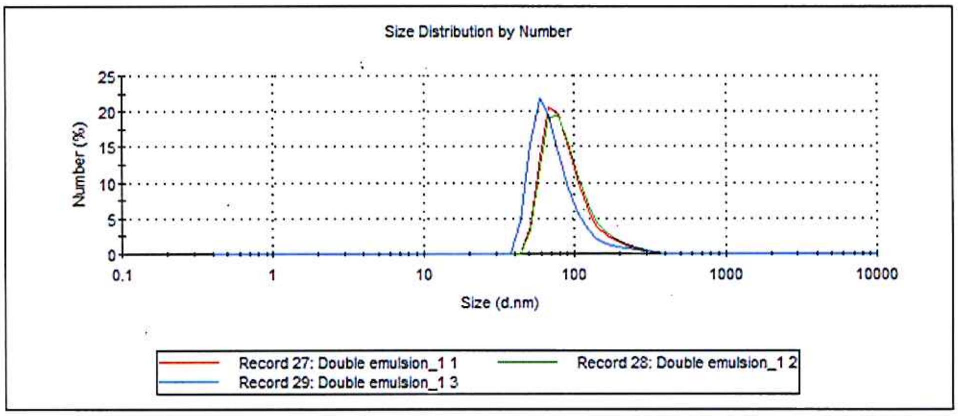

Figure B2: Size Distribution by number of double emulsion at 1:1000 dilution (4.17.2017)

			Diam. (nm)	% Number	Width (nm)
Z-Average (d.nm):	151.8	Peak 1:	100.6	100.0	46.81
PdI:	0.198	Peak 2:	0.000	0.0	0.000
Intercept:	0.948	Peak 3:	0.000	0.0	0.000
Result quality :	Good				

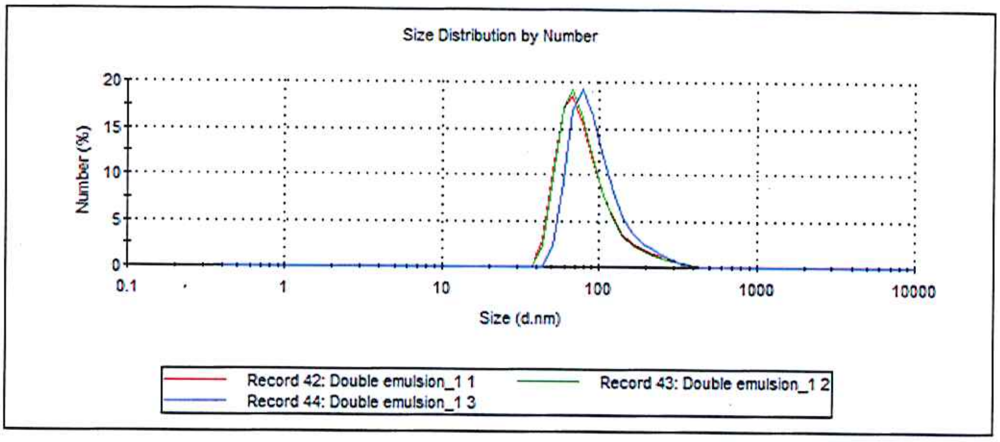

Figure B3: Size Distribution by number of double emulsion at 1:1000 dilution (4.19.2017)

			Diam. (nm)	% Number	Width (nm)
Z-Average (d.nm):	153.4	Peak 1:	91.28	100.0	48.53
PdI:	0.186	Peak 2:	0.000	0.0	0.000
Intercept:	0.943	Peak 3:	0.000	0.0	0.000
Result quality :	Good				

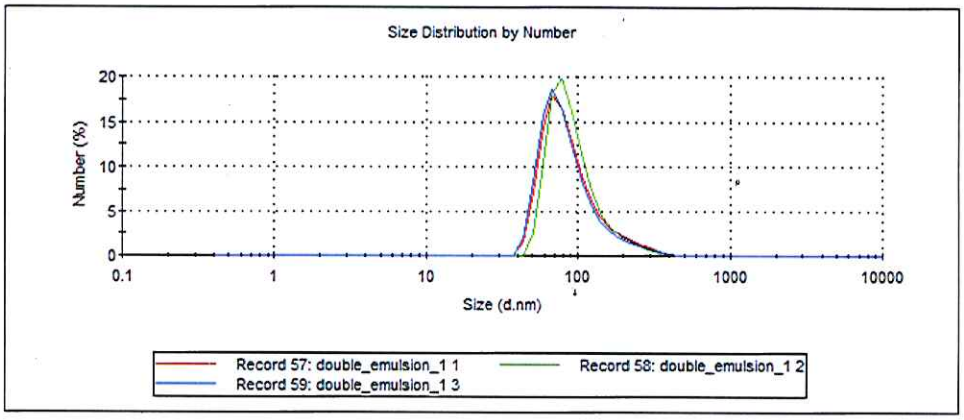

Figure B4: Size Distribution by number of double emulsion at 1:1000 dilution (4.21.2017)

			Diam. (nm)	% Number	Width (nm)
Z-Average (d.nm):	162.8	Peak 1:	104.8	100.0	52.97
PdI:	0.193	Peak 2:	0.000	0.0	0.000
Intercept:	0.951	Peak 3:	0.000	0.0	0.000

Result quality : Good

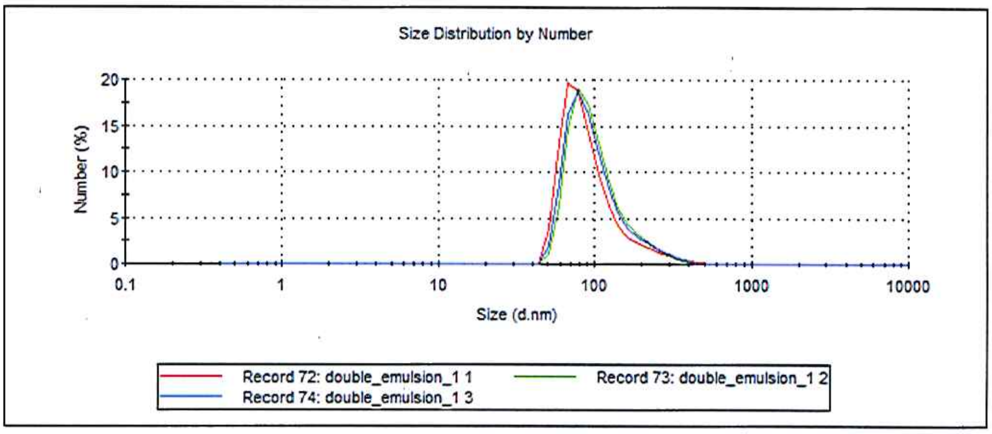

Figure B5: Size Distribution by number of double emulsion at 1:1000 dilution (4.27.2017)

			Diam. (nm)	% Number	Width (nm)
Z-Average (d.nm):	179.8	Peak 1:	170.5	100.0	59.88
PdI:	0.109	Peak 2:	0.000	0.0	0.000
Intercept:	0.953	Peak 3:	0.000	0.0	0.000

Result quality : Good

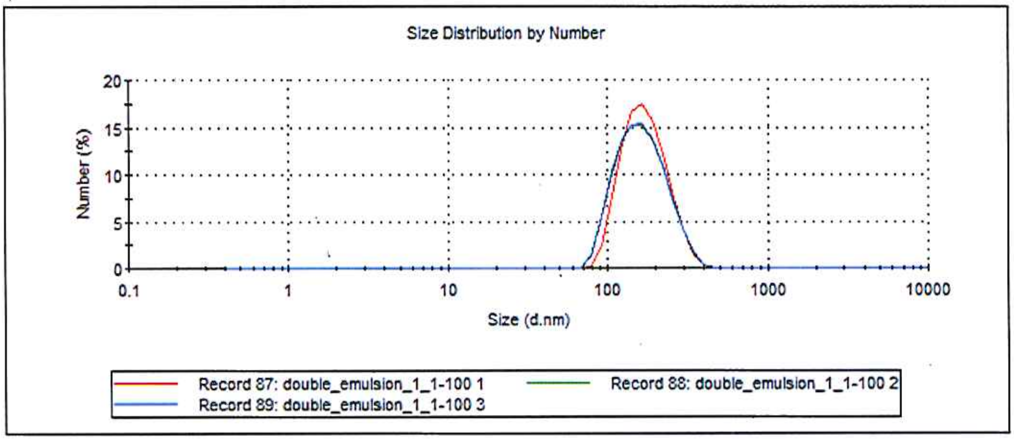

Figure B6: Size Distribution by number of double emulsion at 1:100 dilution (5.10.2017)

APPENDIX C

			Diam. (nm)	% Intensity	Width (nm)
Z-Average (d.nm):	221.6	Peak 1:	258.6	94.9	134.4
PdI:	0.333	Peak 2:	4805	5.1	724.8
Intercept:	0.858	Peak 3:	0.000	0.0	0.000
Result quality :	Good				

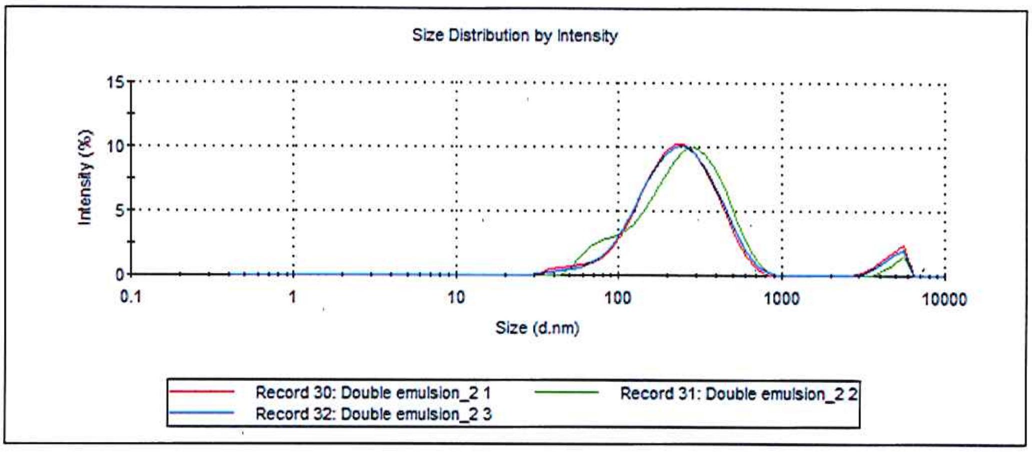

Figure C1: Size Distribution by Intensity of double emulsion with aluminum chlorohydrate at 1:1000 dilution (4.17.2017)

			Diam. (nm)	% Intensity	Width (nm)
Z-Average (d.nm):	170.1	Peak 1:	210.8	90.7	130.1
PdI:	0.422	Peak 2:	4181	9.3	1032
Intercept:	0.947	Peak 3:	0.000	0.0	0.000
Result quality :	Good				

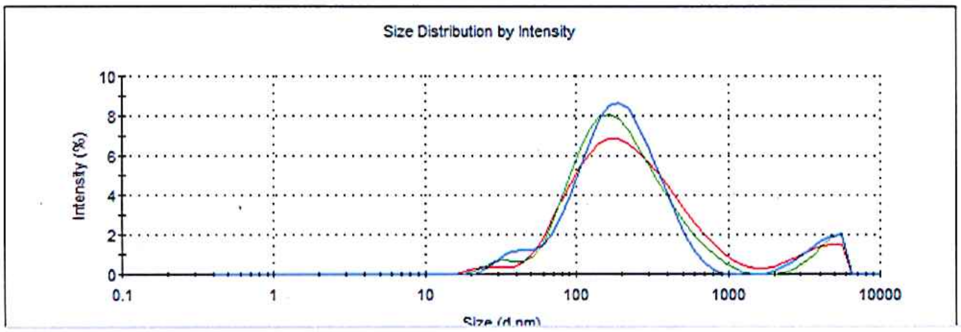

Figure C2: Size Distribution by Intensity of double emulsion with aluminum chlorohydrate at 1:1000 dilution (4.11.2017)

			Diam. (nm)	% Intensity	Width (nm)
Z-Average (d.nm):	152.7	Peak 1:	174.8	100.0	63.05
PdI:	0.121	Peak 2:	0.000	0.0	0.000
Intercept:	0.936	Peak 3:	0.000	0.0	0.000
Result quality :	Good				

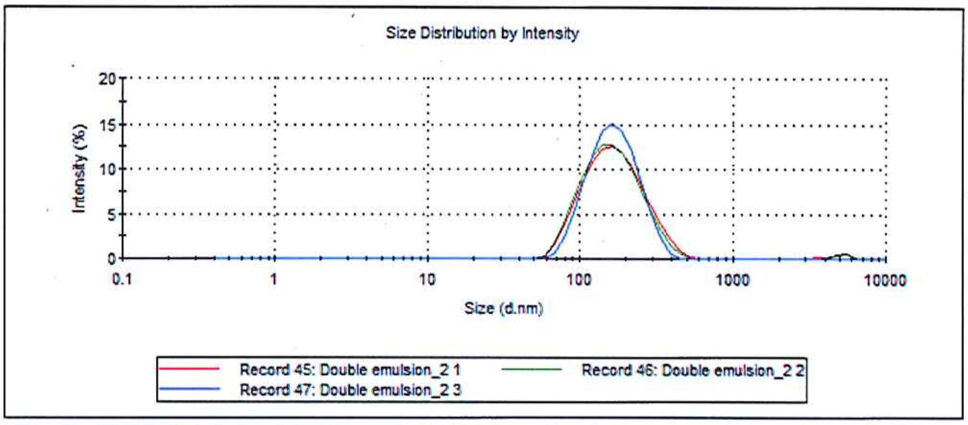

Figure C3: Size Distribution by Intensity of double emulsion with aluminum chlorohydrate at 1:1000 dilution (4.19.2017)

			Diam. (nm)	% Intensity	Width (nm)
Z-Average (d.nm):	152.7	Peak 1:	178.7	100.0	73.18
PdI:	0.132	Peak 2:	0.000	0.0	0.000
Intercept:	0.930	Peak 3:	0.000	0.0	0.000
Result quality :	Good				

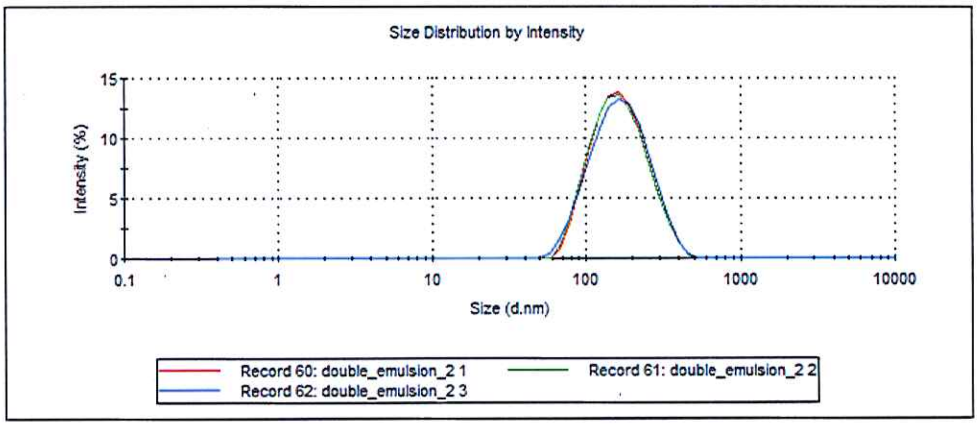

Figure C4: Size Distribution by Intensity of double emulsion with aluminum chlorohydrate at 1:1000 dilution (4.21.2017)

			Diam. (nm)	% Intensity	Width (nm)
Z-Average (d.nm):	159.1	Peak 1:	170.7	97.0	62.30
PdI:	0.187	Peak 2:	4689	3.0	785.1
Intercept:	0.936	Peak 3:	0.000	0.0	0.000
Result quality :	Good				

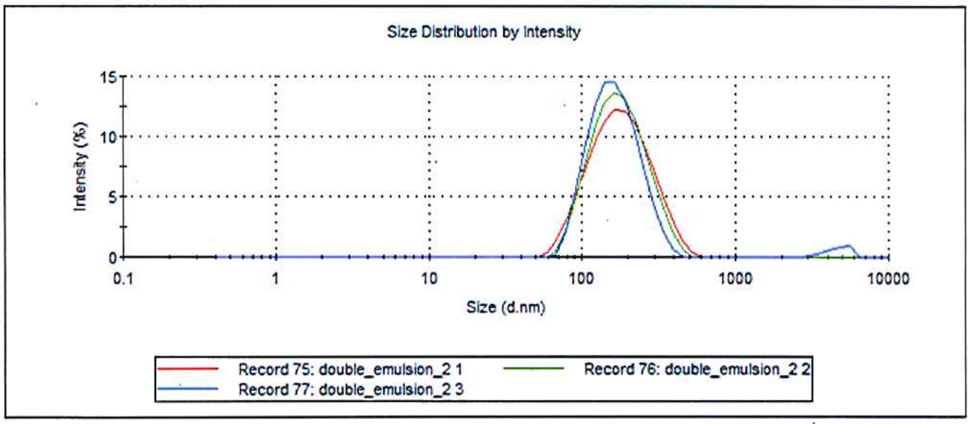

Figure C5: Size Distribution by Intensity of double emulsion with aluminum chlorohydrate at 1:1000 dilution (4.27.2017)

APPENDIX D

			Diam. (nm)	% Number	Width (nm)
Z-Average (d.nm):	221.6	Peak 1:	55.33	100.0	44.24
PdI:	0.333	Peak 2:	0.000	0.0	0.000
Intercept:	0.858	Peak 3:	0.000	0.0	0.000
Result quality :	Good				

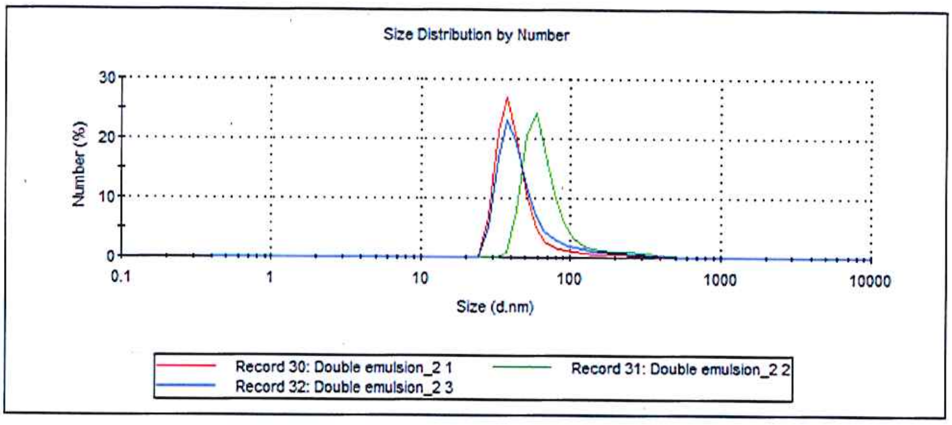

Figure D1: Size Distribution by number of double emulsion with aluminum chlorohydrate at 1:1000 dilution (4.17.2017)

			Diam. (nm)	% Number	Width (nm)
Z-Average (d.nm):	152.7	Peak 1:	117.4	100.0	49.53
PdI:	0.121	Peak 2:	0.000	0.0	0.000
Intercept:	0.936	Peak 3:	0.000	0.0	0.000
Result quality :	Good				

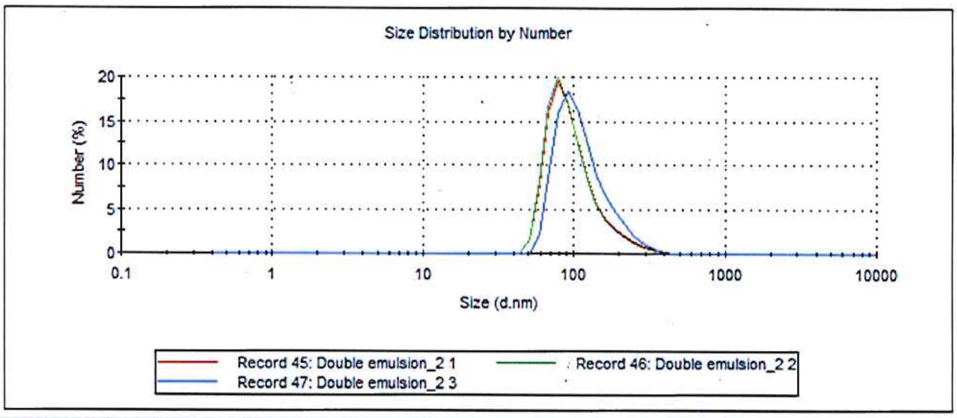

Figure D2: Size Distribution by number of double emulsion with aluminum chlorohydrate at 1:1000 dilution (4.19.2017)

			Diam. (nm)	% Number	Width (nm)
Z-Average (d.nm):	192.6	Peak 1:	97.81	100.0	44.44
PdI:	0.236	Peak 2:	0.000	0.0	0.000
Intercept:	0.941	Peak 3:	0.000	0.0	0.000

Result quality : Good

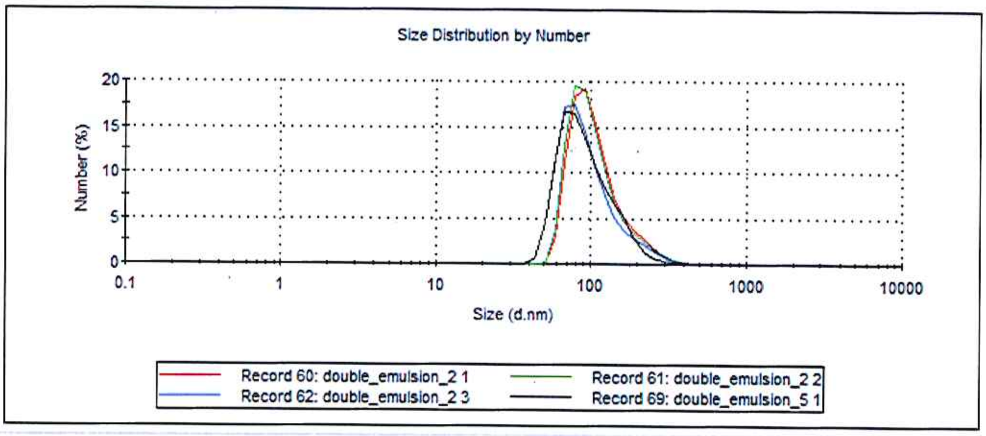

Figure D3: Size Distribution by number of double emulsion with aluminum chlorohydrate at 1:1000 dilution (4.21.2017)

			Diam. (nm)	% Number	Width (nm)
Z-Average (d.nm):	159.1	Peak 1:	118.1	100.0	46.94
PdI:	0.187	Peak 2:	0.000	0.0	0.000
Intercept:	0.936	Peak 3:	0.000	0.0	0.000

Result quality : Good

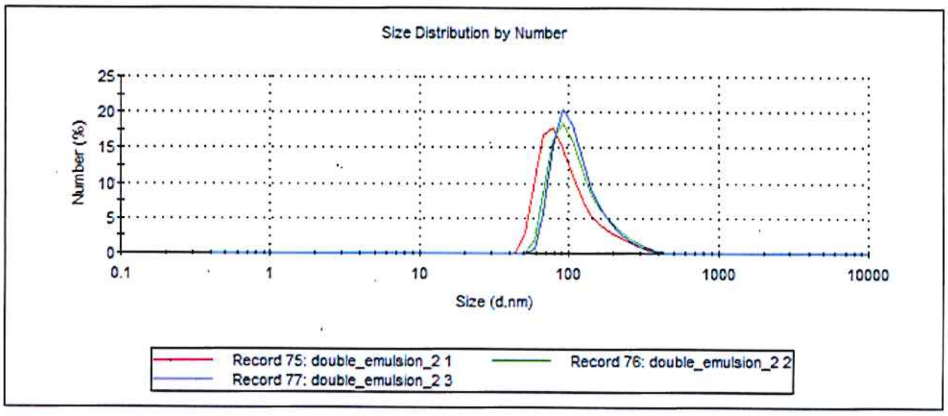

Figure D4: Size Distribution by number of double emulsion with aluminum chlorohydrate at 1:1000 dilution (4.27.2017)

APPENDIX E

			Diam. (nm)	% Intensity	Width (nm)
Z-Average (d.nm):	117.1	Peak 1:	135.6	100.0	57.05
PdI:	0.149	Peak 2:	0.000	0.0	0.000
Intercept:	0.939	Peak 3:	0.000	0.0	0.000
Result quality :	Good				

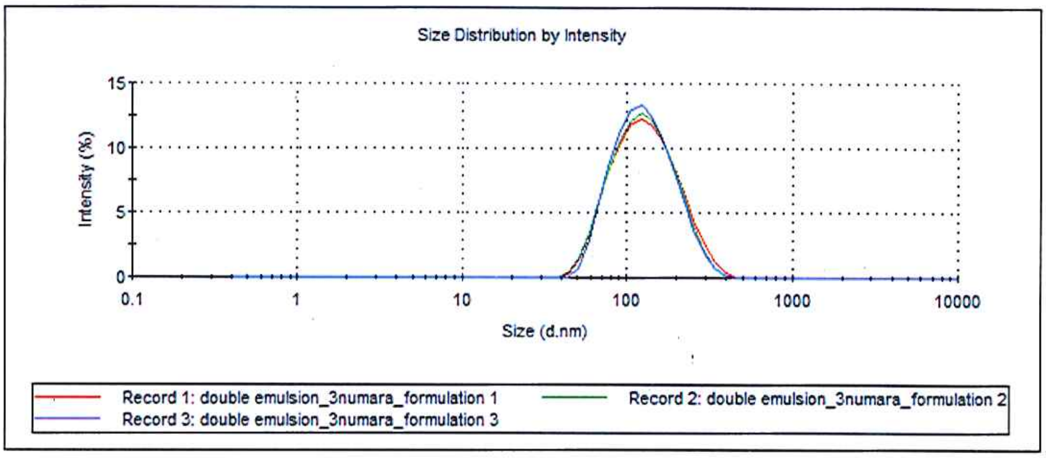

Figure E1: Size Distribution by Intensity of double emulsion with lavender oil at 1:1000 dilution (4.7.2017)

			Diam. (nm)	% Intensity	Width (nm)
Z-Average (d.nm):	124.0	Peak 1:	149.5	100.0	66.37
PdI:	0.160	Peak 2:	0.000	0.0	0.000
Intercept:	0.955	Peak 3:	0.000	0.0	0.000
Result quality :	Good				

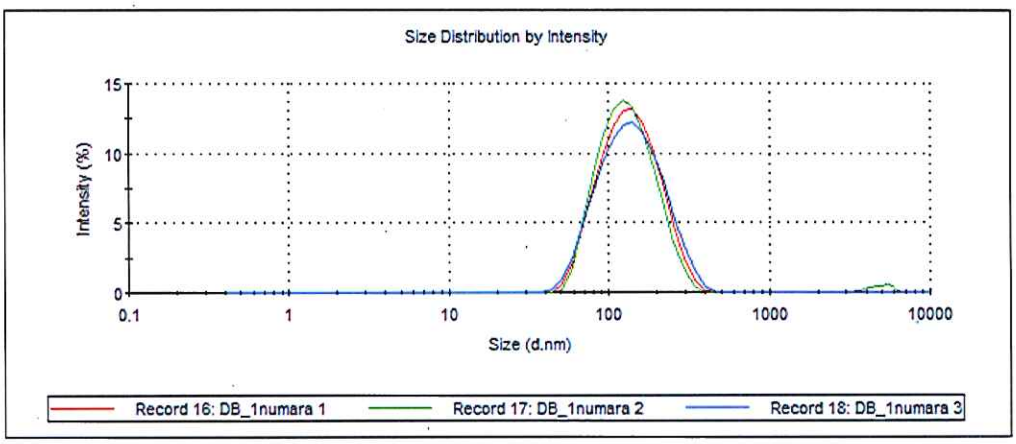

Figure E2: Size Distribution by Intensity of double emulsion with lavender oil at 1:1000 dilution (4.11.2017)

			Diam. (nm)	% Intensity	Width (nm)
Z-Average (d.nm):	169.4	Peak 1:	167.9	99.0	73.32
PdI:	0.368	Peak 2:	5560	1.0	0.000
Intercept:	0.931	Peak 3:	0.000	0.0	0.000
Result quality :	Good				

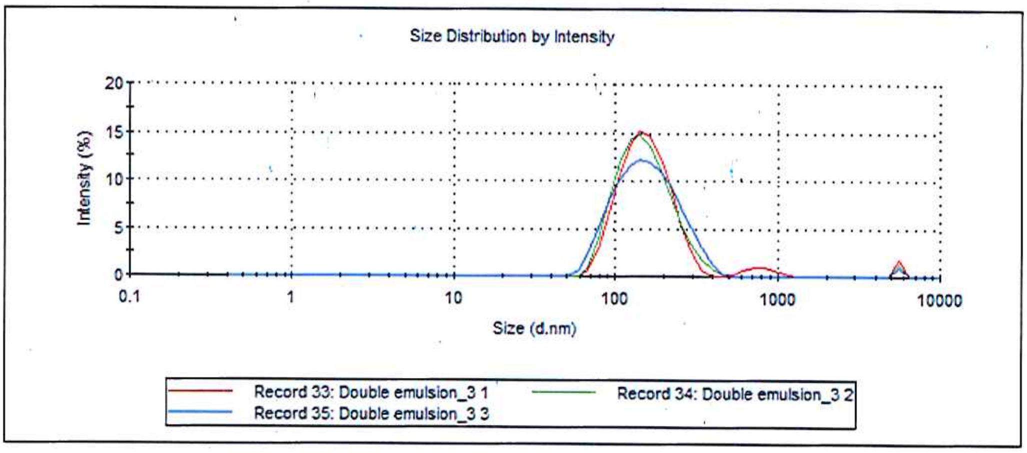

Figure E3: Size Distribution by Intensity of double emulsion with lavender oil at 1:1000 dilution (4.17.2017)

			Diam. (nm)	% Intensity	Width (nm)
Z-Average (d.nm):	232.9	Peak 1:	236.1	94.8	110.4
PdI:	0.405	Peak 2:	5201	5.2	474.1
Intercept:	0.857	Peak 3:	0.000	0.0	0.000
Result quality :	Good				

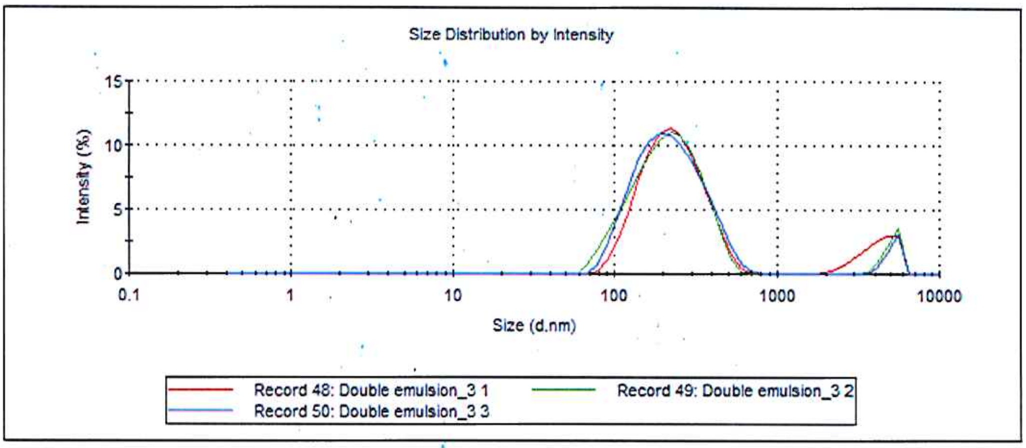

Figure E4: Size Distribution by Intensity of double emulsion with lavender oil at 1:1000 dilution (4.19.2017)

			Diam. (nm)	% Intensity	Width (nm)
Z-Average (d.nm):	185.9	Peak 1:	261.0	100.0	166.6
PdI:	0.238	Peak 2:	0.000	0.0	0.000
Intercept:	0.938	Peak 3:	0.000	0.0	0.000
Result quality :	Good				

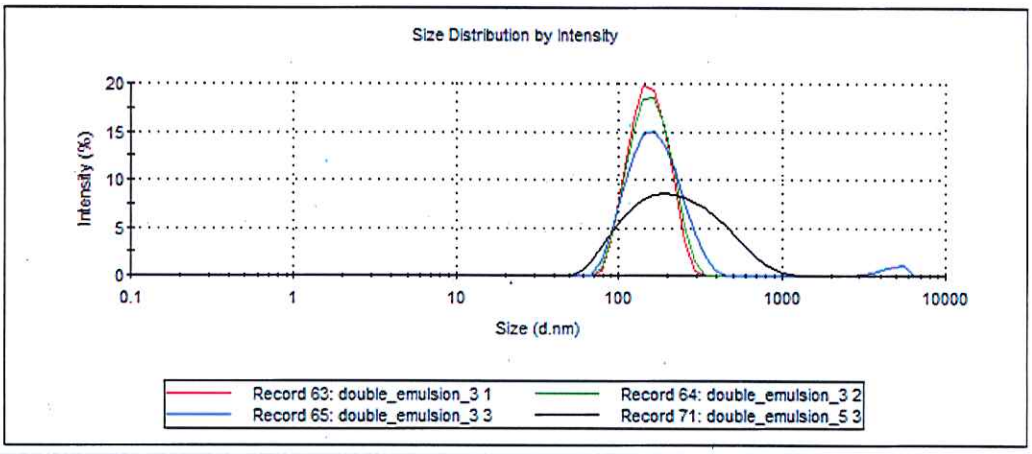

Figure E5: Size Distribution by Intensity of double emulsion with lavender oil at 1:1000 dilution (4.21.2017)

			Diam. (nm)	% Intensity	Width (nm)
Z-Average (d.nm):	180.6	Peak 1:	181.2	100.0	52.91
PdI:	0.203	Peak 2:	0.000	0.0	0.000
Intercept:	0.957	Peak 3:	0.000	0.0	0.000
Result quality :	Good				

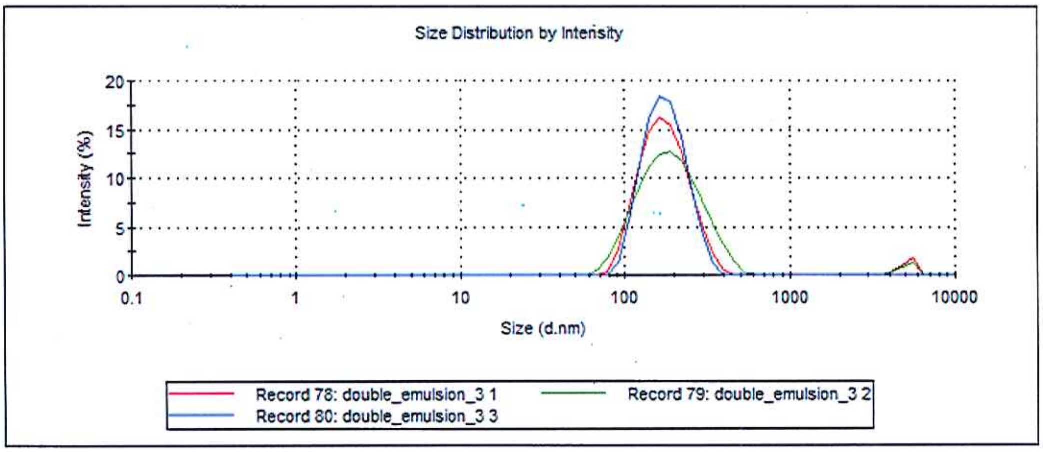

Figure E6: Size Distribution by Intensity of double emulsion with lavender oil at 1:1000 dilution (4.27.2017)

APPENDIX F

			Diam. (nm)	% Number	Width (nm)
Z-Average (d.nm):	117.1	Peak 1:	73.42	100.0	24.76
PdI:	0.149	Peak 2:	0.000	0.0	0.000
Intercept:	0.939	Peak 3:	0.000	0.0	0.000
Result quality :	Good				

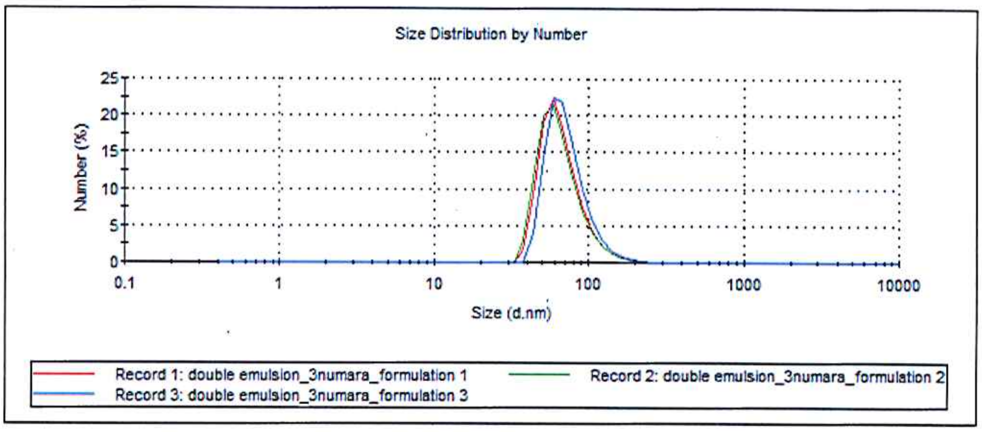

Figure F1: Size Distribution by Number of double emulsion with lavender oil at 1:1000 dilution (4.7.2017)

			Diam. (nm)	% Number	Width (nm)
Z-Average (d.nm):	169.4	Peak 1:	98.15	100.0	45.50
PdI:	0.368	Peak 2:	0.000	0.0	0.000
Intercept:	0.931	Peak 3:	0.000	0.0	0.000
Result quality :	Good				

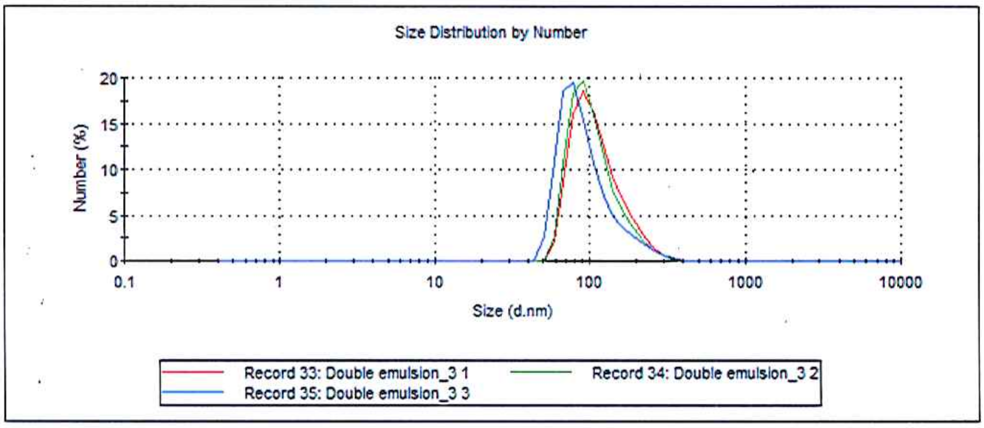

Figure F2: Size Distribution by number of double emulsion with lavender oil at 1:1000 dilution (4.17.2017)

			Diam. (nm)	% Number	Width (nm)
Z-Average (d.nm): 232.9		Peak 1:	150.9	100.0	68.63
PdI: 0.405		Peak 2:	0.000	0.0	0.000
Intercept: 0.857		Peak 3:	0.000	0.0	0.000

Result quality : Good

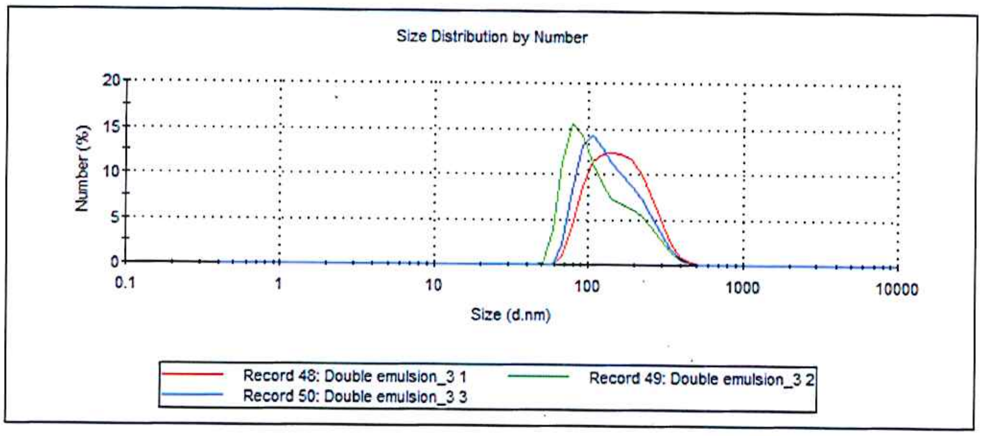

Figure F3: Size Distribution by number of double emulsion with lavender oil at 1:1000 dilution (4.19.2017)

			Diam. (nm)	% Number	Width (nm)
Z-Average (d.nm): 185.9		Peak 1:	93.22	100.0	41.21
PdI: 0.238		Peak 2:	0.000	0.0	0.000
Intercept: 0.938		Peak 3:	0.000	0.0	0.000

Result quality : Good

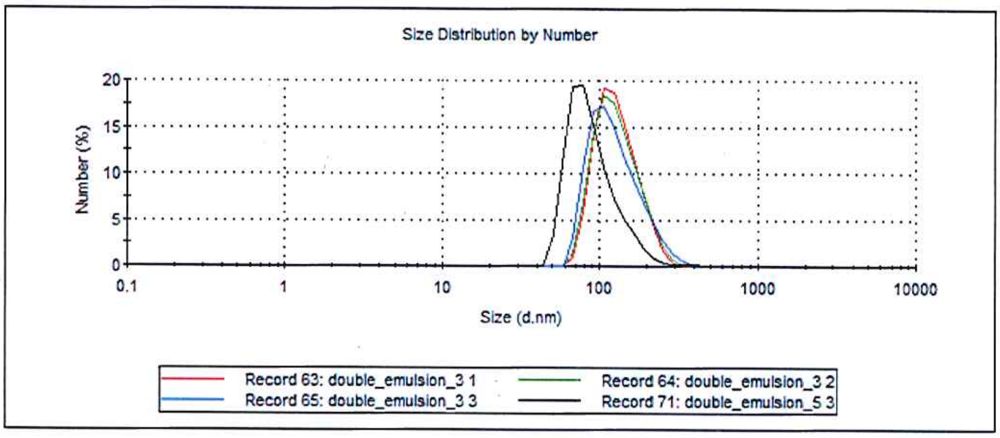

Figure F4: Size Distribution by number of double emulsion with lavender oil at 1:1000 dilution (4.21.2017)

			Diam. (nm)	% Number	Width (nm)
Z-Average (d.nm):	180.6	Peak 1:	155.0	100.0	50.71
PdI:	0.203	Peak 2:	0.000	0.0	0.000
Intercept:	0.957	Peak 3:	0.000	0.0	0.000

Result quality : Good

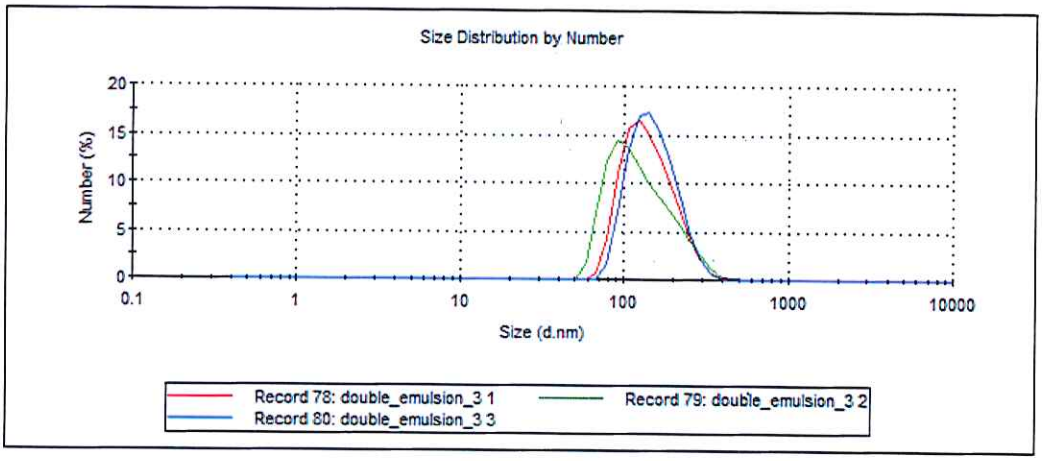

Figure F5: Size Distribution by number of double emulsion with lavender oil at 1:1000 dilution (4.27.2017)

APPENDIX G

			Diam. (nm)	% Intensity	Width (nm)
Z-Average (d.nm):	120.0	Peak 1:	149.6	100.0	76.44
PdI:	0.201	Peak 2:	0.000	0.0	0.000
Intercept:	0.949	Peak 3:	0.000	0.0	0.000
Result quality :	Good				

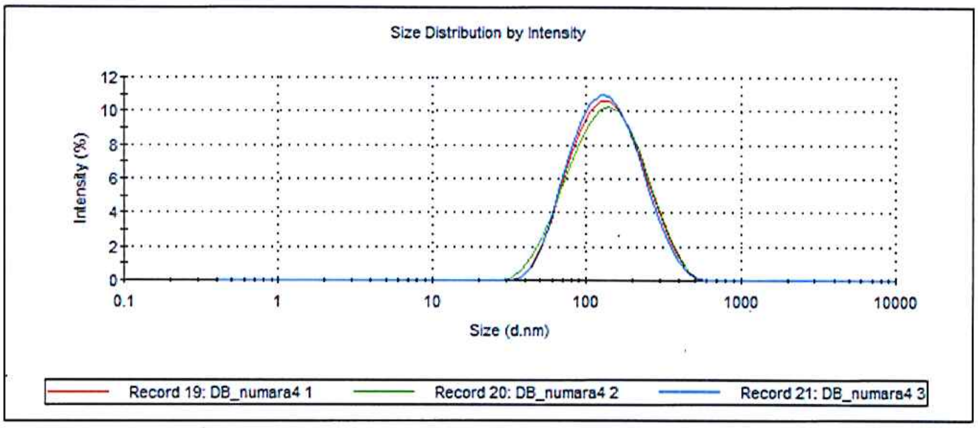

Figure G1: Size Distribution by Intensity of double emulsion with aluminum chlorohydrate and lavender oil at 1:1000 dilution (4.11.2017)

			Diam. (nm)	% Intensity	Width (nm)
Z-Average (d.nm):	203.8	Peak 1:	251.9	94.1	141.2
PdI:	0.346	Peak 2:	4356	5.9	943.6
Intercept:	0.885	Peak 3:	0.000	0.0	0.000
Result quality :	Good				

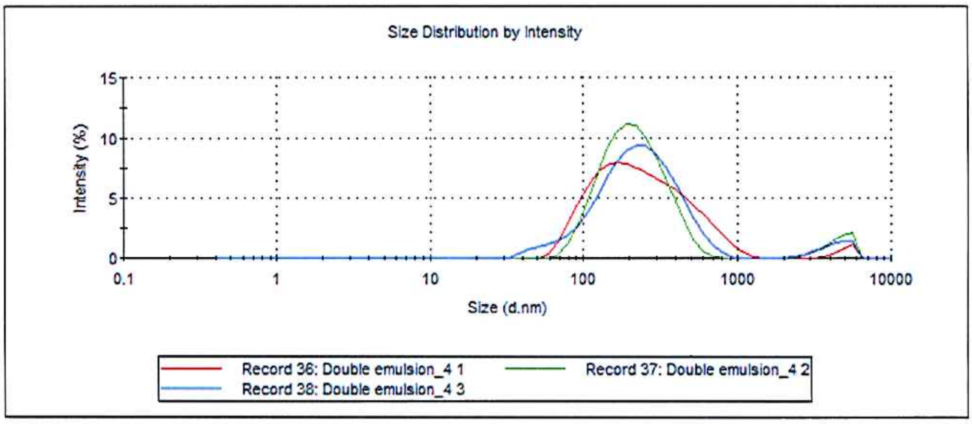

Figure G2: Size Distribution by Intensity of double emulsion with aluminum chlorohydrate and lavender oil at 1:1000 dilution (4.17.2017)

			Diam. (nm)	% Intensity	Width (nm)
Z-Average (d.nm): 163.3		Peak 1:	192.2	96.2	96.13
PdI: 0.246		Peak 2:	4439	3.8	906.2
Intercept: 0.939		Peak 3:	0.000	0.0	0.000
Result quality : Good					

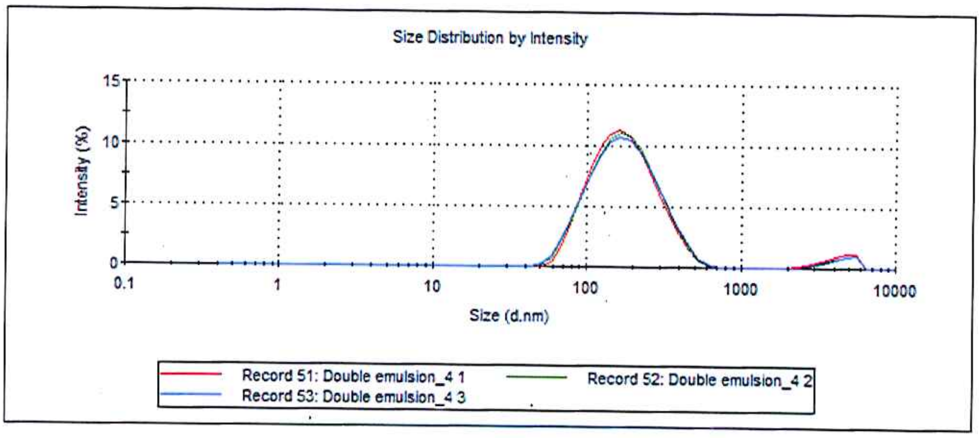

Figure G3: Size Distribution by Intensity of double emulsion with aluminum chlorohydrate and lavender oil at 1:1000 dilution (4.19.2017)

			Diam. (nm)	% Intensity	Width (nm)
Z-Average (d.nm): 231.5		Peak 1:	295.9	96.3	167.4
PdI: 0.362		Peak 2:	4857	3.7	697.2
Intercept: 0.828		Peak 3:	0.000	0.0	0.000
Result quality : Good					

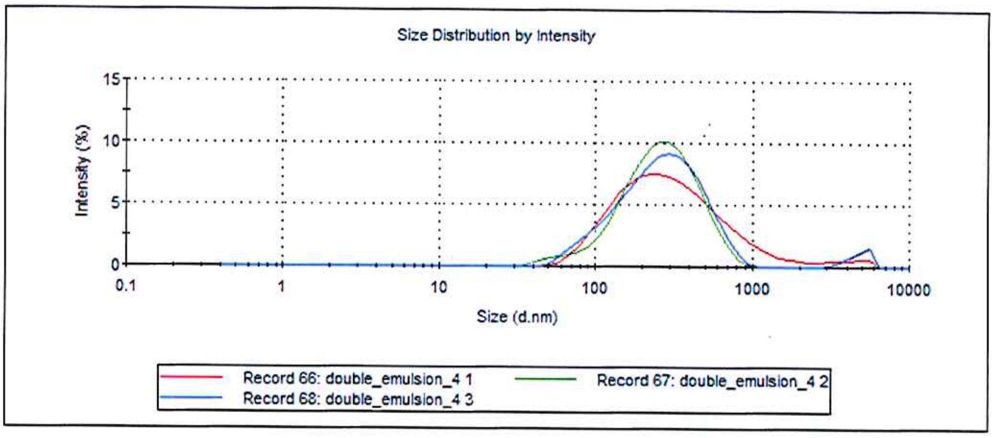

Figure G4: Size Distribution by Intensity of double emulsion with aluminum chlorohydrate and lavender oil at 1:1000 dilution (4.21.2017)

			Diam. (nm)	% Intensity	Width (nm)
Z-Average (d.nm):	165.6	Peak 1:	199.8	98.4	86.67
PdI:	0.238	Peak 2:	5029	1.6	593.0
Intercept:	0.946	Peak 3:	0.000	0.0	0.000
Result quality :	Good				

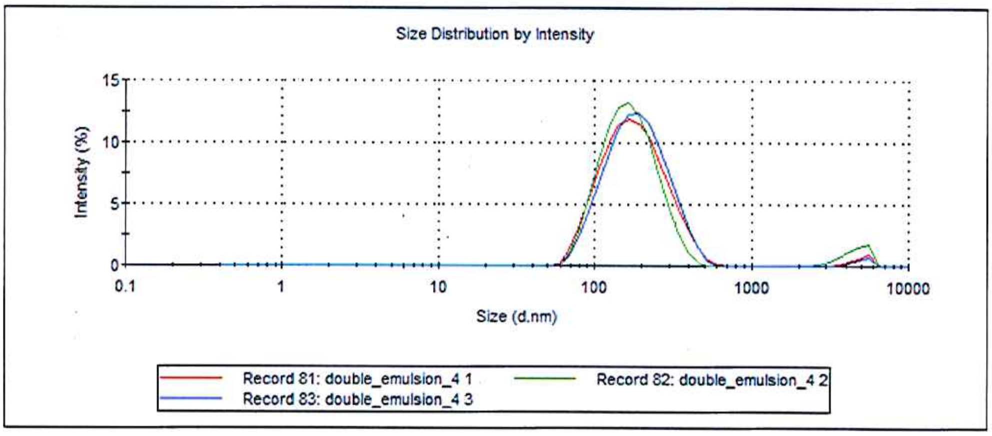

Figure G5: Size Distribution by Intensity of double emulsion with aluminum chlorohydrate and lavender oil at 1:1000 dilution (4.27.2017)

			Diam. (nm)	% Intensity	Width (nm)
Z-Average (d.nm):	178.3	Peak 1:	196.9	100.0	59.33
PdI:	0.096	Peak 2:	0.000	0.0	0.000
Intercept:	0.956	Peak 3:	0.000	0.0	0.000
Result quality :	Good				

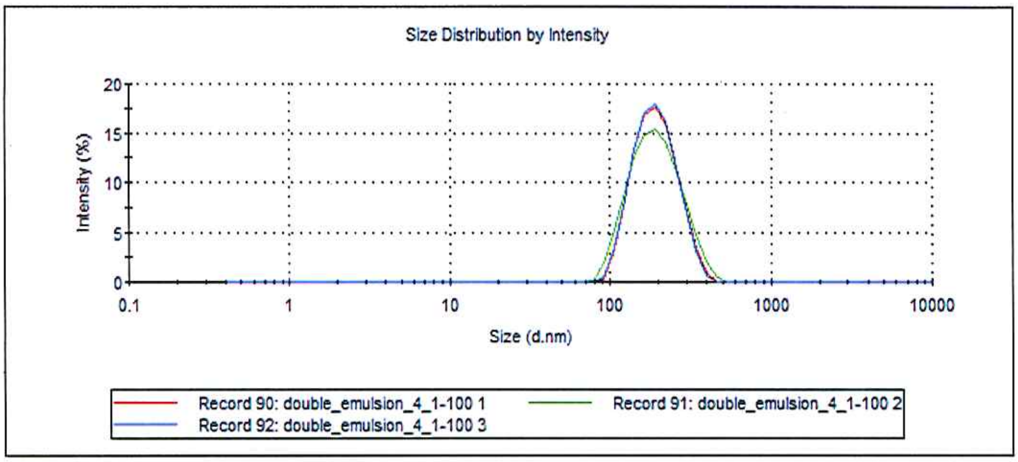

Figure G6: Size Distribution by Intensity of double emulsion with aluminum chlorohydrate and lavender oil at 1:100 dilution (5.10.2017)

APPENDIX H

			Diam. (nm)	% Number	Width (nm)
Z-Average (d.nm):	203.8	Peak 1:	50.38	100.0	25.58
PdI:	0.346	Peak 2:	0.000	0.0	0.000
Intercept:	0.885	Peak 3:	0.000	0.0	0.000

Result quality : Good

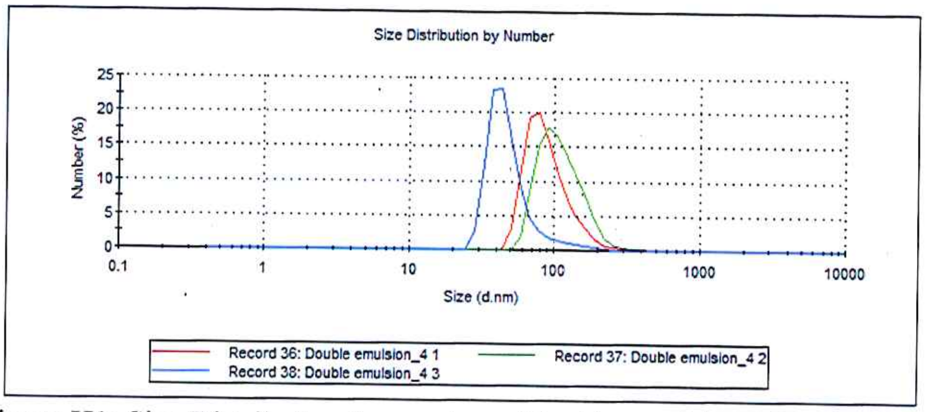

Figure H1: Size Distribution by number of double emulsion with aluminum chlorohydrate and lavender oil at 1:1000 dilution (4.17.2017)

			Diam. (nm)	% Number	Width (nm)
Z-Average (d.nm):	163.3	Peak 1:	83.31	100.0	34.07
PdI:	0.246	Peak 2:	0.000	0.0	0.000
Intercept:	0.939	Peak 3:	0.000	0.0	0.000

Result quality : Good

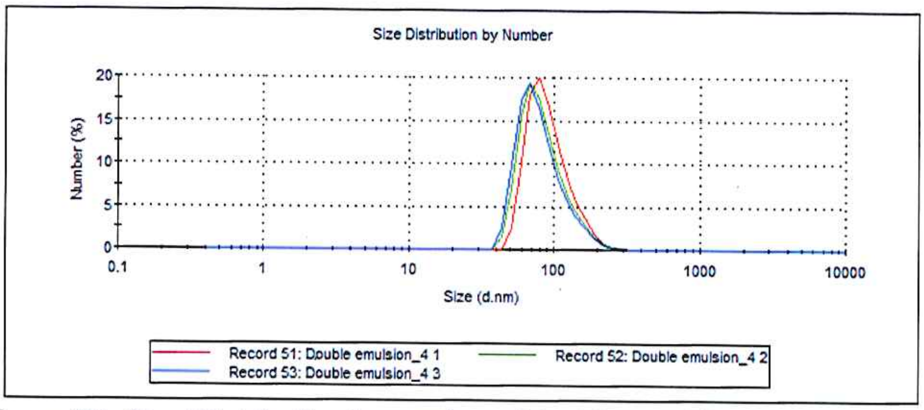

Figure H2: Size Distribution by number of double emulsion with aluminum chlorohydrate and lavender oil at 1:1000 dilution (4.19.2017)

			Diam. (nm)	% Number	Width (nm)
Z-Average (d.nm):	231.5	Peak 1:	78.31	100.0	40.13
PdI:	0.362	Peak 2:	0.000	0.0	0.000
Intercept:	0.828	Peak 3:	0.000	0.0	0.000

Result quality : Good

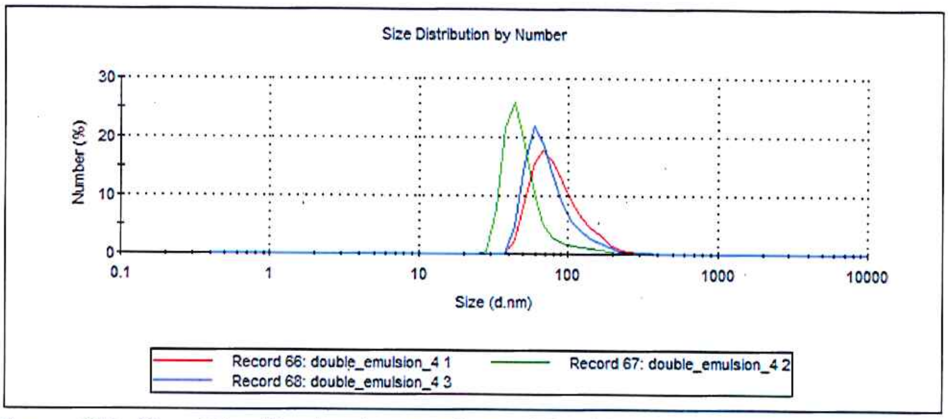

Figure H3: Size Distribution by number of double emulsion with aluminum chlorohydrate and lavender oil at 1:1000 dilution (4.21.2017)

			Diam. (nm)	% Number	Width (nm)
Z-Average (d.nm):	165.6	Peak 1:	117.2	100.0	58.89
PdI:	0.238	Peak 2:	0.000	0.0	0.000
Intercept:	0.946	Peak 3:	0.000	0.0	0.000

Result quality : Good

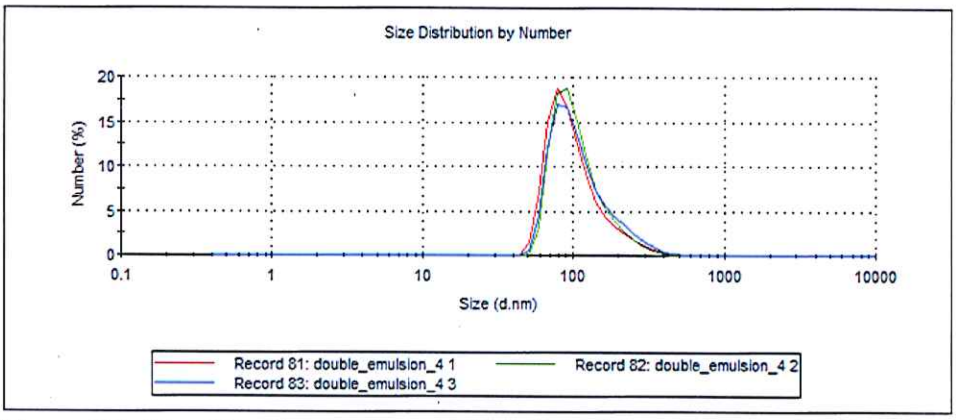

Figure H4: Size Distribution by number of double emulsion with aluminum chlorohydrate and lavender oil at 1:1000 dilution (4.27.2017)

			Diam. (nm)	% Number	Width (nm)
Z-Average (d.nm):	178.3	Peak 1:	172.0	100.0	56.39
PdI:	0.096	Peak 2:	0.000	0.0	0.000
Intercept:	0.956	Peak 3:	0.000	0.0	0.000

Result quality : Good

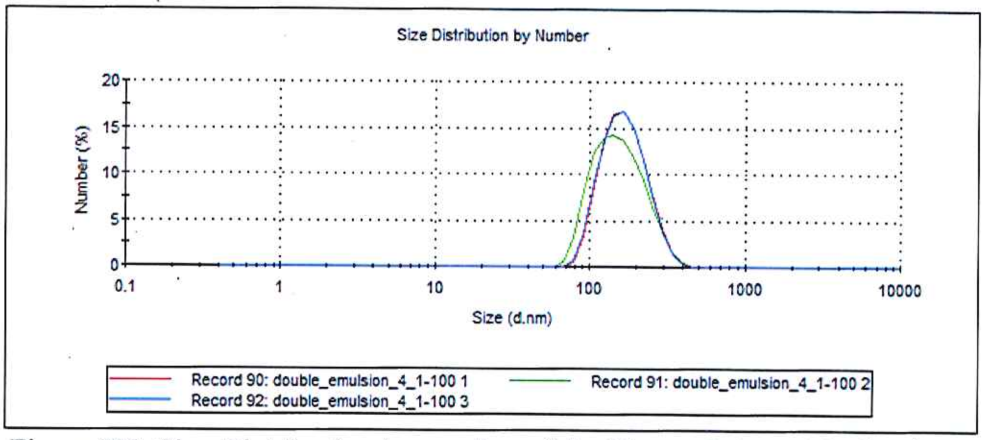

Figure H5: Size Distribution by number of double emulsion with aluminum chlorohydrate and lavender oil at 1:1000 dilution (5.10.2017)

APPENDIX I

			Diam. (nm)	% Intensity	Width (nm)
Z-Average (d.nm):	20.70	Peak 1:	23.21	100.0	7.002
PdI:	0.114	Peak 2:	0.000	0.0	0.000
Intercept:	0.942	Peak 3:	0.000	0.0	0.000
Result quality :	Good				

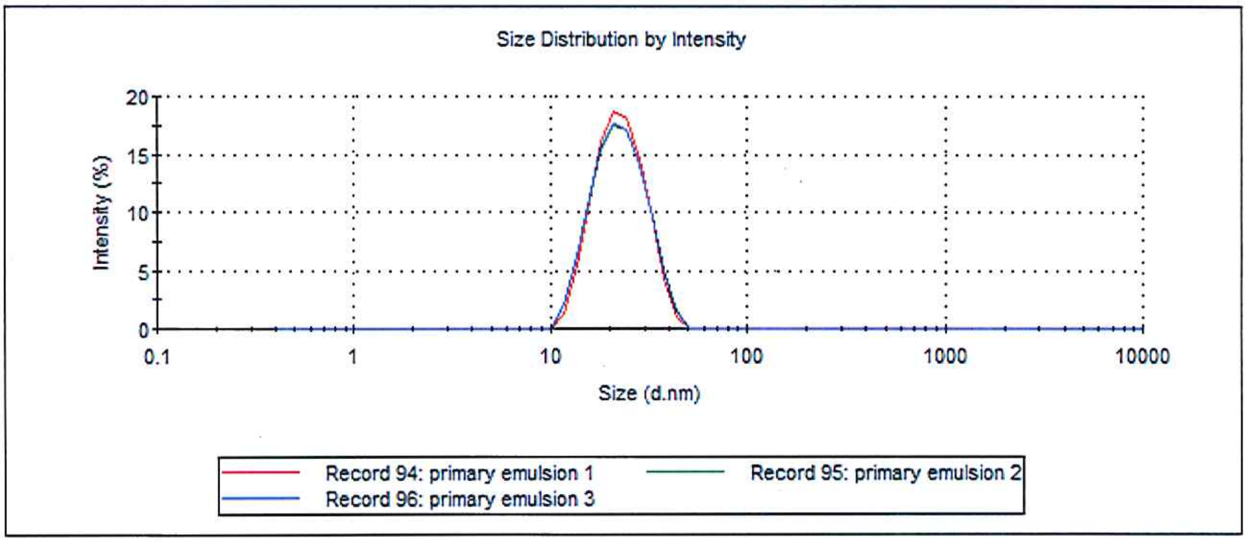

Figure I1: Size Distribution by Intensity of primary emulsion (9.20.2017)

			Diam. (nm)	% Intensity	Width (nm)
Z-Average (d.nm):	20.86	Peak 1:	23.86	100.0	7.904
PdI:	0.132	Peak 2:	0.000	0.0	0.000
Intercept:	0.938	Peak 3:	0.000	0.0	0.000
Result quality :	Good				

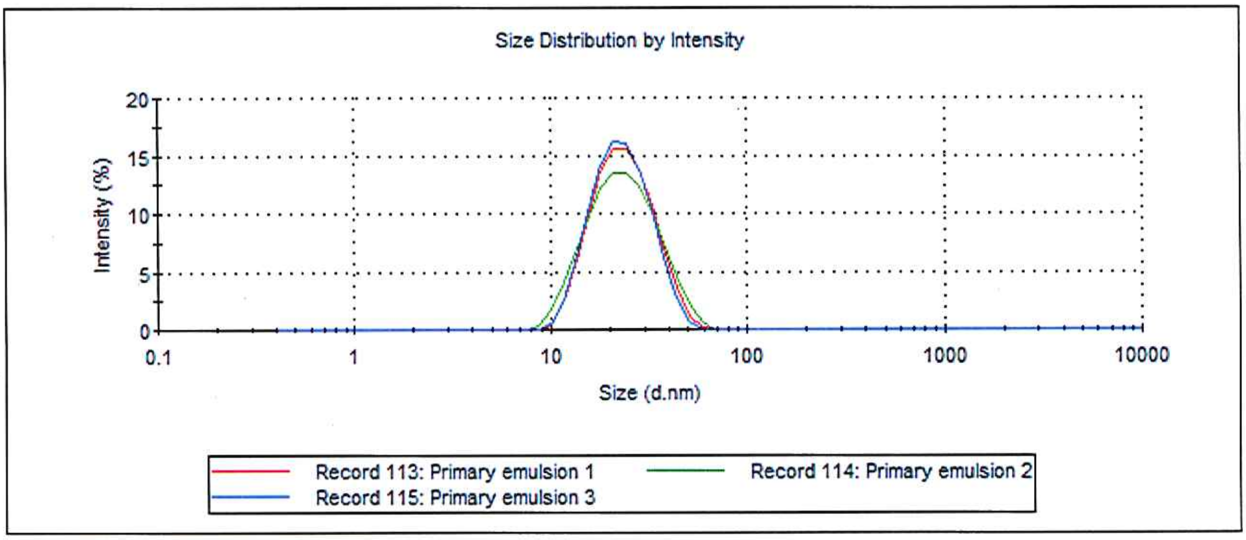

Figure I2: Size Distribution by Intensity of primary emulsion (9.22.2017)

			Diam. (nm)	% Intensity	Width (nm)
Z-Average (d.nm):	20.15	Peak 1:	22.33	100.0	6.183
PdI:	0.102	Peak 2:	0.000	0.0	0.000
Intercept:	0.937	Peak 3:	0.000	0.0	0.000
Result quality :	Good				

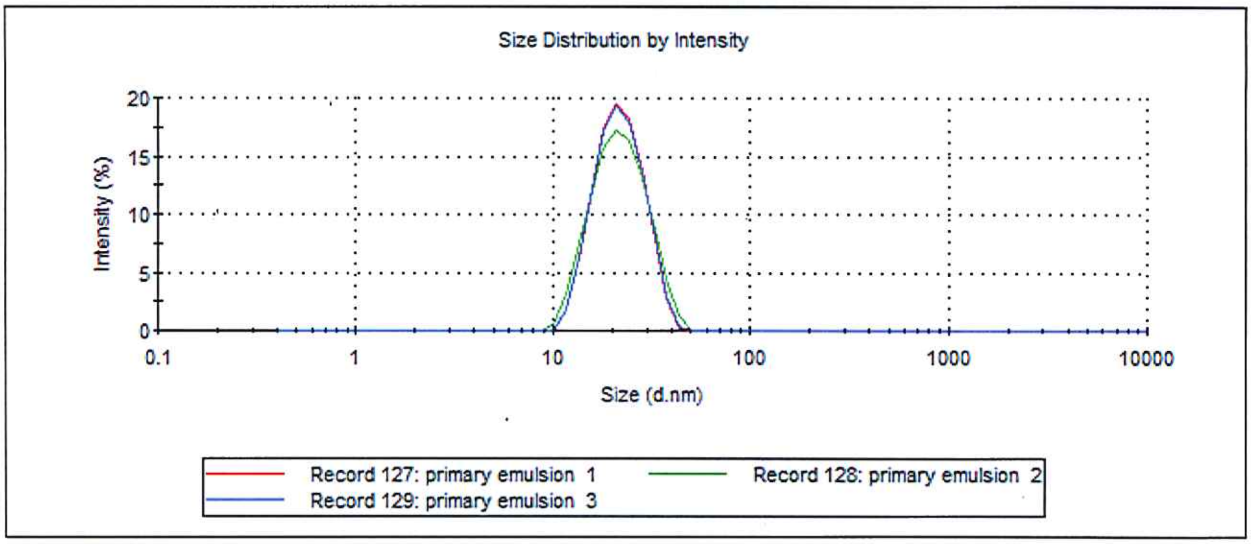

Figure I3: Size Distribution by Intensity of primary emulsion (9.25.2017)

			Diam. (nm)	% Intensity	Width (nm)
Z-Average (d.nm):	21.01	Peak 1:	24.91	100.0	9.880
PdI:	0.167	Peak 2:	0.000	0.0	0.000
Intercept:	0.907	Peak 3:	0.000	0.0	0.000
Result quality :	Good				

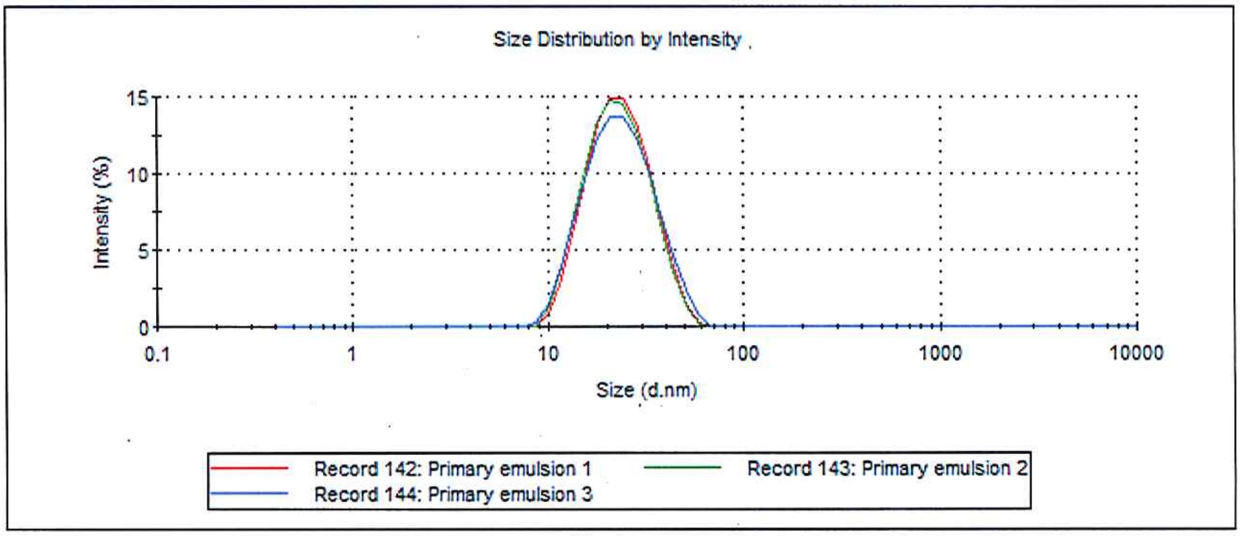

Figure I4: Size Distribution by Intensity of primary emulsion (9.28.2017)

			Diam. (nm)	% Intensity	Width (nm)
Z-Average (d.nm):	19.71	Peak 1:	22.02	100.0	6.482
PdI:	0.109	Peak 2:	0.000	0.0	0.000
Intercept:	0.942	Peak 3:	0.000	0.0	0.000
Result quality :	Good				

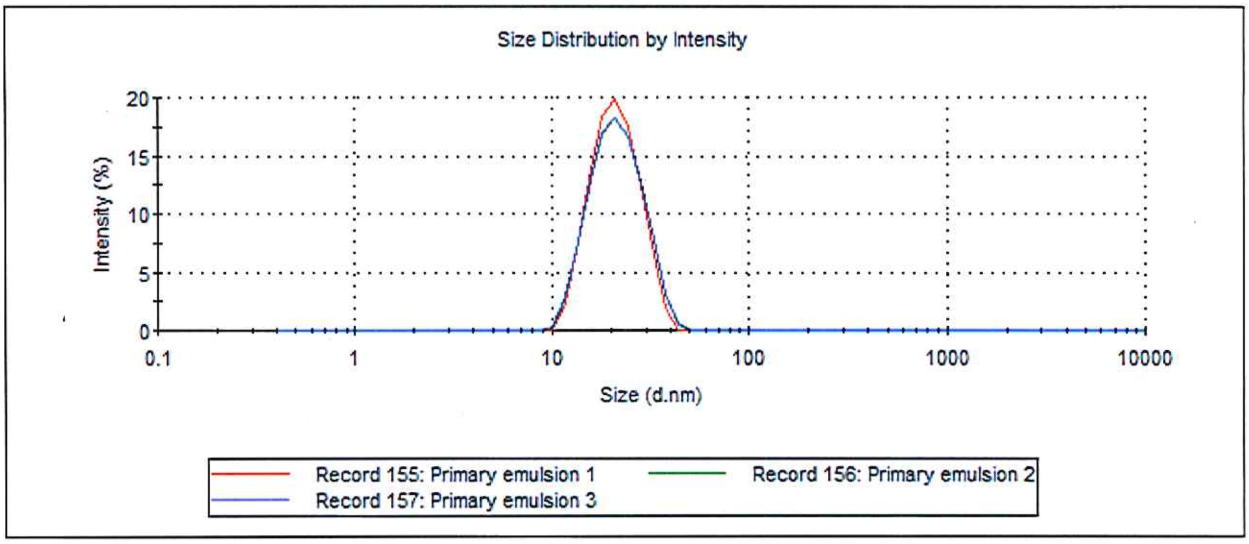

Figure I5: Size Distribution by Intensity of primary emulsion (10.06.2017)

			Diam. (nm)	% Intensity	Width (nm)
Z-Average (d.nm):	288.6	Peak 1:	225.5	88.4	52.14
PdI:	0.480	Peak 2:	5120	11.6	528.3
Intercept:	0.718	Peak 3:	0.000	0.0	0.000
Result quality :	Refer to quality report				

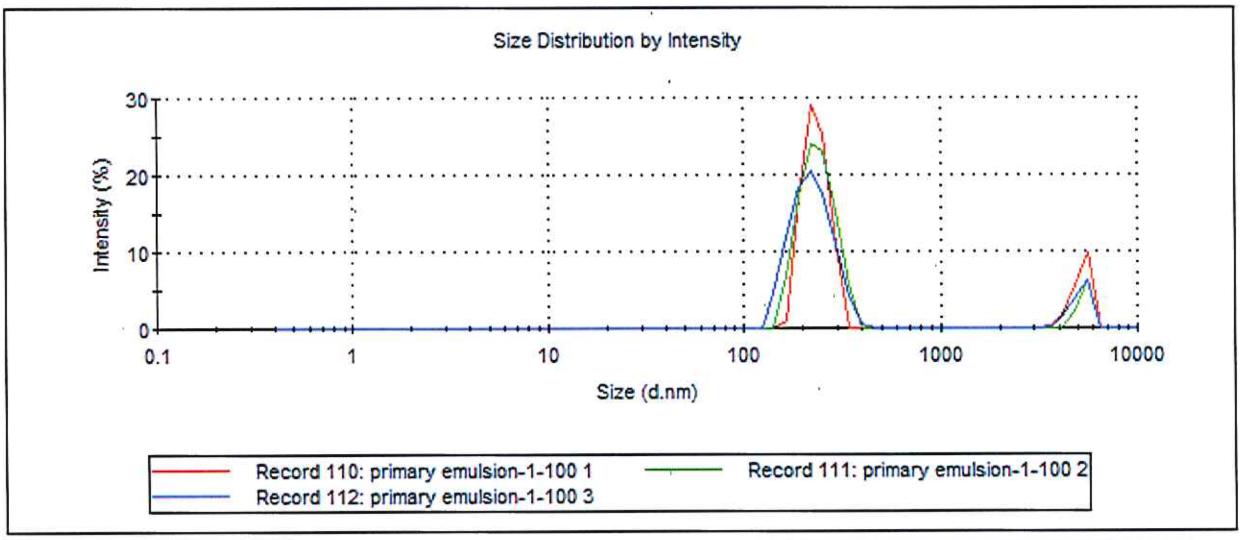

Figure I6: Size Distribution by Intensity of primary emulsion at 1:100 dilution (9.20.2017)

			Diam. (nm)	% Intensity	Width (nm)
Z-Average (d.nm):	666.8	Peak 1:	548.7	100.0	100.1
PdI:	0.274	Peak 2:	0.000	0.0	0.000
Intercept:	0.699	Peak 3:	0.000	0.0	0.000

Result quality : Refer to quality report

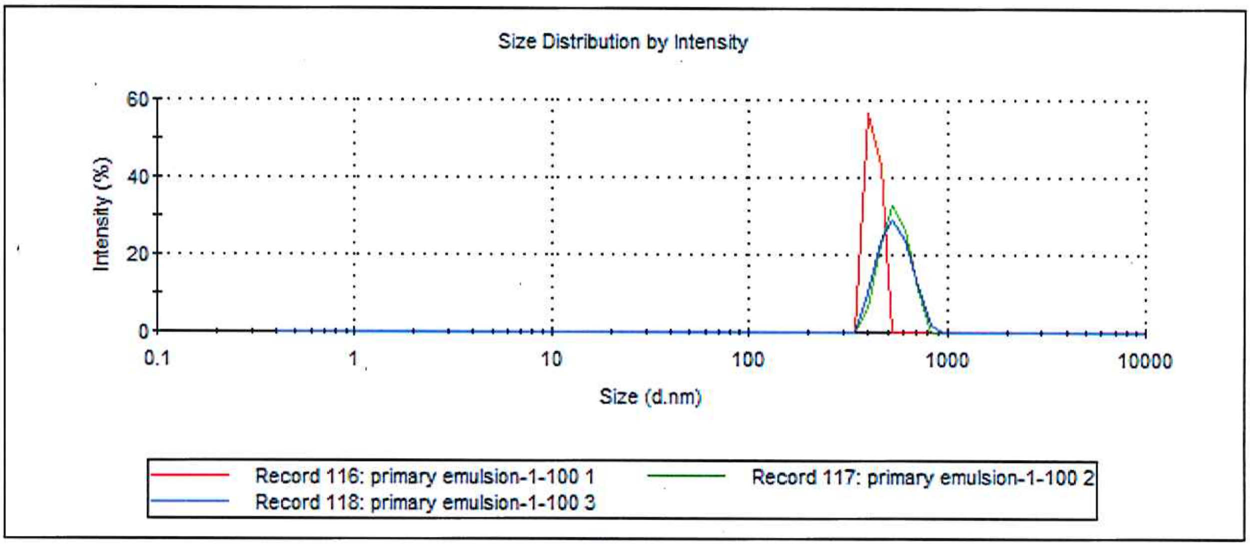

Figure I7: Size Distribution by Intensity of primary emulsion at 1:100 dilution (9.22.2017)

			Diam. (nm)	% Intensity	Width (nm)
Z-Average (d.nm):	722.6	Peak 1:	478.6	100.0	89.50
PdI:	0.114	Peak 2:	0.000	0.0	0.000
Intercept:	0.456	Peak 3:	0.000	0.0	0.000

Result quality : Refer to quality report

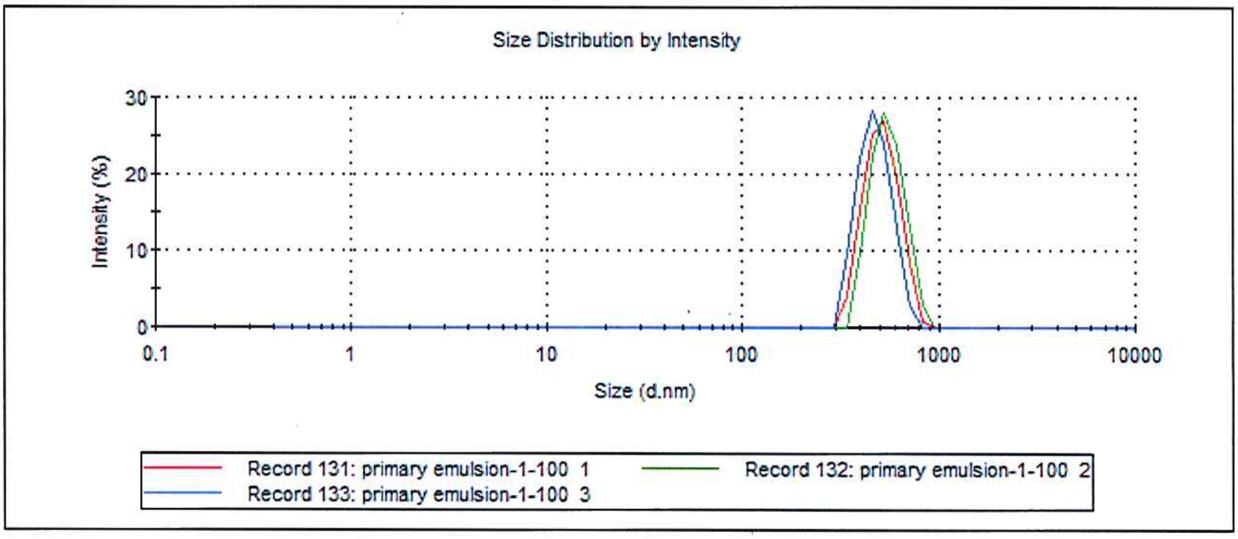

Figure I8: Size Distribution by Intensity of primary emulsion at 1:100 dilution (9.25.2017)

			Diam. (nm)	% Intensity	Width (nm)
Z-Average (d.nm):	528.8	Peak 1:	564.5	100.0	123.3
PdI:	0.242	Peak 2:	0.000	0.0	0.000
Intercept:	0.464	Peak 3:	0.000	0.0	0.000
Result quality :	Refer to quality report				

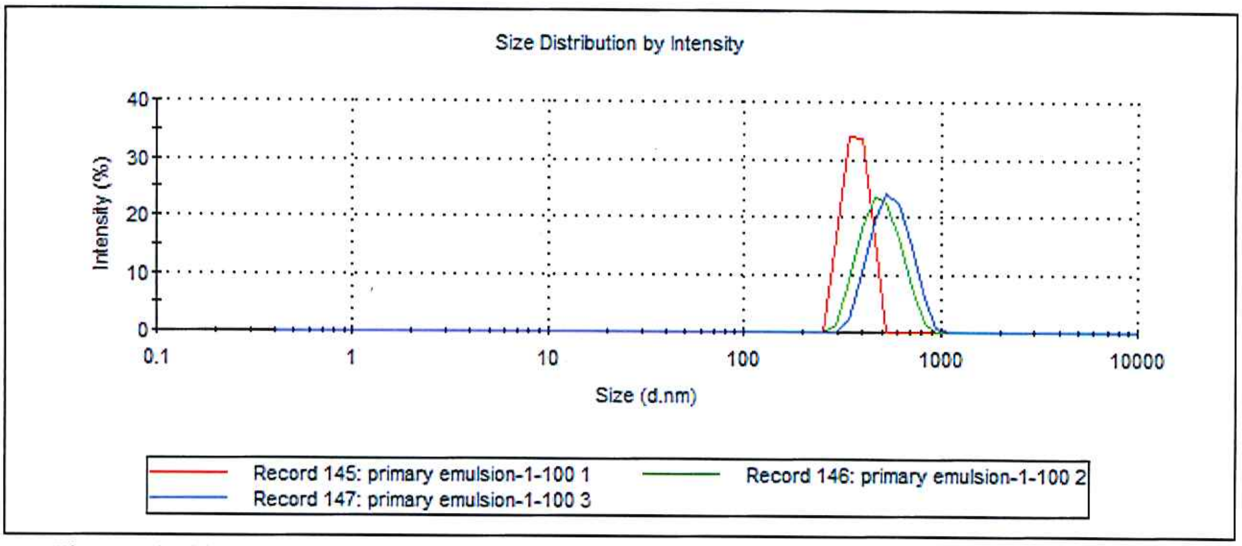

Figure I9: Size Distribution by Intensity of primary emulsion at 1:100 dilution (9.28.2017)

			Diam. (nm)	% Intensity	Width (nm)
Z-Average (d.nm):	693.4	Peak 1:	621.5	100.0	126.4
PdI:	0.413	Peak 2:	0.000	0.0	0.000
Intercept:	0.537	Peak 3:	0.000	0.0	0.000
Result quality :	Refer to quality report				

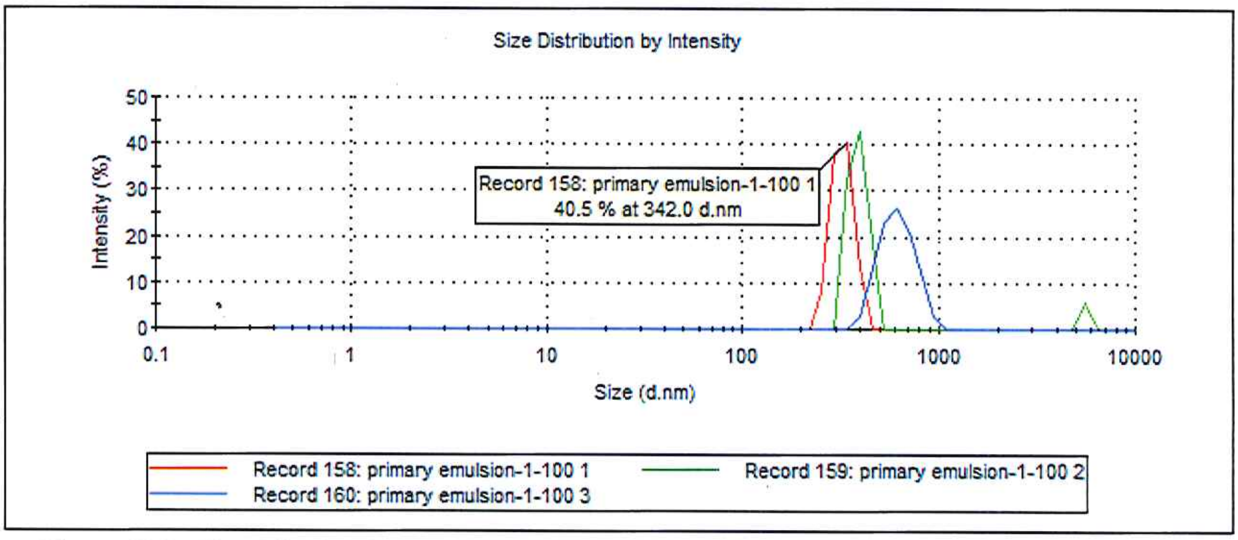

Figure I10: Size Distribution by Intensity of primary emulsion at 1:100 dilution (10.06.2017)

APPENDIX J

			Diam. (nm)	% Number	Width (nm)
Z-Average (d.nm):	20.70	Peak 1:	15.19	100.0	3.809
PdI:	0.114	Peak 2:	0.000	0.0	0.000
Intercept:	0.942	Peak 3:	0.000	0.0	0.000
Result quality :	Good				

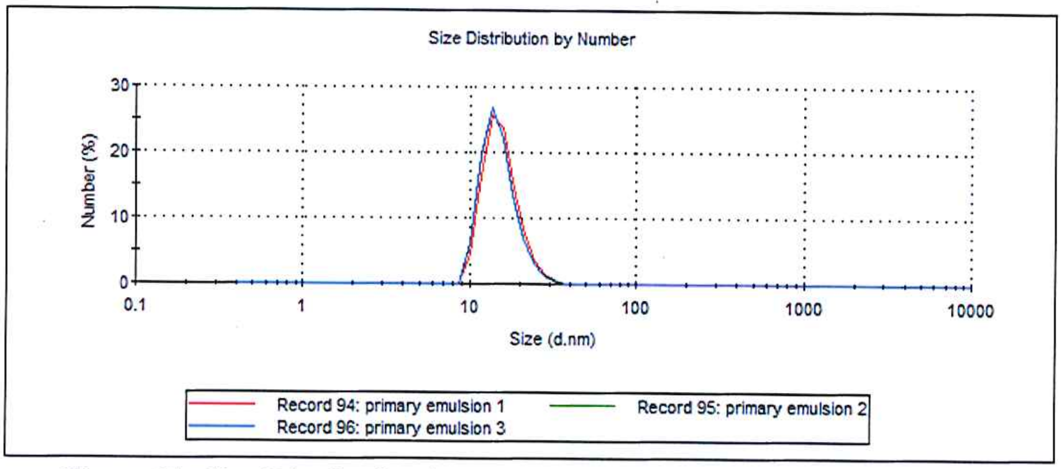

Figure J1: Size Distribution by Number of primary emulsion (9.20.2017)

			Diam. (nm)	% Number	Width (nm)
Z-Average (d.nm):	20.86	Peak 1:	16.79	100.0	5.711
PdI:	0.132	Peak 2:	0.000	0.0	0.000
Intercept:	0.938	Peak 3:	0.000	0.0	0.000
Result quality :	Good				

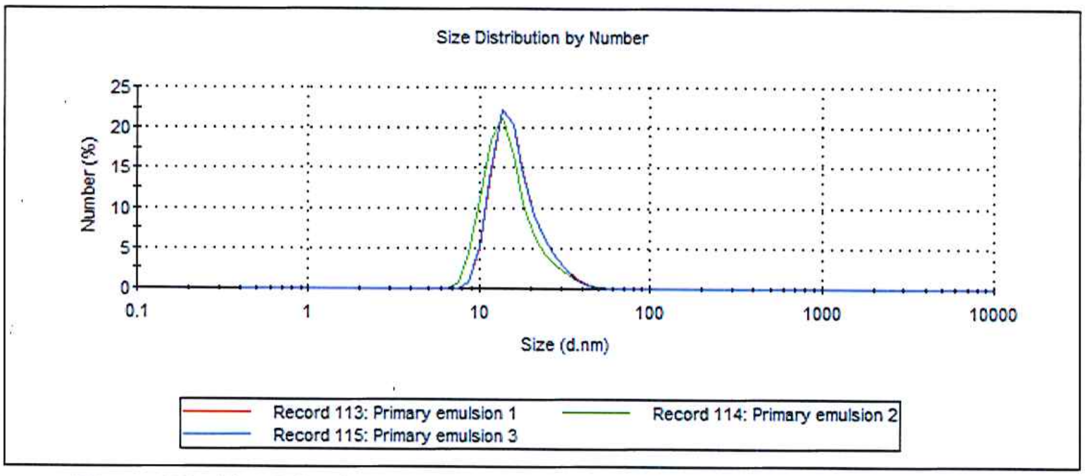

Figure J2: Size Distribution by Number of primary emulsion (9.22.2017)

			Diam. (nm)	% Number	Width (nm)
Z-Average (d.nm):	20.15	Peak 1:	17.14	100.0	5.088
PdI:	0.102	Peak 2:	0.000	0.0	0.000
Intercept:	0.937	Peak 3:	0.000	0.0	0.000

Result quality : Good

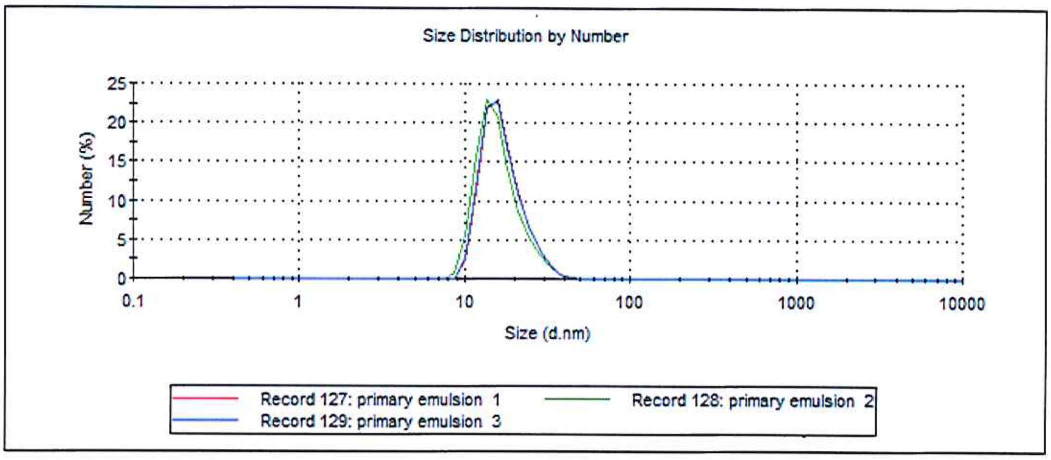

Figure J3: Size Distribution by Number of primary emulsion (9.25.2017)

			Diam. (nm)	% Number	Width (nm)
Z-Average (d.nm):	21.01	Peak 1:	15.76	100.0	5.906
PdI:	0.167	Peak 2:	0.000	0.0	0.000
Intercept:	0.907	Peak 3:	0.000	0.0	0.000

Result quality : Good

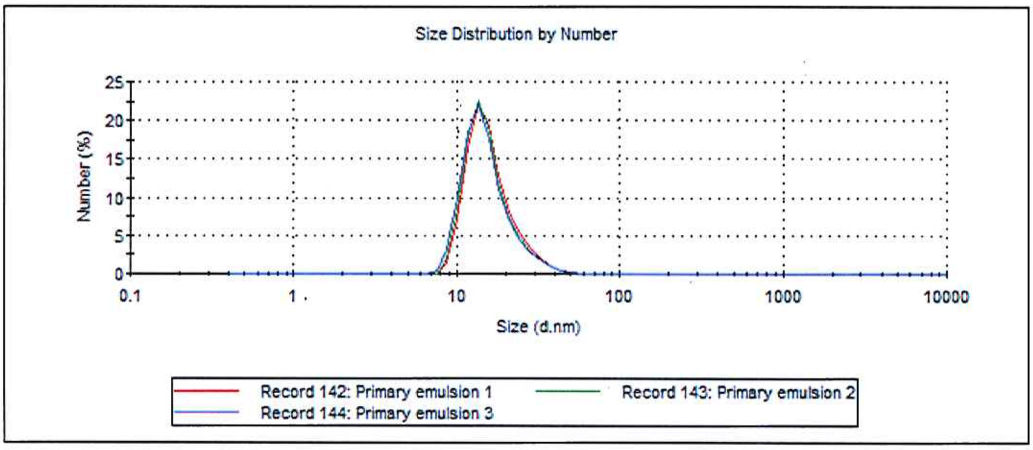

Figure J4: Size Distribution by Number of primary emulsion (9.28.2017)

			Diam. (nm)	% Intensity	Width (nm)
Z-Average (d.nm):	19.71	Peak 1:	22.02	100.0	6.482
PdI:	0.109	Peak 2:	0.000	0.0	0.000
Intercept:	0.942	Peak 3:	0.000	0.0	0.000
Result quality :	Good				

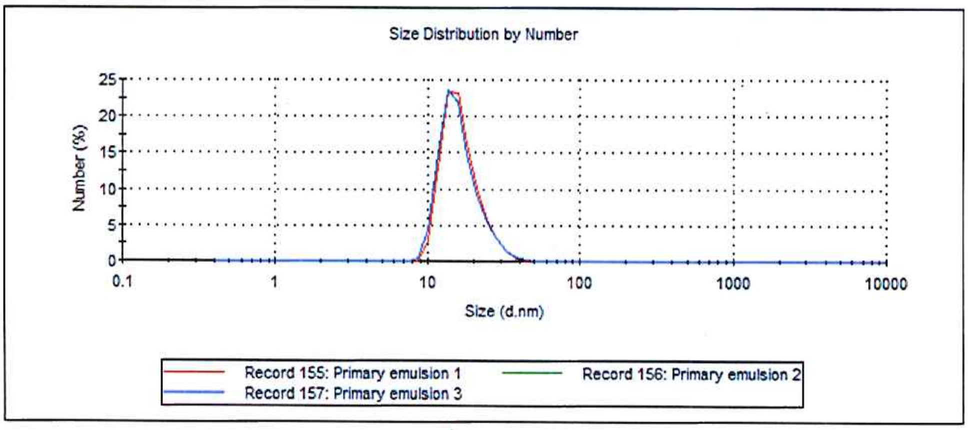

Figure J5: Size Distribution by Number of primary emulsion (10.06.2017)

			Diam. (nm)	% Number	Width (nm)
Z-Average (d.nm):	288.6	Peak 1:	204.9	100.0	54.03
PdI:	0.480	Peak 2:	5077	0.0	769.2
Intercept:	0.718	Peak 3:	0.000	0.0	0.000
Result quality :	Refer to quality report				

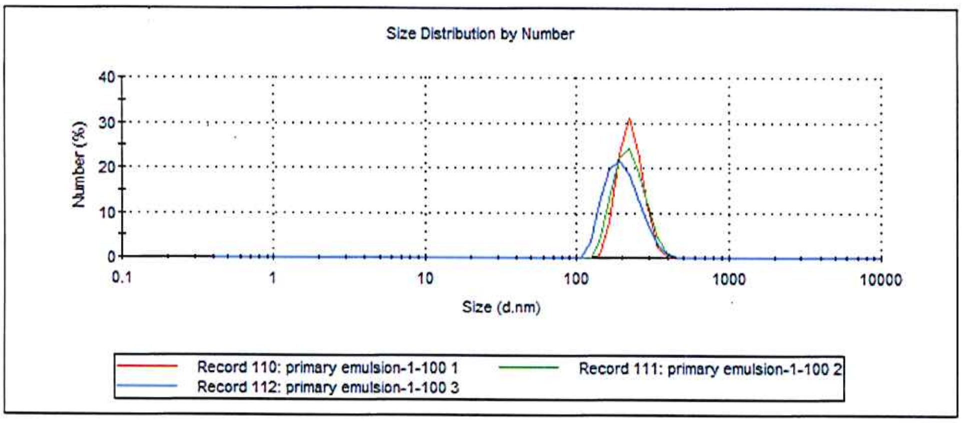

Figure J6: Size Distribution by Number of primary emulsion at 1:100 dilution (9.20.2017)

			Diam. (nm)	% Number	Width (nm)
Z-Average (d.nm):	666.8	Peak 1:	486.2	100.0	92.03
PdI:	0.274	Peak 2:	0.000	0.0	0.000
Intercept:	0.699	Peak 3:	0.000	0.0	0.000

Result quality : Refer to quality report

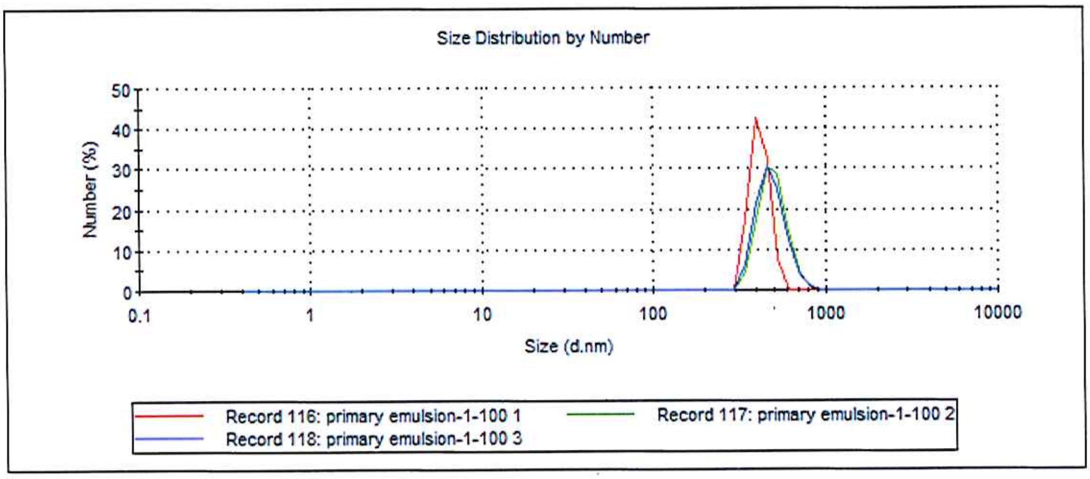

Figure J7: Size Distribution by Number of primary emulsion at 1:100 dilution (9.22.2017)

			Diam. (nm)	% Number	Width (nm)
Z-Average (d.nm):	722.6	Peak 1:	421.6	100.0	84.72
PdI:	0.114	Peak 2:	0.000	0.0	0.000
Intercept:	0.456	Peak 3:	0.000	0.0	0.000

Result quality : Refer to quality report

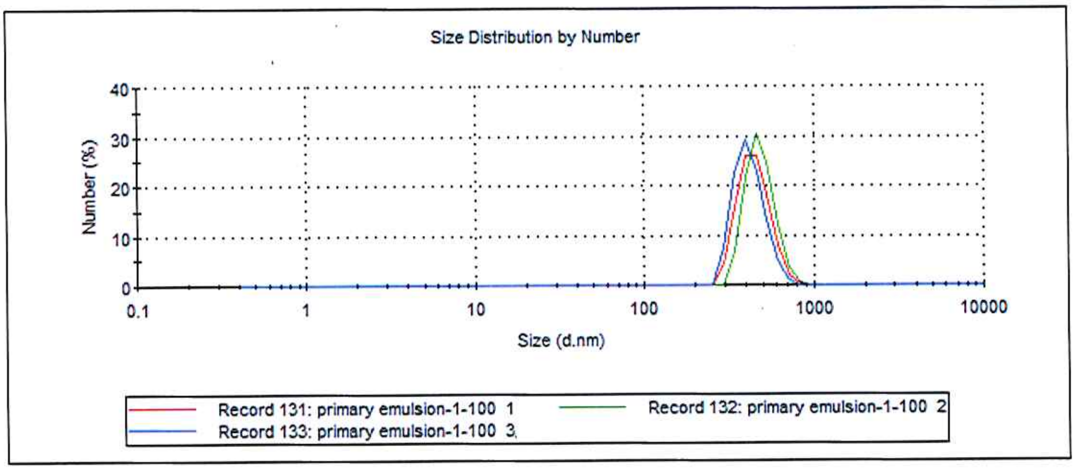

Figure J8: Size Distribution by Number of primary emulsion at 1:100 dilution (9.25.2017)

			Diam. (nm)	% Number	Width (nm)
Z-Average (d.nm):	528.8	Peak 1:	469.0	100.0	104.3
PdI:	0.242	Peak 2:	0.000	0.0	0.000
Intercept:	0.464	Peak 3:	0.000	0.0	0.000

Result quality : Refer to quality report

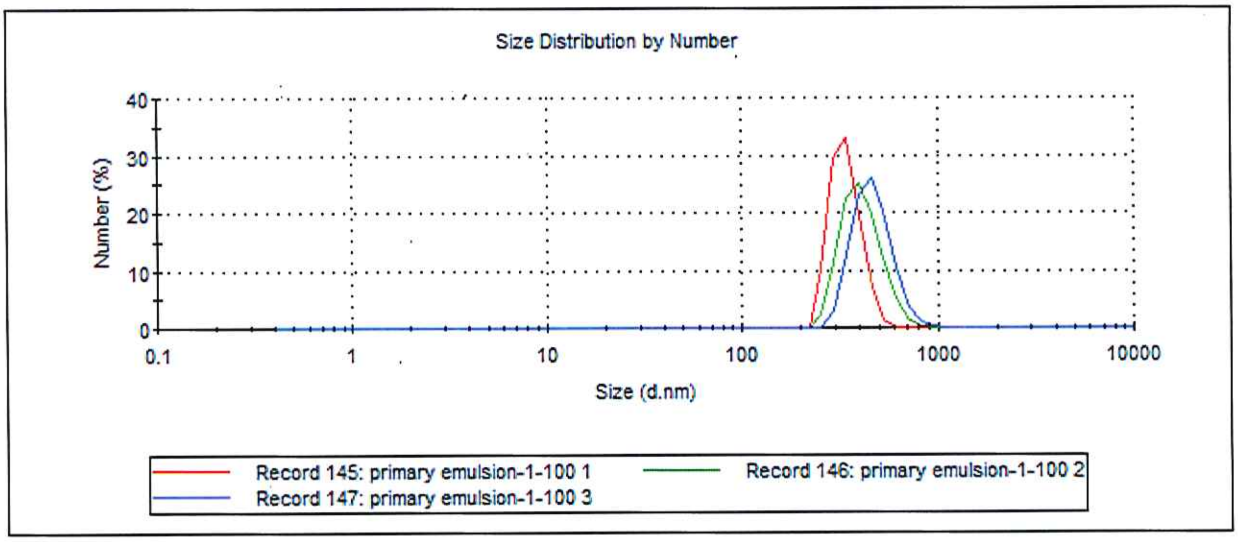

Figure J9: Size Distribution by Number of primary emulsion at 1:100 dilution (9.28.2017)

			Diam. (nm)	% Intensity	Width (nm)
Z-Average (d.nm):	693.4	Peak 1:	621.5	100.0	126.4
PdI:	0.413	Peak 2:	0.000	0.0	0.000
Intercept:	0.537	Peak 3:	0.000	0.0	0.000

Result quality : Refer to quality report

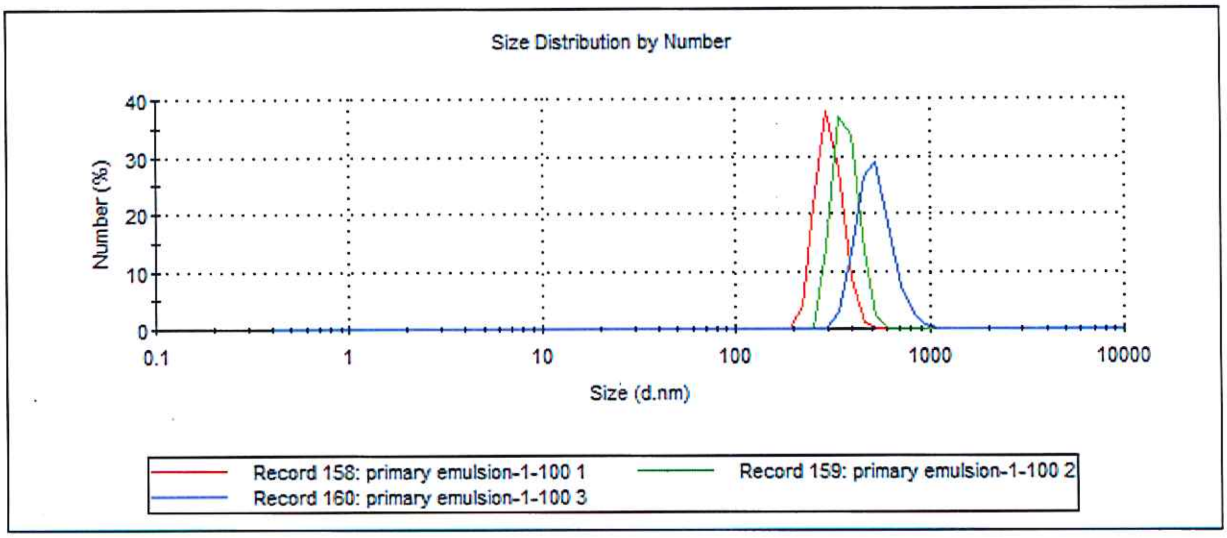

Figure J10: Size Distribution by Number of primary emulsion at 1:100 dilution (10.06.2017)

APPENDIX K

			Diam. (nm)	% Intensity	Width (nm)
Z-Average (d.nm):	14.68	Peak 1:	16.23	98.5	5.665
PdI:	0.170	Peak 2:	4797	1.5	725.0
Intercept:	0.921	Peak 3:	0.000	0.0	0.000
Result quality :	Good				

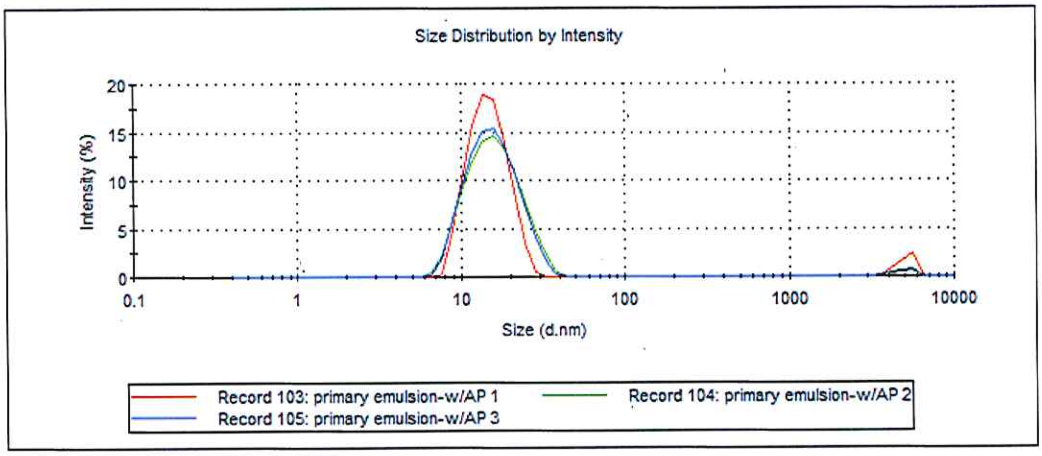

Figure K1: Size Distribution by Intensity of primary emulsion with $Al_2OH_5Cl_2 . 3\ H_2O$ (20.09.2017)

			Diam. (nm)	% Intensity	Width (nm)
Z-Average (d.nm):	15.05	Peak 1:	16.83	96.3	6.505
PdI:	0.227	Peak 2:	4336	3.7	948.9
Intercept:	0.930	Peak 3:	0.000	0.0	0.000
Result quality :	Good				

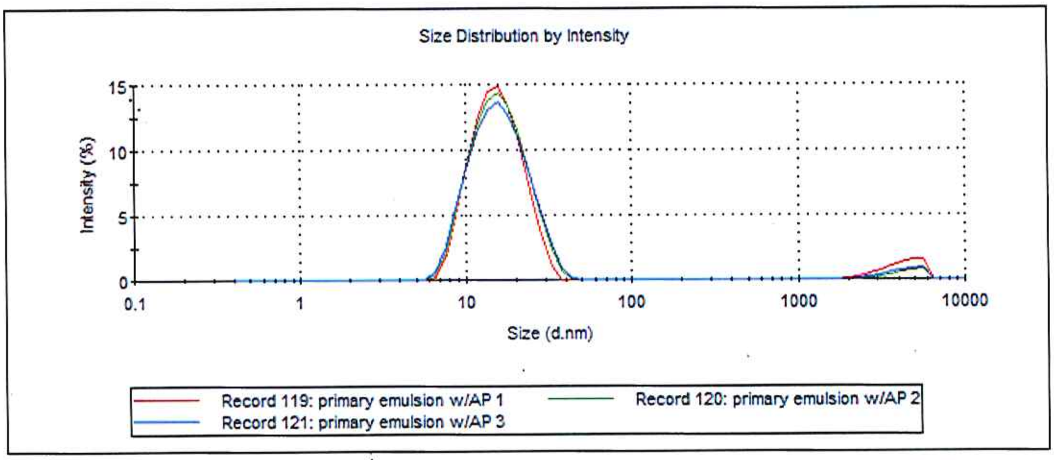

Figure K2: Size Distribution by Intensity of primary emulsion with $Al_2OH_5Cl_2 . 3\ H_2O$ (22.09.2017)

			Diam. (nm)	% Intensity	Width (nm)
Z-Average (d.nm):	15.15	Peak 1:	16.43	96.0	6.010
PdI:	0.212	Peak 2:	4240	4.0	989.3
Intercept:	0.926	Peak 3:	0.000	0.0	0.000
Result quality :	Good				

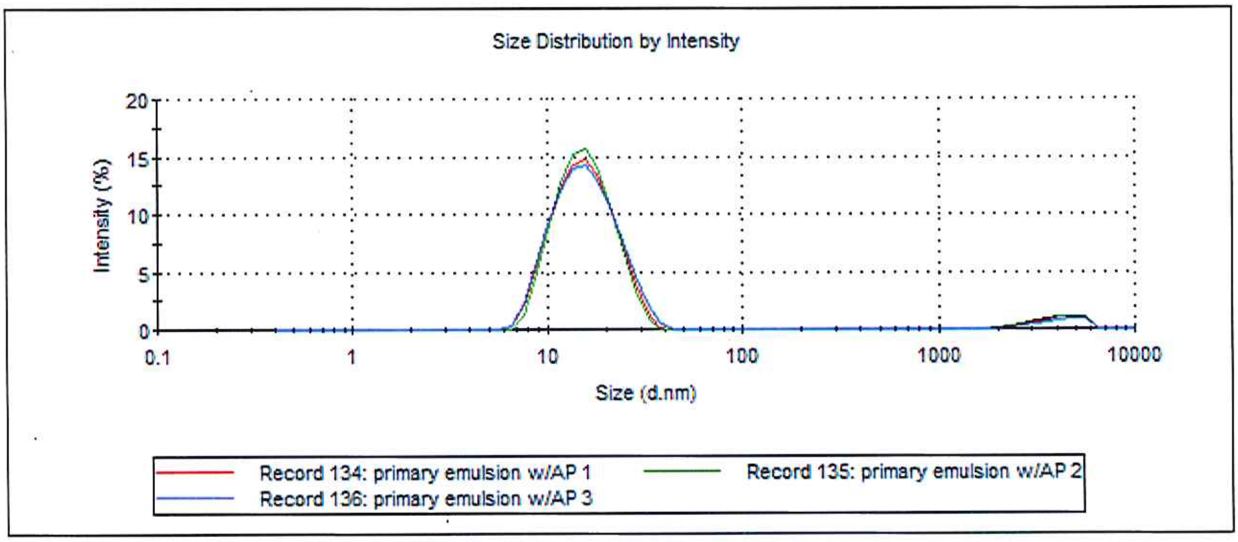

Figure K3: Size Distribution by Intensity of primary emulsion with $Al_2OH_5Cl_2 . 3\ H_2O$ (25.09.2017)

			Diam. (nm)	% Intensity	Width (nm)
Z-Average (d.nm):	16.07	Peak 1:	15.27	86.4	4.440
PdI:	0.305	Peak 2:	806.3	9.8	398.0
Intercept:	0.922	Peak 3:	3895	3.8	1146
Result quality :	Good				

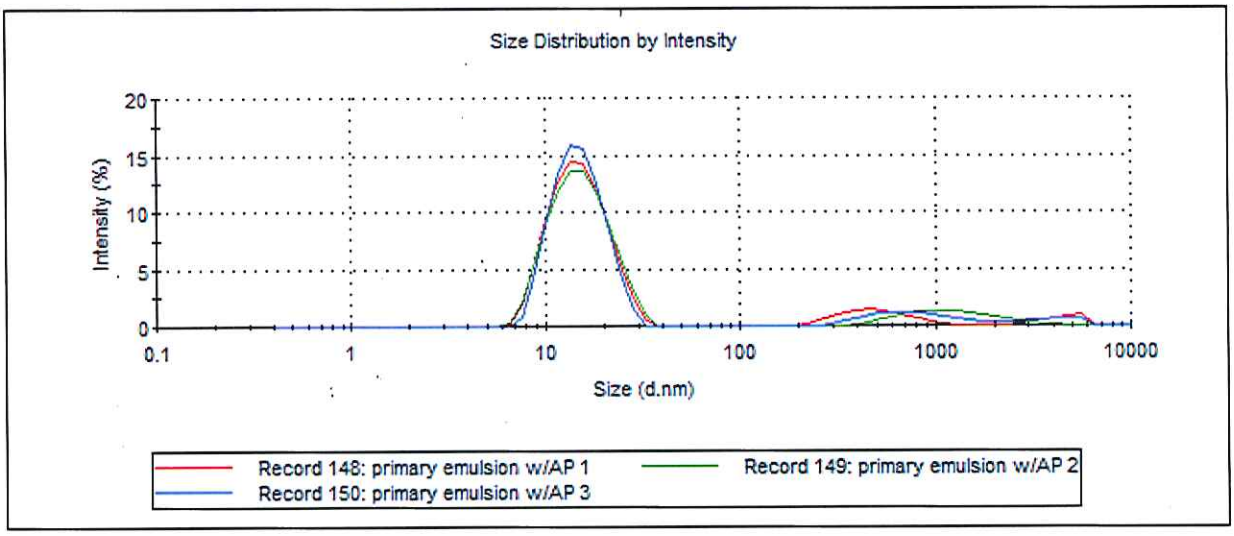

Figure K4: Size Distribution by Intensity of primary emulsion with $Al_2OH_5Cl_2 . 3\ H_2O$ (28.09.2017)

			Diam. (nm)	% Intensity	Width (nm)
Z-Average (d.nm):	43.69	Peak 1:	19.10	64.8	4.953
PdI:	0.447	Peak 2:	4130	33.8	1013
Intercept:	0.542	Peak 3:	280.7	1.4	51.03

Result quality : Refer to quality report

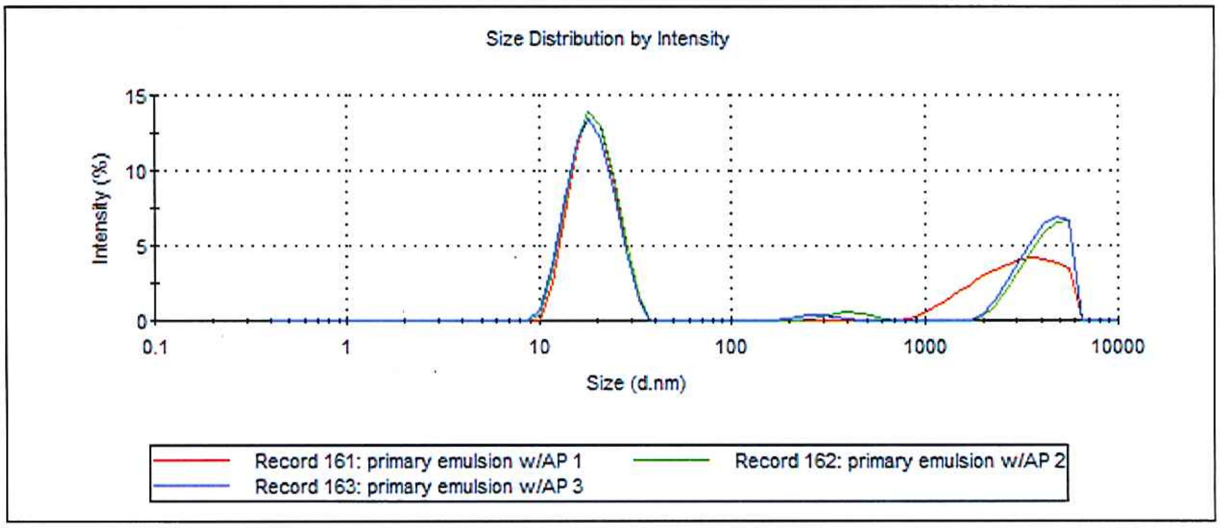

Figure K5: Size Distribution by Intensity of primary emulsion with $Al_2OH_5Cl_2.3\ H_2O$ (10.06.2017)

			Diam. (nm)	% Intensity	Width (nm)
Z-Average (d.nm):	364.2	Peak 1:	399.7	100.0	75.45
PdI:	0.138	Peak 2:	0.000	0.0	0.000
Intercept:	0.690	Peak 3:	0.000	0.0	0.000

Result quality : Refer to quality report

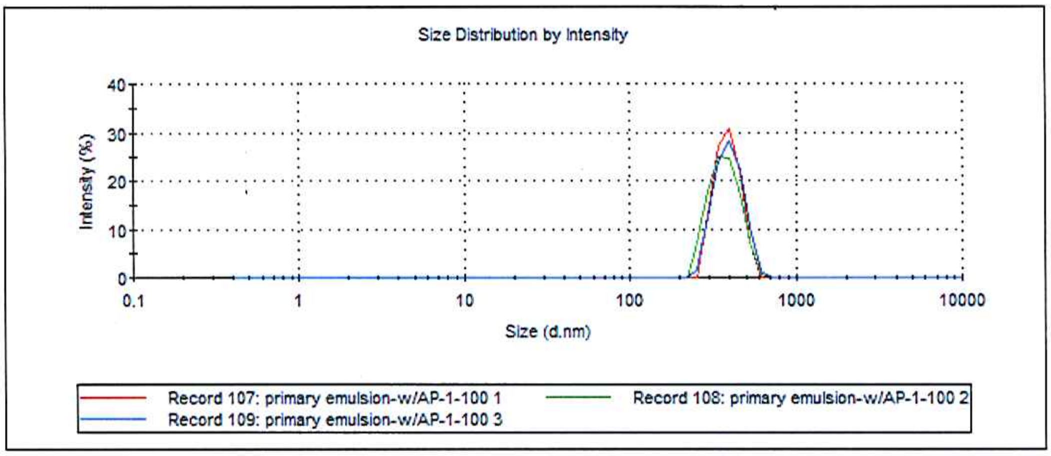

Figure K6: Size Distribution by Intensity of primary emulsion with $Al_2OH_5Cl_2.3\ H_2O$ at 1:100 dilution (20.09.2017)

		Diam. (nm)	% Intensity	Width (nm)
Z-Average (d.nm): 458.4	Peak 1:	371.2	93.1	86.62
PdI: 0.458	Peak 2:	5342	6.9	357.4
Intercept: 0.571	Peak 3:	0.000	0.0	0.000

Result quality : Refer to quality report

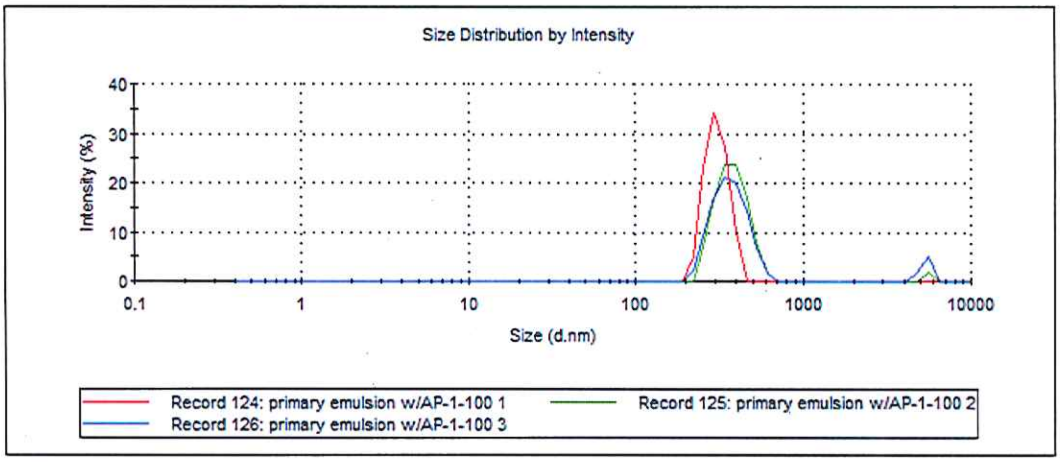

Figure K7: Size Distribution by Intensity of primary emulsion with $Al_2OH_5Cl_2 . 3\ H_2O$ at 1:100 dilution (22.09.2017)

		Diam. (nm)	% Intensity	Width (nm)
Z-Average (d.nm): 494.0	Peak 1:	304.5	96.4	51.30
PdI: 0.365	Peak 2:	5560	3.6	6.104e-5
Intercept: 0.557	Peak 3:	0.000	0.0	0.000

Result quality : Refer to quality report

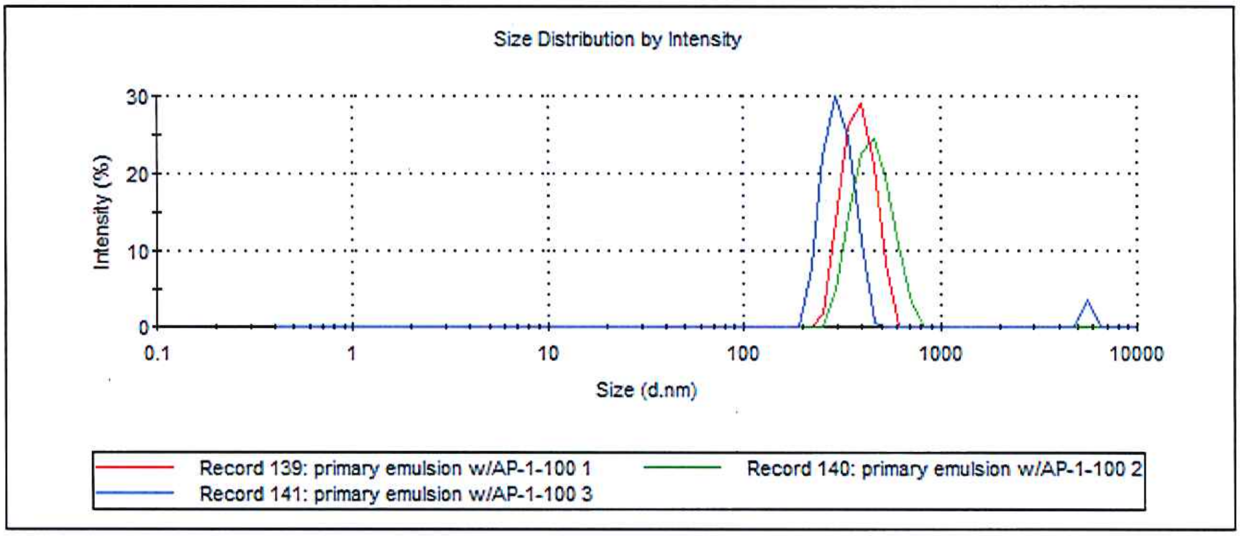

Figure K8: Size Distribution by Intensity of primary emulsion with $Al_2OH_5Cl_2 . 3\ H_2O$ at 1:100 dilution (25.09.2017)

			Diam. (nm)	% Intensity	Width (nm)
Z-Average (d.nm):	479.4	Peak 1:	392.6	100.0	68.80
PdI:	0.351	Peak 2:	0.000	0.0	0.000
Intercept:	0.612	Peak 3:	0.000	0.0	0.000

Result quality : Refer to quality report

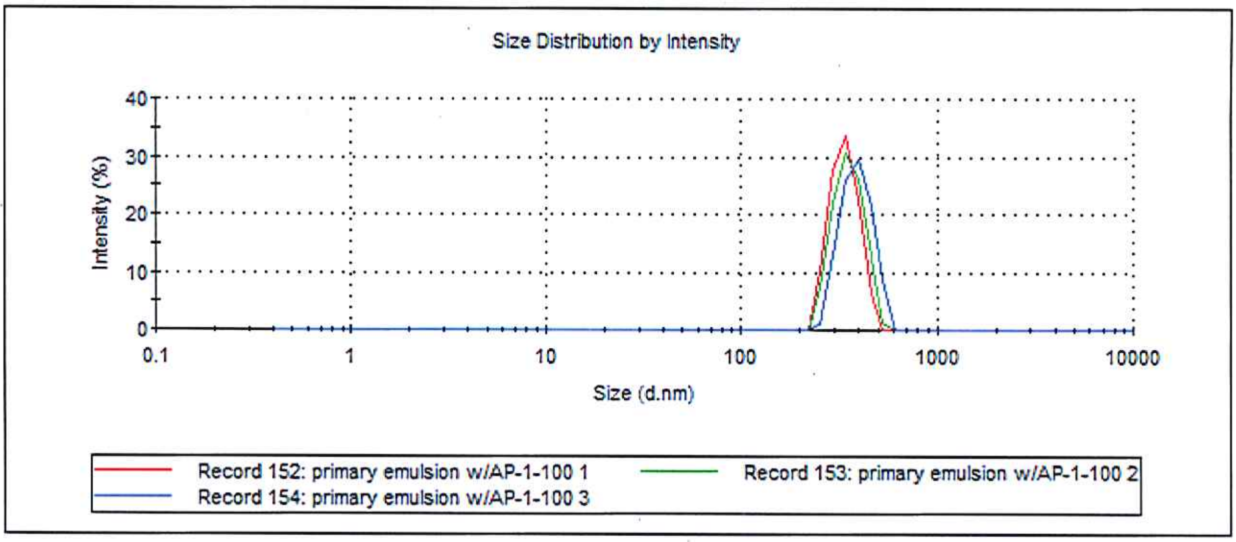

Figure K9: Size Distribution by Intensity of primary emulsion with $Al_2OH_5Cl_2 . 3\ H_2O$ at 1:100 dilution (28.09.2017)

			Diam. (nm)	% Intensity	Width (nm)
Z-Average (d.nm):	707.8	Peak 1:	640.0	100.0	120.7
PdI:	0.300	Peak 2:	0.000	0.0	0.000
Intercept:	0.617	Peak 3:	0.000	0.0	0.000

Result quality : Refer to quality report

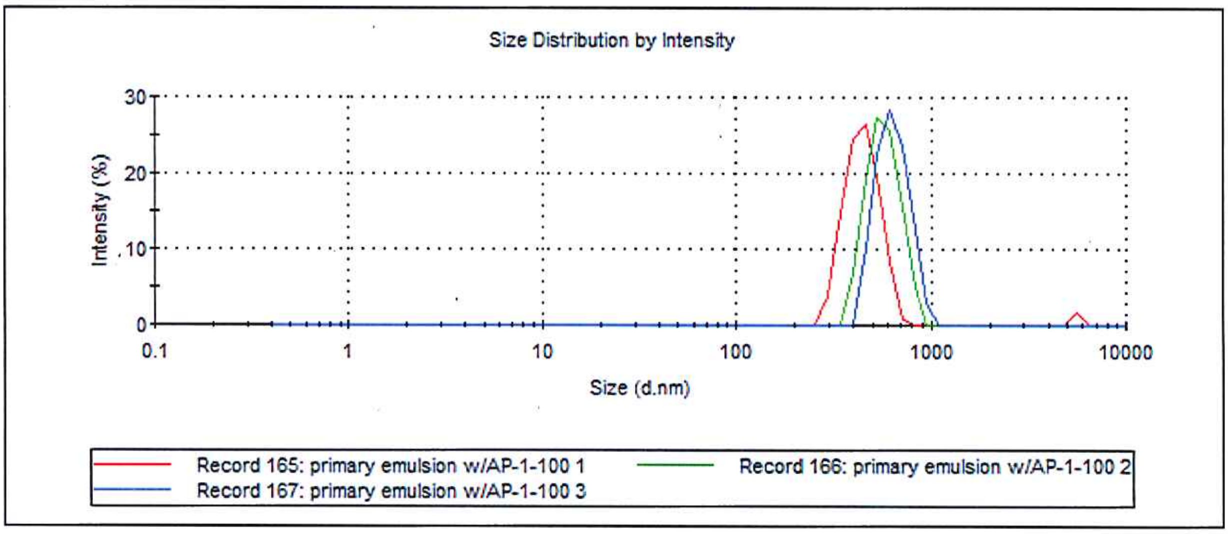

Figure K10: Size Distribution by Intensity of primary emulsion with $Al_2OH_5Cl_2 . 3\ H_2O$ at 1:100 dilution (10.06.2017)

APPENDIX L

			Diam. (nm)	% Number	Width (nm)
Z-Average (d.nm):	14.68	Peak 1:	9.665	100.0	2.542
PdI:	0.170	Peak 2:	0.000	0.0	0.000
Intercept:	0.921	Peak 3:	0.000	0.0	0.000

Result quality : Good

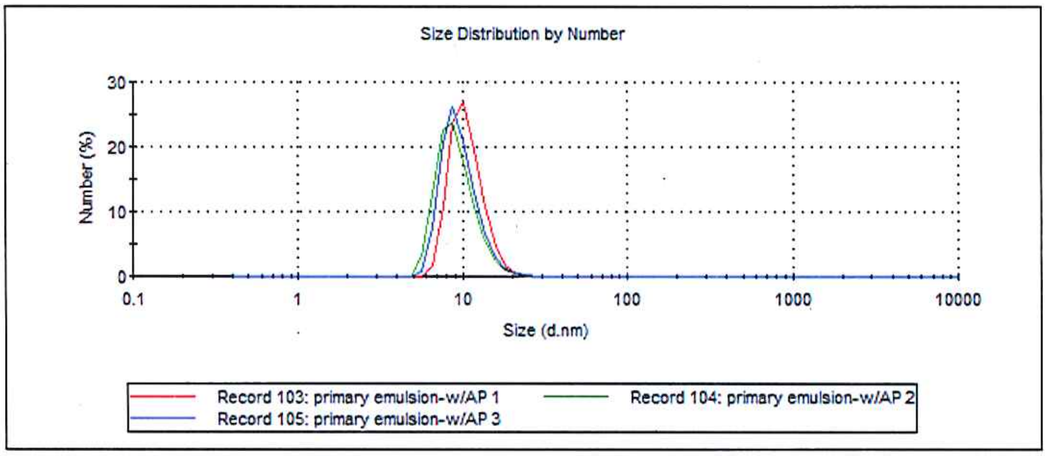

Figure L1: Size Distribution by Number of primary emulsion with $Al_2OH_5Cl_2 . 3\ H_2O$ (20.09.2017)

			Diam. (nm)	% Number	Width (nm)
Z-Average (d.nm):	15.05	Peak 1:	11.59	100.0	3.859
PdI:	0.227	Peak 2:	0.000	0.0	0.000
Intercept:	0.930	Peak 3:	0.000	0.0	0.000

Result quality : Good

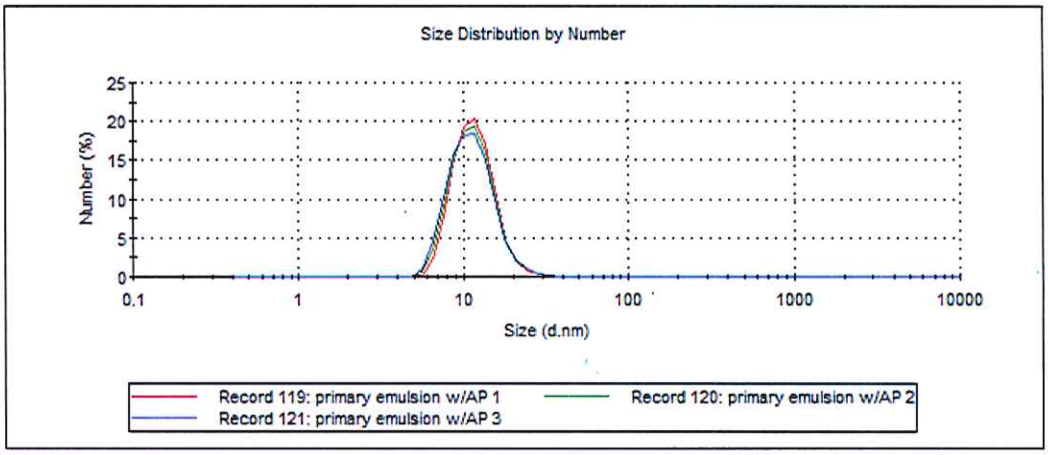

Figure L2: Size Distribution by Number of primary emulsion with $Al_2OH_5Cl_2 . 3\ H_2O$ (22.09.2017)

			Diam. (nm)	% Number	Width (nm)
Z-Average (d.nm):	15.15	Peak 1:	11.76	100.0	3.696
PdI:	0.212	Peak 2:	0.000	0.0	0.000
Intercept:	0.926	Peak 3:	0.000	0.0	0.000

Result quality : Good

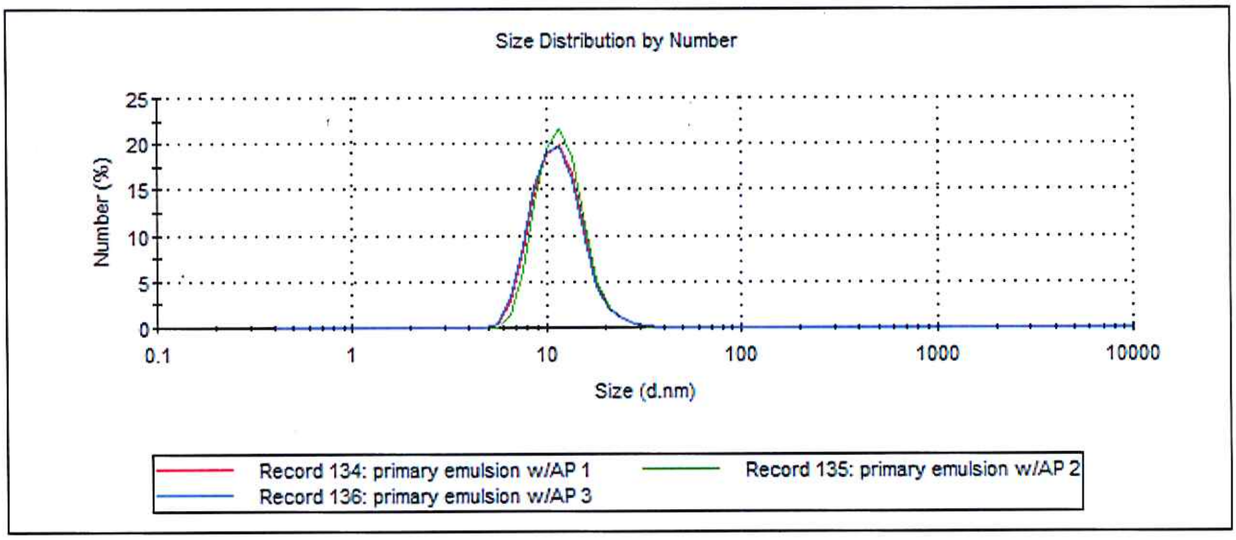

Figure L3: Size Distribution by Number of primary emulsion with $Al_2OH_5Cl_2 . 3\ H_2O$ (25.09.2017)

Z-Average (d.nm):	16.07	Peak 1:	12.16	100.0	3.230
PdI:	0.305	Peak 2:	0.000	0.0	0.000
Intercept:	0.922	Peak 3:	0.000	0.0	0.000

Result quality : Good

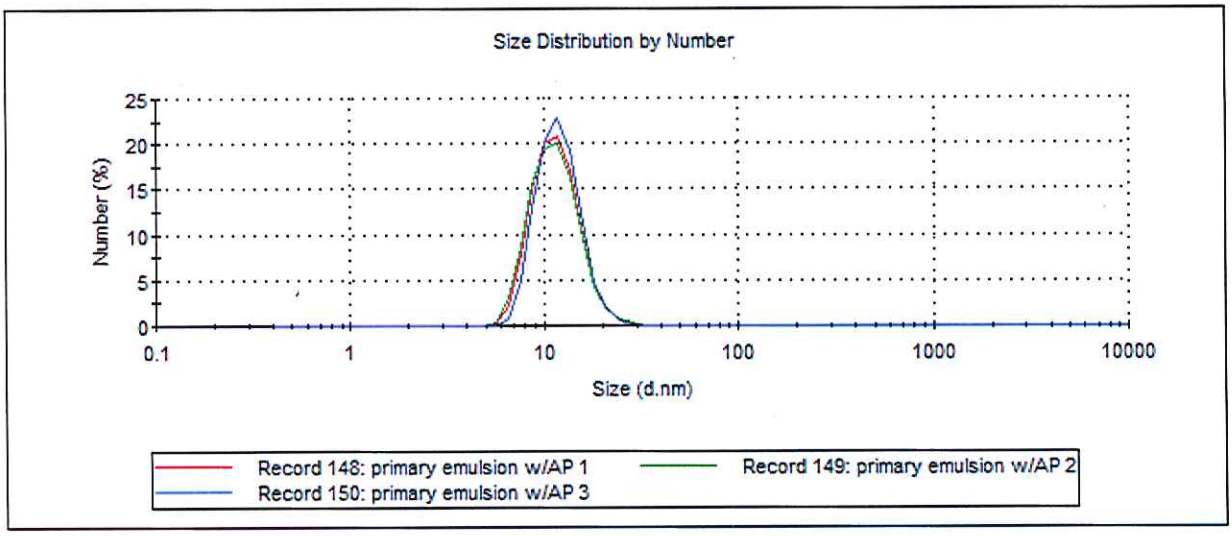

Figure L4: Size Distribution by Number of primary emulsion with $Al_2OH_5Cl_2 . 3\ H_2O$ (28.09.2017)

			Diam. (nm)	% Intensity	Width (nm)
Z-Average (d.nm):	43.69	Peak 1:	19.10	64.8	4.953
PdI:	0.447	Peak 2:	4130	33.8	1013
Intercept:	0.542	Peak 3:	280.7	1.4	51.03

Result quality : Refer to quality report

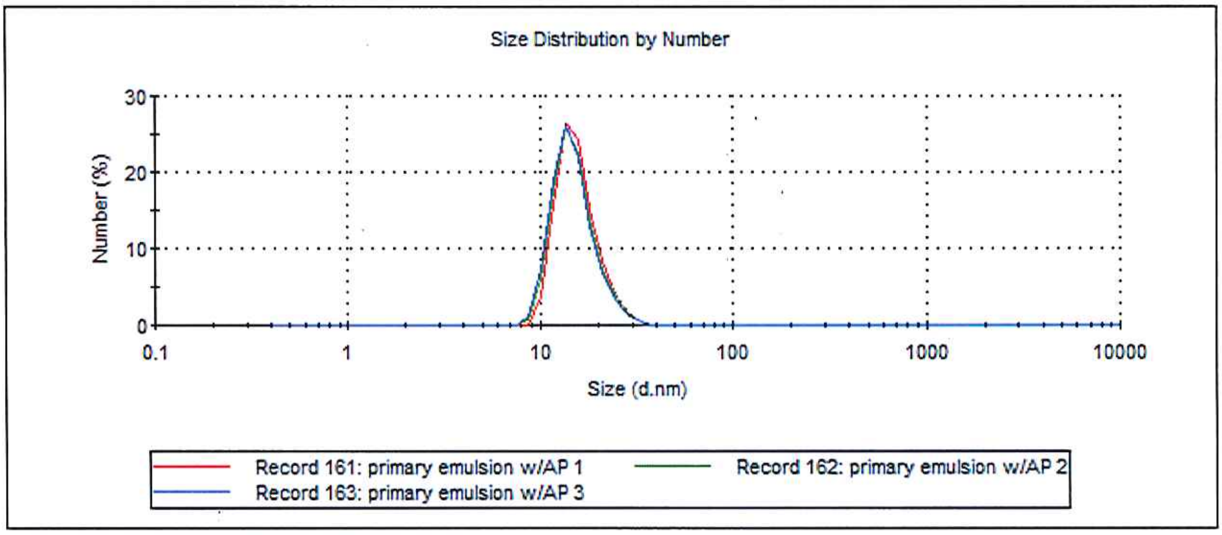

Figure L5: Size Distribution by Number of primary emulsion with $Al_2OH_5Cl_2 . 3\ H_2O$ (10.06.2017)

			Diam. (nm)	% Number	Width (nm)
Z-Average (d.nm):	364.2	Peak 1:	385.2	100.0	83.73
PdI:	0.138	Peak 2:	0.000	0.0	0.000
Intercept:	0.690	Peak 3:	0.000	0.0	0.000

Result quality : Refer to quality report

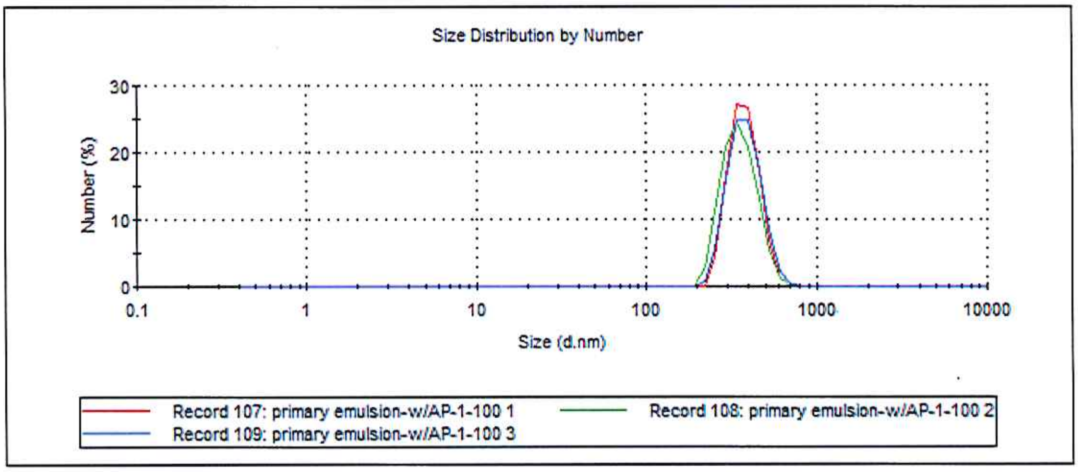

Figure L6: Size Distribution by Number of primary emulsion with $Al_2OH_5Cl_2 . 3\ H_2O$ at 1:100 dilution (20.09.2017)

			Diam. (nm)	% Number	Width (nm)
Z-Average (d.nm):	458.4	Peak 1:	307.4	100.0	69.53
PdI:	0.458	Peak 2:	0.000	0.0	0.000
Intercept:	0.571	Peak 3:	0.000	0.0	0.000

Result quality : Refer to quality report

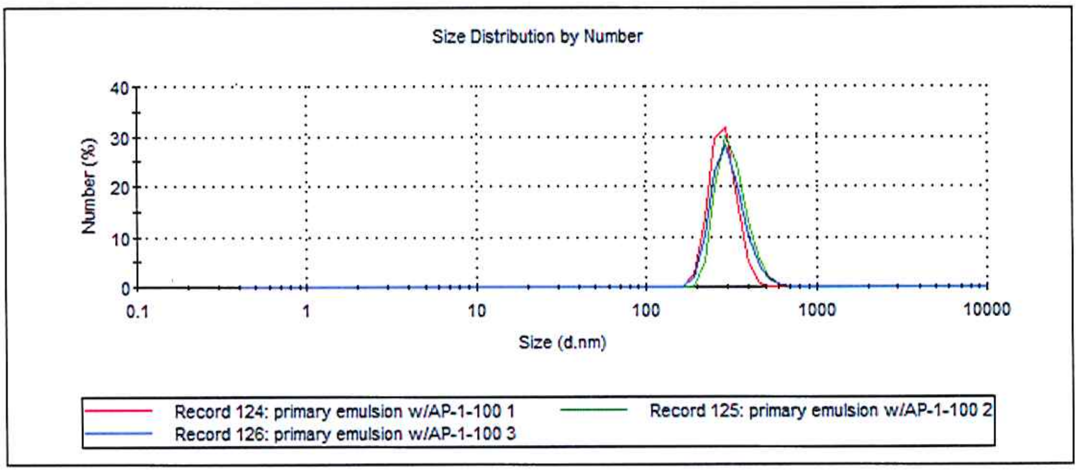

Figure L7: Size Distribution by Number of primary emulsion with $Al_2OH_5Cl_2 . 3\ H_2O$ at 1:100 dilution (22.09.2017)

			Diam. (nm)	% Number	Width (nm)
Z-Average (d.nm):	494.0	Peak 1:	279.8	100.0	51.34
PdI:	0.365	Peak 2:	0.000	0.0	0.000
Intercept:	0.557	Peak 3:	0.000	0.0	0.000

Result quality : Refer to quality report

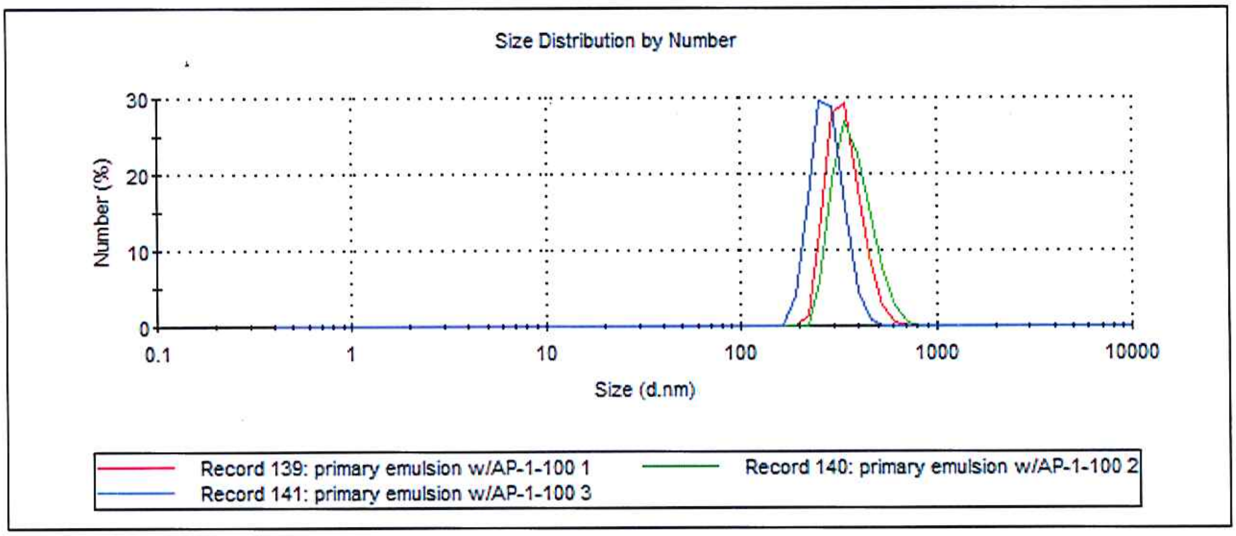

Figure L8: Size Distribution by Number of primary emulsion with $Al_2OH_5Cl_2 . 3\ H_2O$ at 1:100 dilution (25.09.2017)

			Diam. (nm)	% Number	Width (nm)
Z-Average (d.nm):	479.4	Peak 1:	344.9	100.0	68.14
PdI:	0.351	Peak 2:	0.000	0.0	0.000
Intercept:	0.612	Peak 3:	0.000	0.0	0.000

Result quality : Refer to quality report

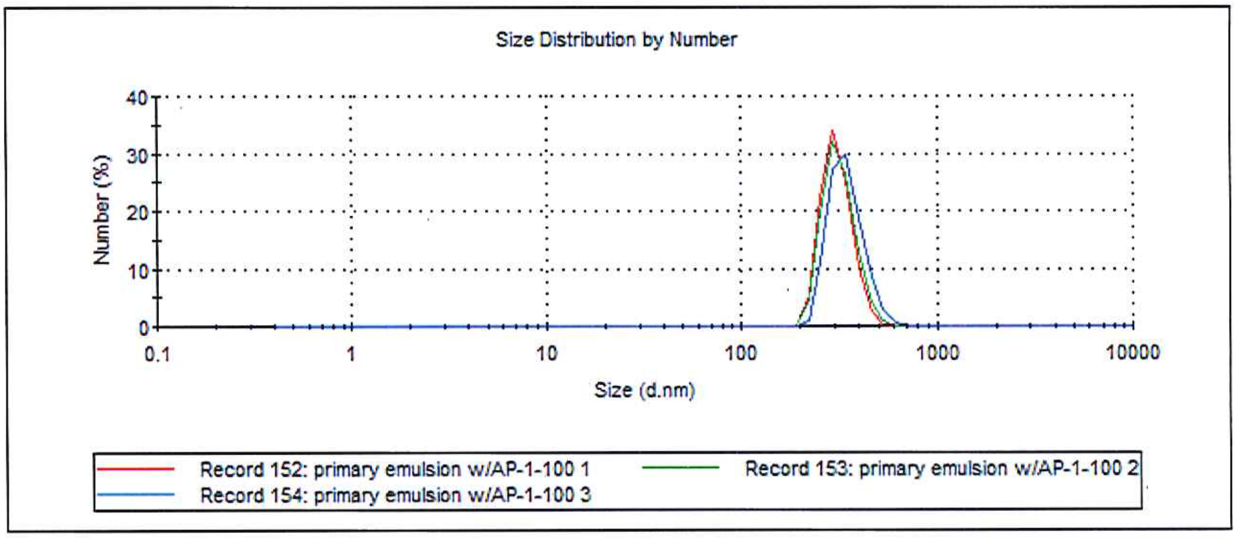

Figure L9: Size Distribution by Number of primary emulsion with $Al_2OH_5Cl_2 . 3\ H_2O$ at 1:100 dilution (28.09.2017)

			Diam. (nm)	% Intensity	Width (nm)
Z-Average (d.nm):	707.8	Peak 1:	640.0	100.0	120.7
PdI:	0.300	Peak 2:	0.000	0.0	0.000
Intercept:	0.617	Peak 3:	0.000	0.0	0.000

Result quality : Refer to quality report

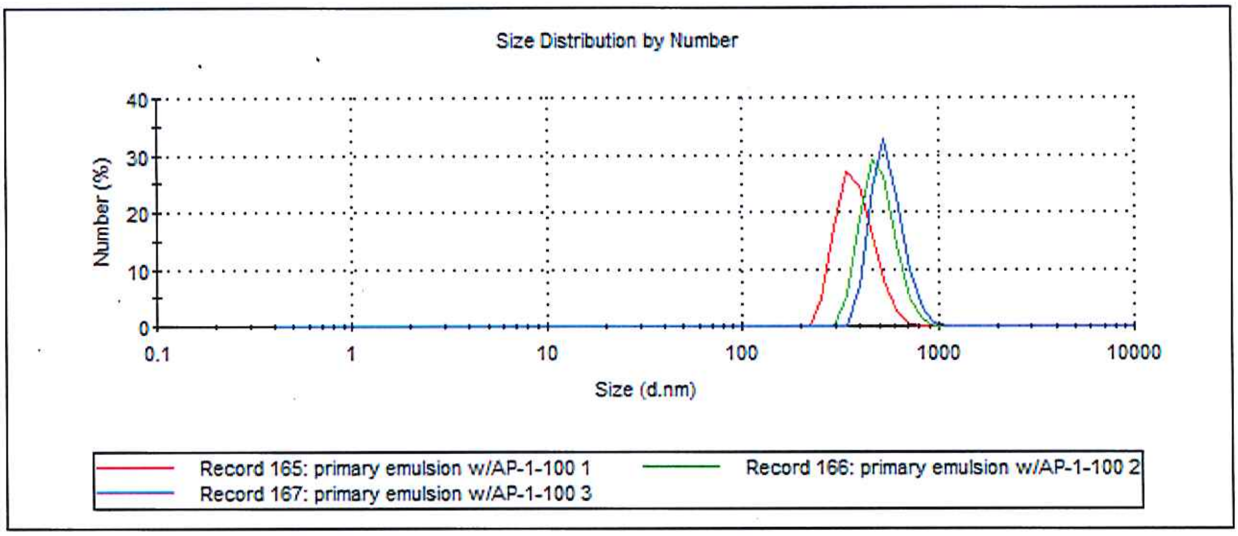

Figure L10: Size Distribution by Number of primary emulsion with $Al_2OH_5Cl_2 . 3\ H_2O$ at 1:100 dilution (10.06.2017)

APPENDIX M

Temperature (°C):	25.0	Duration Used (s):	60
Count Rate (kcps):	516.7	Measurement Position (mm):	0.85
Cell Description:	Disposable sizing cuvette	Attenuator:	5

			Diam. (nm)	% Intensity	Width (nm)
Z-Average (d.nm):	293.5	Peak 1:	342.5	94.7	188.3
PdI:	0.404	Peak 2:	5020	5.3	600.4
Intercept:	0.772	Peak 3:	0.000	0.0	0.000
Result quality :	Good				

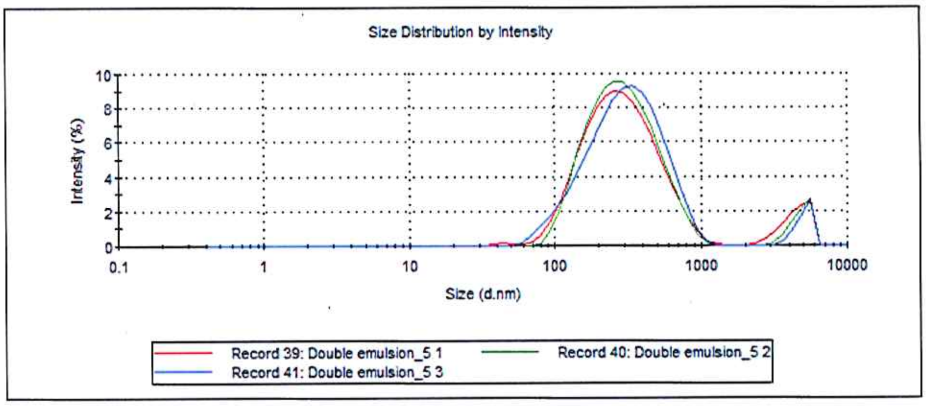

Figure M1: Size Distribution by Intensity of secondary emulsion at 1:1000 dilution (4.17.2017)

			Diam. (nm)	% Intensity	Width (nm)
Z-Average (d.nm):	184.5	Peak 1:	229.0	98.1	122.1
PdI:	0.235	Peak 2:	4671	1.9	796.1
Intercept:	0.938	Peak 3:	0.000	0.0	0.000
Result quality :	Good				

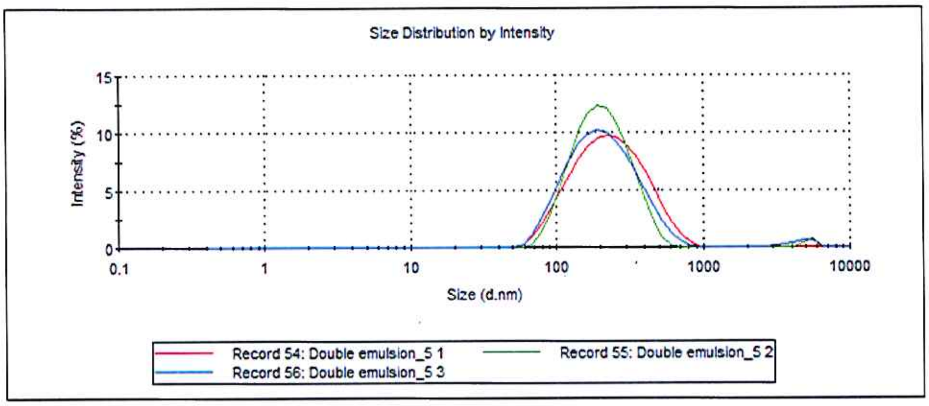

Figure M2: Size Distribution by Intensity of secondary emulsion at 1:1000 dilution (4.19.2017)

			Diam. (nm)	% Intensity	Width (nm)
Z-Average (d.nm):	185.9	Peak 1:	261.0	100.0	166.6
PdI:	0.238	Peak 2:	0.000	0.0	0.000
Intercept:	0.938	Peak 3:	0.000	0.0	0.000
Result quality :	Good				

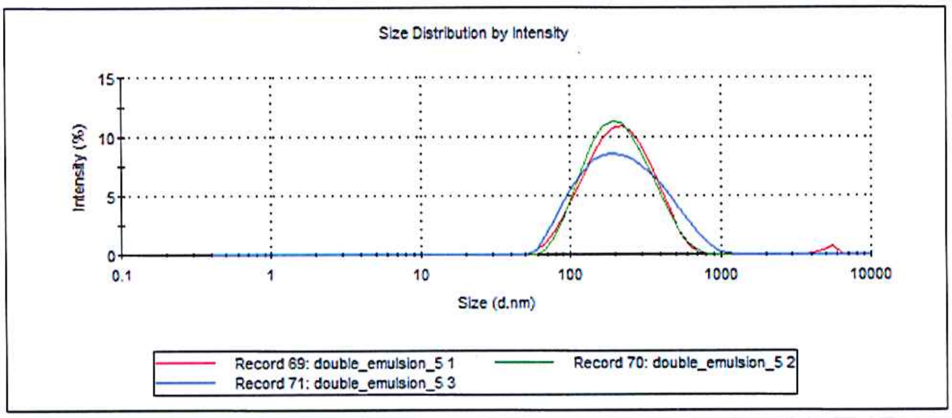

Figure M3: Size Distribution by Intensity of secondary emulsion at 1:1000 dilution (4.21.2017)

			Diam. (nm)	% Intensity	Width (nm)
Z-Average (d.nm):	197.1	Peak 1:	248.5	100.0	123.7
PdI:	0.243	Peak 2:	0.000	0.0	0.000
Intercept:	0.940	Peak 3:	0.000	0.0	0.000
Result quality :	Good				

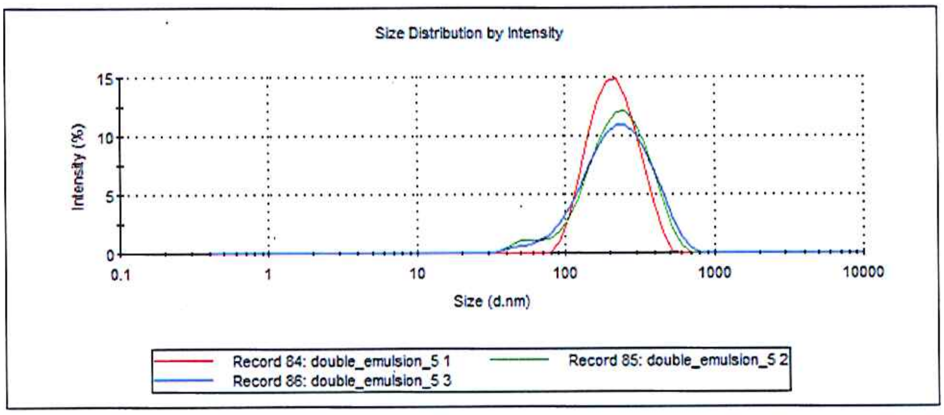

Figure M4: Size Distribution by Intensity of secondary emulsion at 1:1000 dilution (4.27.2017)

APPENDIX N

			Diam. (nm)	% Number	Width (nm)
Z-Average (d.nm):	293.5	Peak 1:	127.8	100.0	84.75
PdI:	0.404	Peak 2:	0.000	0.0	0.000
Intercept:	0.772	Peak 3:	0.000	0.0	0.000
Result quality :	Good				

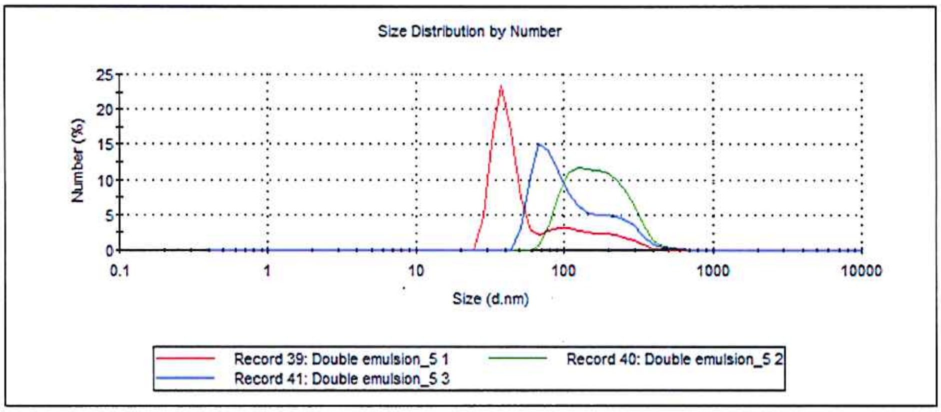

Figure N1: Size Distribution by Number of secondary emulsion at 1:1000 dilution (4.17.2017)

			Diam. (nm)	% Number	Width (nm)
Z-Average (d.nm):	184.5	Peak 1:	99.47	100.0	42.32
PdI:	0.235	Peak 2:	0.000	0.0	0.000
Intercept:	0.938	Peak 3:	0.000	0.0	0.000
Result quality :	Good				

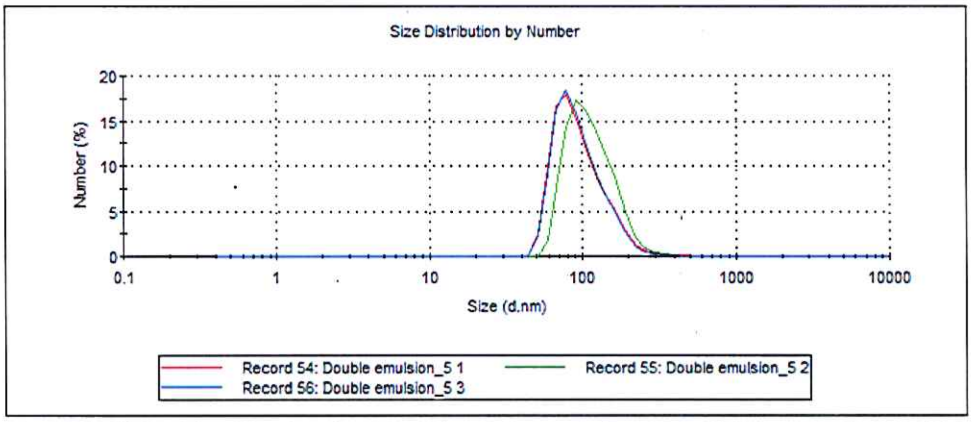

Figure N2: Size Distribution by Number of secondary emulsion at 1:1000 dilution (4.19.2017)

			Diam. (nm)	% Number	Width (nm)
Z-Average (d.nm):	185.9	Peak 1:	93.22	100.0	41.21
PdI:	0.238	Peak 2:	0.000	0.0	0.000
Intercept:	0.938	Peak 3:	0.000	0.0	0.000

Result quality : Good

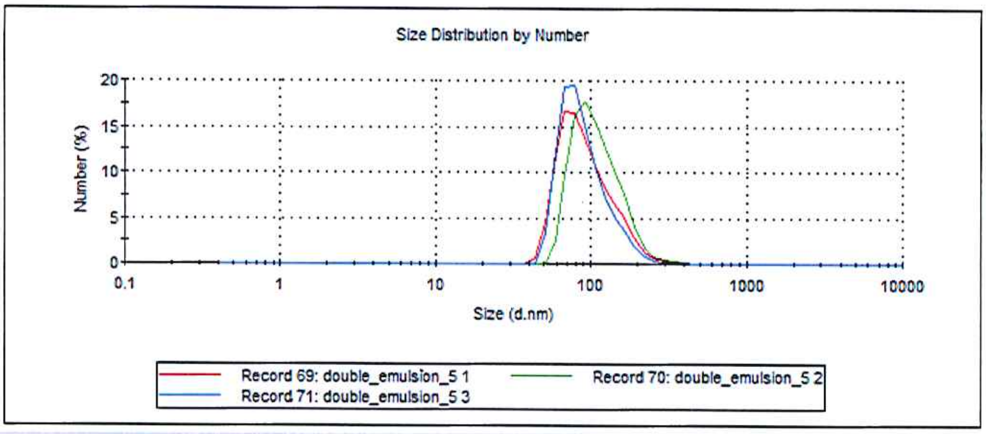

Figure N3: Size Distribution by Number of secondary emulsion at 1:1000 dilution (4.21.2017)

			Diam. (nm)	% Number	Width (nm)
Z-Average (d.nm):	197.1	Peak 1:	52.83	100.0	31.37
PdI:	0.243	Peak 2:	0.000	0.0	0.000
Intercept:	0.940	Peak 3:	0.000	0.0	0.000

Result quality : Good

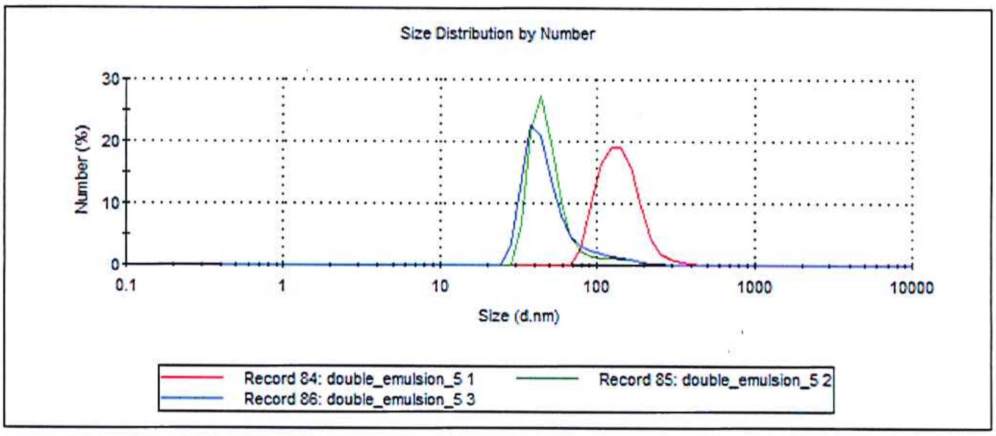

Figure N4: Size Distribution by Number of secondary emulsion at 1:1000 dilution (4.27.2017)